TRIBHUVAN UNIVERSITY

INSTITUTE OF ENGINEERING

PULCHOWK CAMPUS

THESIS NO.: M-117-MSESPM-2018/2020

Optimal Placement of Dynamic Voltage Restorer for Voltage Sag Mitigation using Artificial Neural Network

by

Archana Ghimire

A THESIS

SUBMITTED TO DEPARTMENT OF MECHANICAL AND AEROSPACE ENGINEERING IN PARTIAL FULFILLMENT OF THE REQUIREMENT FOR THE DEGREE OF MASTER OF SCIENCE IN

ENERGY SYSTEMS PLANNING AND MANAGEMENT

DEPARTMENT OF MECHANICAL AND AEROSPACE ENGINEERING

LALITPUR, NEPAL

JULY, 2020

COPYRIGHT

TRIBHUVAN UNIVERSITY

INSTITUTE OF ENGINEERING

PULCHOWK CAMPUS

DEPARTMENT OF MECHANICAL AND AEROSPACE ENGINEERING

The undersigned certify that they have read, and recommend to the Institute of Engineering for acceptance, a thesis entitled "**Optimal Placement of Dynamic Voltage Restorer for Voltage Sag Mitigation using Artificial Neural Network**" submitted by Archana Ghimire in partial fulfillment of the requirements for the degree of Master in Energy Systems Planning and Management.

_____

Supervisor, Dr. Nawraj Bhattarai
Associate Professor, Department of Mechanical and Aerospace Engineering, Pulchowk Campus

_____

Supervisor, Laxman Motra
Assistant Professor, Department of Mechanical and Aerospace Engineering, Pulchowk Campus

_____

External Examiner, Birendra Kumar Jha
Deputy Manager, Nepal Electricity Authority

_____

Committee Chairperson, Dr. Nawraj Bhattarai
Head, Department of Mechanical and Aerospace Engineering, Pulchowk Campus

Date: July 31, 2020

ABSTRACT

Voltage sag is one of the most critical and frequently occurring events in electric power systems and more prominent in radial distribution systems. When the uninterrupted operation of a load is desired, there is a necessity of a mechanism to dynamically compensate the voltage in the grid. Custom power electronics devices are used to achieve such dynamic compensation of which Dynamic voltage restorer (DVR) is extensively used because of its fast operation, the competence of compensating active and reactive power, fewer harmonics injection and its ability to operate for both voltage sags/swells apart from being compact in size and cheaper in cost. Based on the nature of the network and equipment served, the unit of DVRs to be placed in a system also varies. It becomes not only economically infeasible to provide DVR to every load in a system, but also, such placement of a large number of DVRs violate the operation of the system. Thus, the optimal placement of this device must be determined so that it maximizes the system performance. This study focuses on the Artificial neural network method in order to optimally locate DVR in a radial distribution network. The working model of a DVR developed in MATLAB/SIMULINK simulation environment has been implemented to restore the node voltages back to the pre-fault conditions dynamically. In order to analyze the influence of various parameters affecting the operation of DVR in radial distribution networks, sensitivity analysis has been implemented. The developed DVR model has been optimally located in the network using the ANN-based approach, which uses the Levenberg Marquardt backpropagation algorithm with a target of minimizing the voltage deviation of the buses from their rated operating values. Optimization results obtained by using ANN have then been verified by finding the optimal location using a different approach, which involves the minimization of System Average RMS Frequency Index (SARFI).

Sensitivity analysis shows that the developed DVR model can bring the bus voltages back to a safe operating range above 0.9p.u. for more than 90% of the simulated cases. Optimal placement of DVR is found to be at line 2-3 for IEEE 15 bus system and line 2-6 for Thimi-Sallaghari radial distribution systems. Simulation results with DVR placed in the optimal location for both the systems show a consequential enhancement in voltage profile of systems with DVR being able to restore the voltage sags at neighboring buses to more than 90% of the nominal rated voltage at each bus.

ACKNOWLEDGEMENTS

I would like to express my sincere appreciation towards my thesis supervisors Associate Prof. Dr. Nawraj Bhattarai and Assistant Prof. Laxman Motra, for their expert guidance, constant support, and suggestions whenever required and continuous encouragement throughout the course of the research.

My humble honor goes to the Department of Mechanical and Aerospace Engineering and the Institute of Engineering for providing me the opportunity to carry out research work on the topic of my interest. I am extremely thankful to Associate Prof. Dr. Shree Raj Shakya, coordinator, MS-ESPM, for providing an environment conducive to carrying out my thesis work and also to the entire committee members for their perspective insights, comments, and guidance throughout different stages of the thesis. I owe my special thanks to Er. Sourav Dhungana, Er. Bikram Gaihre, Er. Anjay Sah and all friends of 074MSESPM for their constant motivation.

I take this opportunity to extend my sincere gratitude and indebtedness to my family members and colleagues for their encouragement during the entire period of thesis work.

TABLE OF CONTENTS

LIST OF FIGURES

LIST OF TABLES

LIST OF ACRONYMS AND ABBREVIATIONS

PQ	:	Power Quality
DG	:	Distributed Generation
DVR	:	Dynamic Voltage Restorer
CPDs	:	Custom power devices
PCC	:	Point of common coupling
UPS	:	Uninterruptible power supplies
DSTATCOM	:	Distribution Static Synchronous Compensator
UPQC	:	Unified Power Quality Conditioner
SVC	:	Static VAR Compensator
VSC	:	Voltage Source Converter
ANN	:	Artificial Neural Network
LM	:	Levenberg-Marquardt
BP	:	Back Propagation
MSE	:	Mean Square Error
kV	:	Kilo-Volt
kVA	:	Kilovolt Ampere
kVAR	:	Kilovolt Ampere Reactive
IEEE	:	Institute of Electrical and Electronics Engineers
MATLAB	:	Matrix Laboratory
SLD	:	Single line Diagram
RMS	:	Root mean square
p.u.	:	Per unit
SARFI	:	System Average RMS frequency Index

CHAPTER ONE: INTRODUCTION

1.1 Background

Electricity is considered one of the most important sources of energy for almost all populations throughout the world. Its demand is increasing day by day for the consumers with an expectation of easy access fulfilling the good quality requirements in the most economical way. For maintaining the quality, the power distribution system must supply the smooth sinusoidal form of electricity in an undisturbed form to maintain the amplitude as well as the frequency of the supply. For this, the Electricity Regulation of Nepal has established a system that has a certain rule for voltages and frequency. For the voltages below 33kV in a distribution system, the amplitude must remain under ±5%, and the value of frequency must remain under ±2.5% of 50 Hz (SARI/Energy, 2003).

Power quality problems are taken as a prominent issue, and its solution must be obtained by taking the system as a unit rather than trying to solve each unit discretely. Due to improvement in technology and restriction of quality requirements, nowadays modern devices require a highly stable and undisturbed power supply in a continuous manner to maintain its high efficiency (Soni, et al., 2013). Power quality issues can be understood as the events of occurrence of a highly undisturbed supply of power with the fluctuations of voltages/currents as well as the frequency which may affect the user's devices. Some of the power quality issues such as voltage swell and sag distortion of harmonics, flickering, interruptions, time-dependent transient conditions, as well as the flow of power in reverse directions, cause adverse effects in the power system devices leading to the generation of extra heat and losses or damage of various devices (Renders, et al., 2007).

The most severe problem among the disturbances in the voltage are events that occurred due to the harmonics and sagging of voltage as these directly affect both the suppliers as well as the users. The voltage sags definition may vary from place to place as per the need of quality. Still, the most common definition includes the decrement of the RMS value of voltage below 90 % up to 10% for a specific period of time in a one-half cycle to a minute (IEEE, 1994). Voltage sag occurs in a frequent manner and has high effects on the devices.

The power quality problems can be mitigated with the help of many applications among them, injection of distributed generation and installing the capacitor banks are used, but the approach of connecting the Custom Power Devices (CPDs) has been considered to be the most efficient method for compensating the reactive powers, stabilizing the voltage, correcting the power factors and maintaining the level of harmonics. CPDs are considered as the most useful as they provide the solution to most of the power quality problems in an economical way and also avoid the utilities from bearing the burden of installation of additional feeders to the system. Among several CPDs, the requirement of the system and level of operations determine the selection. DVR is a series-connected device, which is considered as one of the efficient CPDs that can tackle both the problem of swelling and sagging by injecting and absorbing both reactive as well as active power. The installation of DVR in an optimal location of the system can reduce the economic burden as well as can maintain the power quality in an efficient and reliable way without interfering with the smooth operation of the whole system.

The problem of optimally selecting the location of CPDs has been a wide area of research, and several approaches like metaheuristics method, sensitive index method, Artificial intelligence (AI) techniques, etc. have been implemented for determining the optimal location of CPDs. This study mainly focuses on providing an approach for locating DVR optimally in a distribution system by using Artificial Neural Network as ANN has become very popular in finding the solution to a multi-objective optimization problem that would otherwise involve complex computations and measurements

1.2 Problem Statement

There are numerous loads that are very critical regarding the voltage and frequency at which they operate, and even a small variation of voltage/frequency in them leads to their abnormal operation and even tripping of the circuits with those loads causing the malfunctioning of the device and an enormous economic impact. Poor power quality is considered a prominent issue in developing countries such as Nepal, which causes financial as well as technical consequences.

As there is a requirement of stable and defect-free supply, whenever a voltage sag occurs, a mechanism that boosts the bus voltage dynamically is required to fill the voltage sag during that temporary period. Whenever there is a presence of a fault in any of the feeder, it instantly affects the performance of another feeder also due to increment

in the voltage drop across the reactance of the source. It is required to eradicate this effect caused by the sagging of voltage during the fault period through some dynamic compensation. The compensating device should be such that it operates instantaneously after the fault initiation, is able to provide both active/reactive power support, performs during both sagging and swelling of voltage, minimizing harmonic injection into the system during the whole period of compensation. Among many Custom Power Devices (CPDs), Dynamic Voltage Restorer offers the above-mentioned operating characteristics while being compact in size and cost sufficient for operation in radial distribution networks. However, the installation of DVR must enhance the performance of the complete system as well as some sections of it under the conditions of voltage sag. In order to increase the resulting benefits from the DVR, the location of DVR must be optimized. Although while installing DVR, there occur the power losses, fluctuations in voltage value as well as increased in economic burden so for maximizing system performance such that it is economically viable and meets required quality and reliability, the device must be optimally placed in the distribution system such that the number of nodes benefitting from its operation maximize.

1.3 Rationale of the Study

Several works have been carried out to study the operation of CPDs and to locate these devices in different systems using different techniques optimally. To minimize power loss, improve voltage profile, save energy costs, and to improve reliability and stability of power systems, CPDs are extensively used. Various techniques are involved for finding out of the optimal location of CPDs, and among the available studies, the use of Artificial Neural Network (ANN) as a tool for optimization has been limited. Also, most of the work among the few available, are based on transmission systems, and there seems to be a dearth of research in medium voltage distribution networks. This study contributes to filling this gap, proposing an ANN-based technique for optimally locating DVR in radial distribution systems.

Analyzing the impacts of various faults on power quality of the distribution system of radial type, a design of DVR that will be operated in series during the faulted condition that brings the voltage of the load-node back to the state of pre-fault by supplying the desired voltage without significant changes in the system operational variations has been proposed. The efficacy of DVR has been investigated for different uncertainties

of load and line length. Optimal utilization of electric networks is necessary for the economic viability and reliability of the system. Since ANN has been used extensively as an optimization tool, the ANN-based approach has been taken with the goal of minimizing the voltage deviation from the pre-fault voltages for determining the optimal location. Such type of formulation helps to determine Mean Square Error (MSE) of different buses, which provides information about the optimal bus for placement of DVR. Thus, the analysis will be helpful to ensure the use of DVR for reliable and stable operation and boost the system performance by placing of the DVR in the optimal location.

1.4 Objectives

1.4.1 Main Objective

The main objective of this thesis is to determine the optimal location to place a DVR in radial distribution systems in order to restore the pre-fault operating voltage at the buses affected by voltage sag during fault using ANN.

1.4.2 Specific Objectives

The study was carried out to meet the following specific objectives:

- To develop a SIMULINK model of DVR and integrate it in a radial distribution system to investigate its effectiveness.
- To perform sensitivity analysis to investigate the performance of DVR under the change in load power and distribution line length.
- To find the location for the optimal placement of DVR in the IEEE 15 bus system and a study with Thimi-Sallaghari radial distribution system using ANN.
- To validate the results of optimal location using SARFI (System Average RMS Frequency Index) approach.

1.5 Assumptions and Limitations

- The study is limited to 11kV radial distribution system
- Voltage disturbances due to faults have only been considered
- The number of DVR integrated into a distribution system is limited to one
- The magnitude of voltage has only been considered
- Unequal voltage profile has not been taken into consideration

CHAPTER TWO: LITERATURE REVIEW

2.1 Power Quality (PQ) Issues

One of the major concerns of the electric power network is the power quality problems, which are the vital issues for industrial along with domestic consumers as it leads to the economic as well as technical losses. With the rapid growth of power electronics devices in the distribution system, power quality issues are rising expeditiously. In order to operate electrical equipment precisely, it is necessary to supply the electrical power of good quality without variation in frequency, the voltage required, and waveform distortion together with the reliability of the supply. Deterioration of power quality is generally caused by faults, high starting currents, switching of heavy loads, nonlinear loads, equipment failure, etc. which results in malfunctioning of protective devices and damage the sensitive equipment's. Power quality problems occur when a small and sudden deviation from the desired value of voltage or current takes place, which includes voltage fluctuations, interruptions, voltage sag, voltage swell, transients, harmonic distortions, etc.

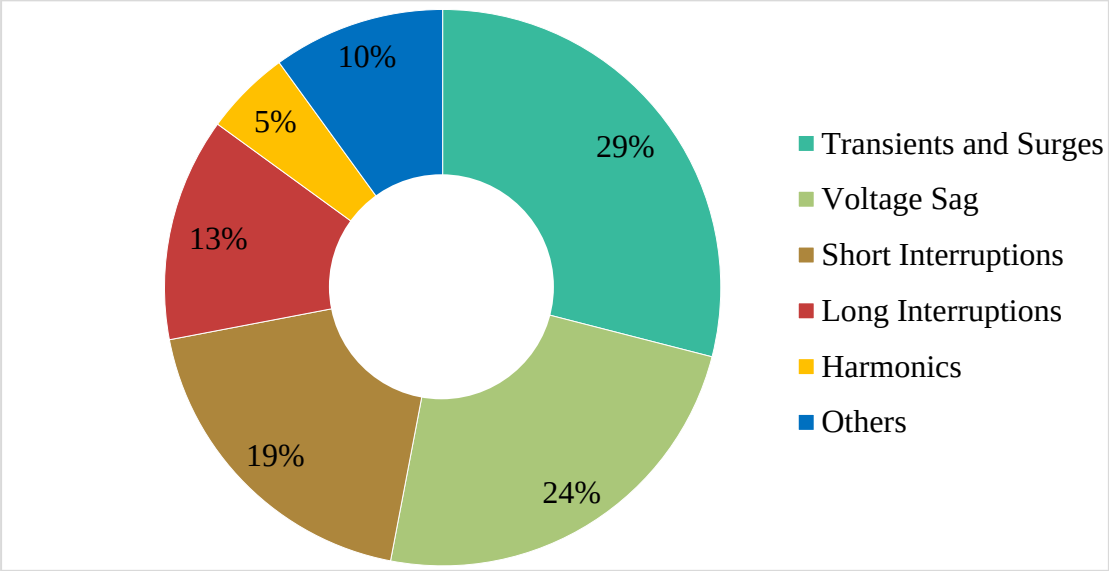

Figure 2.1: Causes of PQ problems (LPQI study)

The major problems faced by industrial and domestic consumers are related to the standards of supply, as concluded by the survey of Electric Power Research Institute (EPRI) conducted in various utilities of the USA as mentioned by (McGranaghan, et al., 1993). The problems related to the quality of power that are frequently experienced by consumers are sag/swells, harmonics, wiring/grounding, capacitor switching, load

interactions, and others with 48%, 22%, 15%, 6%, 5% and 4% shares respectively. Another power quality survey conducted in different countries in Europe concluded that the significant earning loss for consumers is occupied by sag and disturbance of voltage and harmonics with the respective share of 56% and 5%. Similarly, the decline in the revenue can rise by only 0.15% - 0.2% for the network operators due to the effect of harmonics. This survey was conducted by Leonardo Power Quality Initiative (LPQI) (Tamjis & Lau, 2006).

Although voltage sag, among various power quality problems, is an event occurring for a small fraction of time, it is considered as a prominent factor for deteriorating the daily usage of power appliances by imposing a highly unbalanced disturbance.

2.1.1 Voltage Sag

Even though the voltage sag phenomenon has been consistently present in the electric networks, customers became more aware of the inconvenience caused by them only during the past decades. Voltage sag happens when the root mean square (RMS) voltage decreases between 0.1 to 0.9 p.u. for a period of 0.5 cycles to 1 minute. (IEEE, 1994).

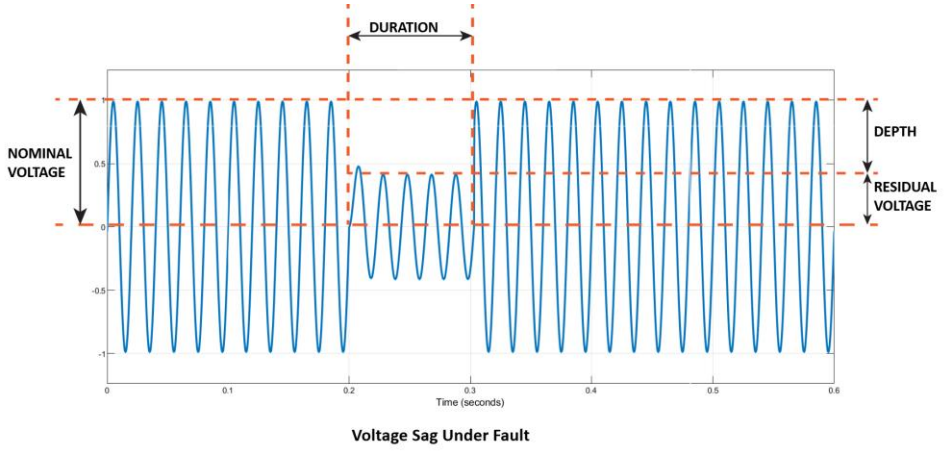

Figure 2.2: Example of voltage sag

The characteristics of voltage sag that determine the behavior of equipment are the magnitude and duration of the sag. Based on the duration of sag, voltage sag can be classified as instantaneous, momentary, and temporary sag with a duration of 0.5 to 30 cycle, 30 cycles to 3 sec, and 3sec to 1 min, respectively.

Faults in the distribution system, overloading of the electrical network, high starting current, and switching operation are the most common reason for the occurrence of

voltage sag which results in, the failure of the protective devices, malfunctioning of information technology equipment's, power fluctuation which diminish the competence of the electrical devices (Edomah, 2009).

During the occurrence of voltage sag due to fault, the parameters of the fault, i.e., type of fault and fault impedance affects the magnitude of the sag. When a balanced fault occurs in the system, then the sag magnitude is equal in all three phases, and during an unbalanced fault, sag magnitude is uneven.

2.1.2 Mitigation of Voltage Sag

Due to the random existence of the faults in the electrical network, it is a strenuous task to alleviate the voltage sag. Placement of capacitors, distributed generation (DG) sources, and power electronics devices at a suitable location are common techniques used for improving the voltage profile of the system. Out of different methods, power electronics devices are widely used for minimizing the voltage sags. While electronic power controllers on transmission level are used to control the flow of power and also to increase the stability, devices on the distribution level, often called Custom Power Devices (CPDs), are mostly used for improving the quality of power delivered to customers. Due to the ability of the CPDs to provide the fast and dynamic VAR support during the voltage disturbances, it can be considered as a better solution to voltage instability (Leon & Taylor, 2002). As voltage sag evaluation depends upon the impedance of the system, so CPDs devices are the most suitable option to mitigate the voltage sag. The critical problem of voltage sag can be diminished through these devices by injecting the voltage into the distribution grid. The commonly used CPDs are Distribution Static Synchronous Compensator (D-STATCOM), which is a shunt device, Dynamic Voltage Restorer (DVR), which is a series-connected device, and Unified Power Quality Conditioner (UPQC) which has a series and shunt compensation capabilities.

Based on the comparison among other CPDs, DVR a series compensating device has a rapid speed of operation, provide active along with reactive power support, reduce voltage sag and voltage swell issues, is also cheaper, compact, and has minimal harmonics insertion into the grid (Singh & Singh, 2015).

2.2 Dynamic Voltage Restorer (DVR)

DVR is a device based on power electronics that works as a compensator and protects the sensitive loads from supply-side disturbances by injecting voltage in series through injection transformer, which is controlled as required. It is capable of supplying and absorbing both real and reactive power where real and reactive power is generated by energy storage and internally by DVR, respectively (Ghosh & Ledwich, 2001).

When the voltage of the system is normal, DVR will remain in still condition, but as the voltage disturbances occur, DVR keeps injecting the voltage until the injected voltage restores the load voltage within a certain specified threshold value. The factors that affect the voltage compensation are the types of voltage sag, the voltage level at which DVR is connected, and load conditions. There are different methods of voltage injection: both voltage magnitude and phase angle are compensated in the Pre-sag Compensation method, only voltage magnitude is compensated through In-phase compensation method, and Phase-Advance Compensation method uses only reactive power injection to compensate sag instead of active power (Haque, 2001).

2.2.1 Mathematical Model of DVR

Mathematically, a DVR can be modeled as a series voltage source with its impedance connected between source and load, as shown in Figure 2.3. During a fault, no matter the type and configuration, system voltage will always decrease, and in such condition, it is required that DVR keeps injecting series voltage V_{DVR} in order to restores the load voltage V_L.

The voltage injected by DVR is given by;

$$V_{DVR} = V_L + Z_{LINE} * I_L - V_{SOURCE} \qquad \text{Equation 2.1}$$

Where V_L is the load voltage, Z_{LINE} is the line impedance, I_L is load current, and V_{SOURCE} is the source voltage throughout the faulty state.

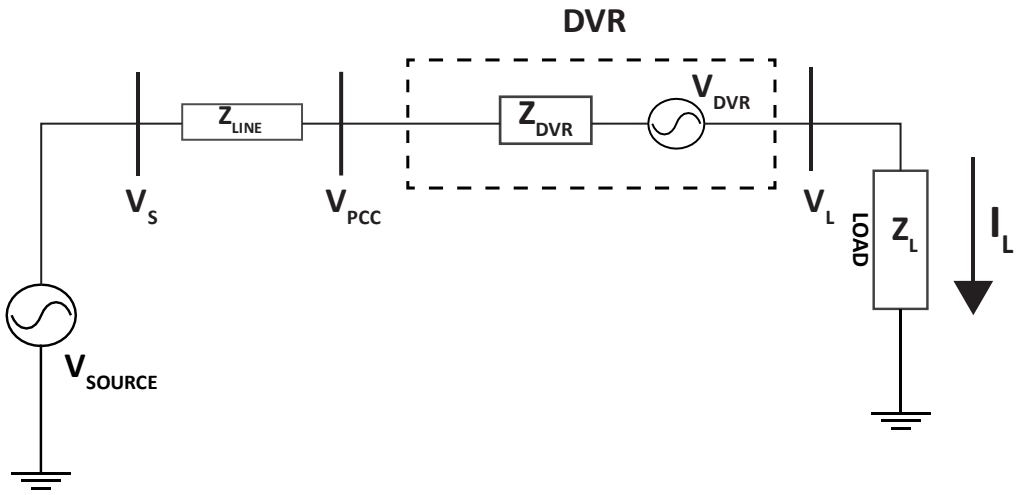

Figure 2.3: DVR equivalent circuit diagram

The current through DVR, which is same as load current since it is series with the load is given by

$$I_L = (P_L + jQ_L)/V_L \qquad \text{Equation 2.2}$$

With V_L taken as reference,

$$V_{DVR}<\alpha = V_L< 0 + Z_{LINE}I_L < (\beta - \Phi) - V_{SOURCE}< \delta \qquad \text{Equation 2.3}$$

where α , β, and δ are the angles of V_{DVR}, Z_{LINE}, and V_{SOURCE} respectively and Φ is load power angle:

$$\Phi = \tan^{-1}\left(\frac{Q_L}{P_L}\right) \qquad \text{Equation 2.4}$$

The power injection from DVR can be expressed as:

$$S_{DVR} = V_{DVR}\, I_L^* \qquad \text{Equation 2.5}$$

The voltage V_{DVR} needs to be controlled and adjusted properly to maintain the desired load voltage.

2.2.2 Working Principle of DVR

DVR basically operates by taking the measure of the amount by which system voltage has sagged/swelled through its internal control and then dynamically compensating that amount of voltage in series with the line through an injection transformer during the event of sag/swell.

When a disturbance occurs in a feeder, a healthy feeder also experienced an impact of the fault and experiences voltage sag as depicted. Under such situation, DVR control block senses this voltage deviation and internally calculated the voltage to be injected into the line so that at any time, the voltage seen by the load is a constant rated voltage, which is represented by a sinusoidal signal of constant amplitude and phase in the figure.

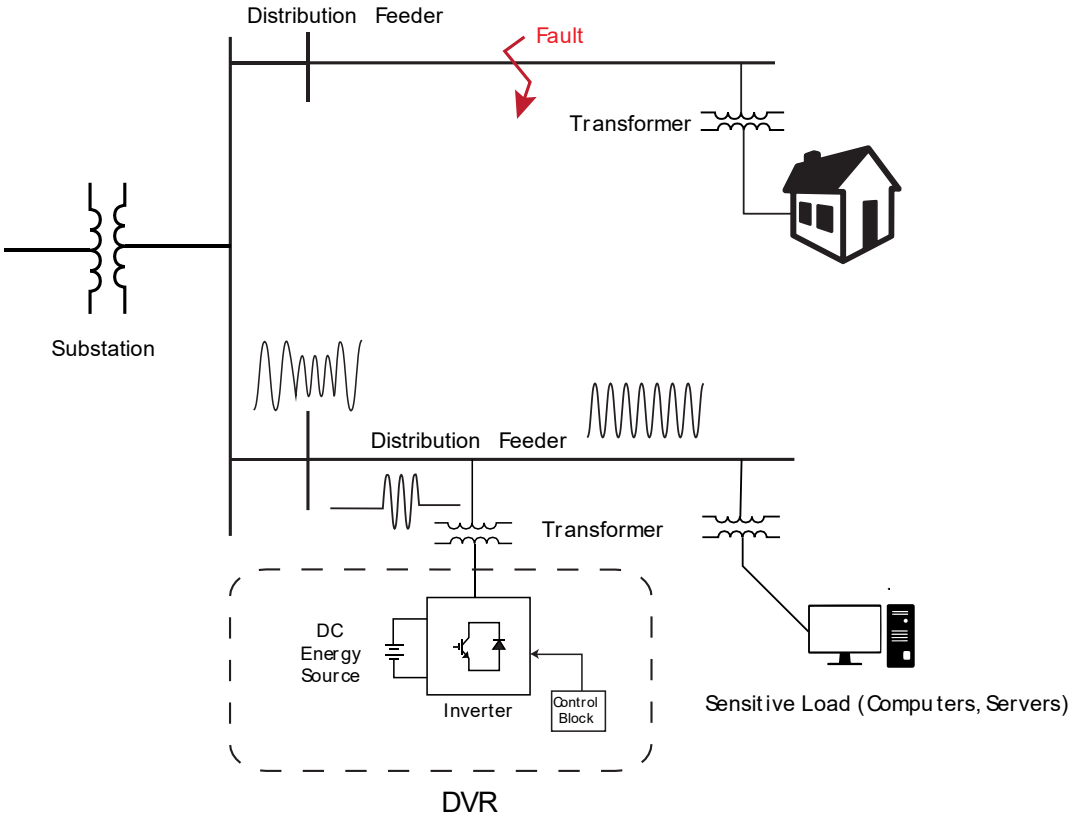

Figure 2.4: Operating principle of DVR

DVR basically operates in three different operating modes —protection mode, standby mode, and injection mode. If load current, which is also the current through the DVR in a radial system, becomes more significant than the safe operating value DVR operates in protection mode, bypassing the current by providing another path to prevent damage to the internal power electronics part of the DVR. In standby mode, DVR does not inject any voltage or injects a small amount of voltage to take care of the line drops and losses. In injection mode (V_{DVR}>0), DVR injects voltage to compensate for the sag/swell through an injection transformer by internally detecting and calculating the amount of voltage sag/swell.

2.2.3 Structure of DVR

DVR basically consists of five main components: Voltage Source Converter, Energy Storage, Control system, Harmonic filter, and Injection/Booster Transformer, as shown in figure 2.5. The details on different components of DVR have been discussed in this section.

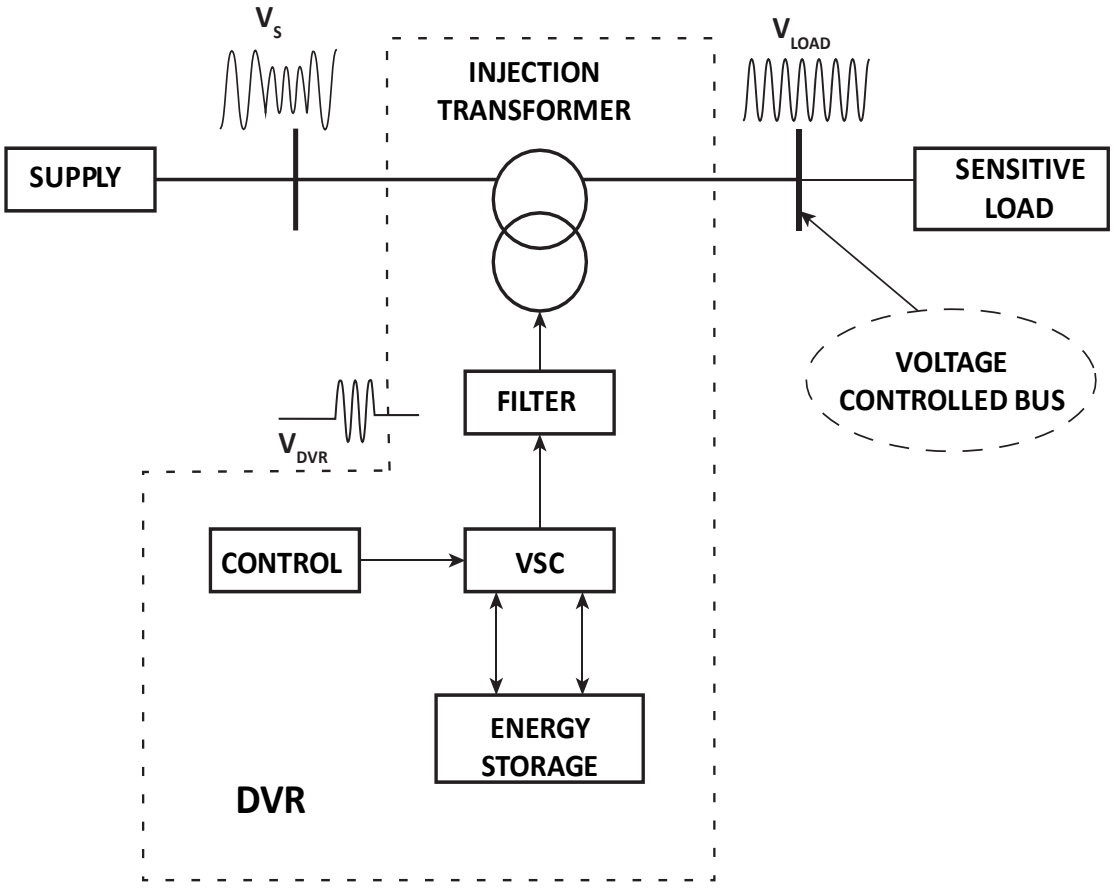

Figure 2.5: Schematic diagram of typical DVR structure

i. Energy Storage

The energy storage device serves as an essential component for the DVR as it serves as the power bank to supply voltage support during voltage sags and absorbs the excess power from the grid during voltage swell.

ii. Voltage Source Converter (VSC)

It is required that the DC voltage in the battery to be injected into the grid as AC power, for this purpose a VSC has controlled switches that enable it to generate a sinusoidal waveform of voltage with desired magnitude, frequency, and phase. Proper operation and control of this inverter are required so that it only injects the desired amount of voltage to the line.

iii. Filter

The filter is provided in DVR with the purpose of dampening the high-frequency harmonics introduced in the system during the control of Inverter (Converter). Second-order LC, RC or RLC filters are extensively used in DVR based upon the functionality and operating system requirements.

iv. Control System

The control system continuously monitors the source voltage and compares it with the reference voltage detecting any change in voltage. When this change is detected, it internally computes the amount of voltage to be injected and operates the switching of inverter such the wanted level of compensation is achieved.

v. Injection Transformer

As a series-operated device, it is required that DVR has some mechanism through which it injects power in series to the line. An injection facilitates this purpose. An injection transformer used with DVR is typically composed of three single transformers connected with delta/open star winding. DVR circuit has electronic components that will be damaged under high voltages and current in the grid. Injection transformer not only provides the electrical isolation of DVR circuit from the grid but also reduces the power requirement of the VSC– while stepping up the voltage from the inverter into the grid the voltage ratings of the inverter to be used can be lowered for the same power to be injected into the grid.

2.2.4 Optimal Placement of DVR

Various research has been followed out in CPDs modeling and its optimal placement in order to lessen the voltage sag issues. Very few works are available focusing on placement of CPDs in the large network for mitigating the sag at the number of buses as most of the studies have been aligned towards the mitigating voltage sag at a particular load. The installation location of CPD in the power system will affect the voltage sag performance of the whole network (Milanovic & Zhang, 2010). Therefore, the placement of these devices must be chosen optimally with an appropriate approach in order to ratify the purpose of connecting to the system. Power loss minimization, voltage fluctuations reduction, improving voltage stability, and reliability of the system are the major objectives of the optimal allocation of CPDs. Different approaches have

been carried out for determining the optimal location, such as Metaheuristics method, sensitivity-based approach, Artificial intelligence (AI) techniques, analytical approach, etc.

Among different approaches, one of the AI techniques, ANN technique, is considered as an effective method as ANN has become very popular in finding solutions to a multi-objective optimization problem that would otherwise involve complex computations and measurements and provide the possibility of solving an infinite number of complex tasks.

2.3 Artificial Neural Network (ANN)

ANN incorporated a large number of artificial neurons, which consists of input, hidden, and output layers connected to each other and are enumerated by a neuron model, architecture, and a training algorithm. All types of processing operations are performed by neuron model where the set of processing units, connections between units are arranged in architecture, and a learning algorithm trained the network by adjusting the weights, and the process is repeated till outputs do not match with desired outputs (Wilamowski, 2009).

Neuron model

Several neurons can be situated in parallel, forming a layer, and several layers can be connected in cascade, forming a multilayer structure. A neuron embodied an input that is associated with weights through a set of links, an adder function that computes the weighted sum of inputs, activation function to regulate the range of neuron output, and an external parameter known as bias (Tagliarini & Christ, 1991).

The input data $x_1, x_2 .. x_m$ flow through the weight of the synapse w_{jm} which strengthens or weakens the input signal and added at additive junction represented by sigma ($\sum$) along with bias b. In an ANN, a lot of parameters (weights and biases) should need to be tuned.

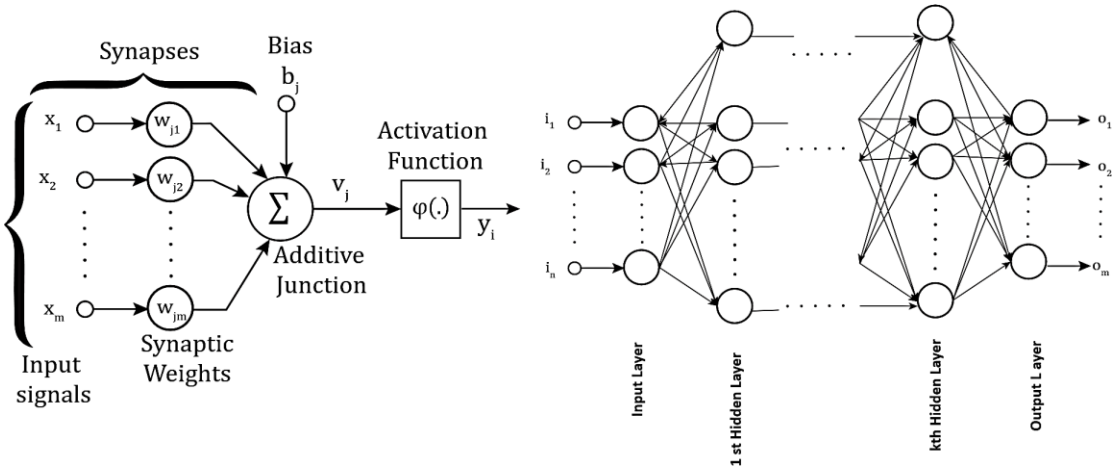

Figure 2.6: Schematic structure of Artificial Neuron and ANN

Architecture of Neural Network

Based on the topology, neural networks can be classified as feedforward and feedback neural networks. The signal in feed-forward neural network flows in one direction from input to output while in feedback network signal can be fed back into the input. The neural network can be further divided into single-layered and multi-layered networks based on the number of layers.

Training Rule

The training of the neural network takes place in order to generate a required output, and a similar process is repeated until outputs of the given input data do not match with desired outputs. Training input data is a set of samples required to train the network. Training of neural networks once on each sample of training data is defined as an epoch, and the training process requires many epochs to meet its best performance. Before training, the samples are categorized into training, testing, and validation samples. There are two types of learning rules: unsupervised and supervised learning. In unsupervised learning, only input parameters are known, whereas in supervised learning input parameters along with the desired output parameters are known.

2.3.1 Backpropagation Algorithm

Feedforward neural network is generally trained using a backpropagation algorithm, which has two phases i.e., forward pass and backward pass. During forward pass, the

output values are calculated, and then backward pass computes the loss function and transmits the error backward (Reynaldi, et al., 2012).

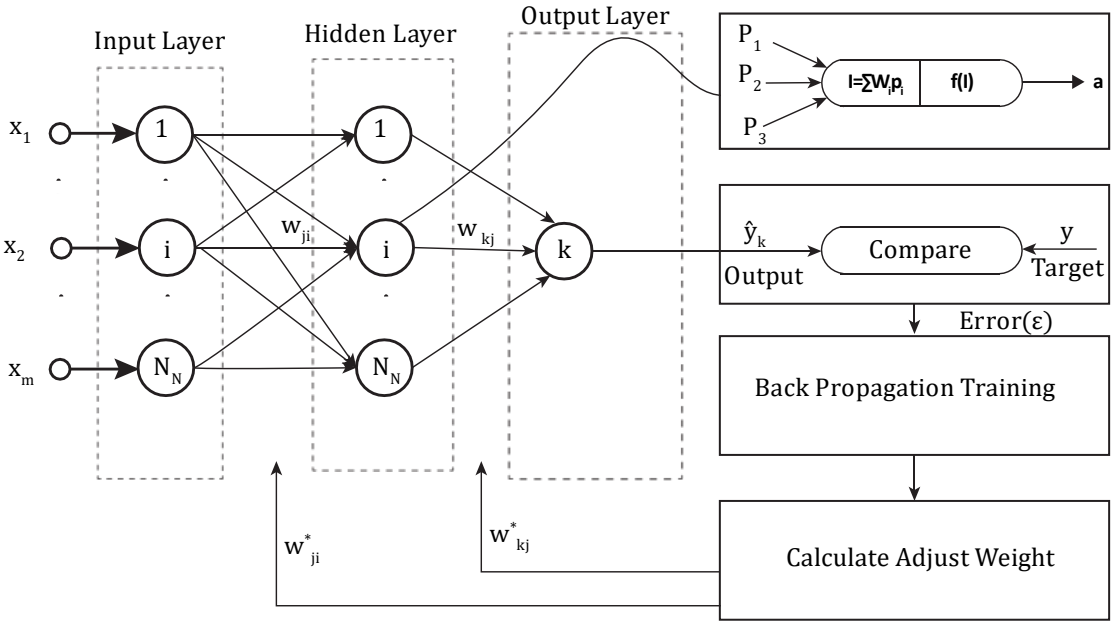

Figure 2.7: Architecture of feedforward backpropagation network

There are different kinds of backpropagation algorithms, among which the Levenberg-Marquardt (LM) learning algorithm is generally used as it is an efficient method for solving nonlinear problems.

2.4 Survey of Earlier Works

The study on various voltage injection method and modeling of DVR generating sine vector for mitigating the various power quality issues like voltage sag and swell have been discussed (Bhonde, et al., 2017).

The study on the mitigation of disturbance due to voltage variation in distribution networks, voltage profile enhancement and reliability improvement of secondary distribution system using a dynamic compensator known as DVR has been presented (Ogunboyo, et al., 2018).

The basic schematic structure, operating principle, electrical model, operation modes, voltage injection methods, parameter design and control scheme of series compensating device, DVR has been discussed (Remya, et al., 2018)

Placement of shunt compensation device using one of the AI techniques has been performed at an interconnected IEEE 15 bus system in order to reduce the voltage sag caused due to symmetrical and asymmetrical fault in the system (Singh, et al., 2011).

DVR placement based on reducing the number of sagged bus and outage load has been presented, and the PSO based approach has been used to solve the DVR optimization problems considering capital costs of DVR installation and interruption costs due to interruption of the load. (Mohammadi, 2013).

Placement of D-STATCOM in the optimal location with the objective of minimizing the power loss and improving the voltage profile of the network using an analytical approach has been presented (Husain & Subbaramiah, 2013).

Efficacy of the ANN-based technique for placement of CPDs in the distribution system of radial type has been presented by implementing the proposed approach on a radial feeder situated in Hunsinkere, Hassan (Y.K & G.K, 2015)

A PSO technique has been formulated for locating the optimal position of DVR in IEEE 33 bus system with the objective of minimizing power losses (Reddy, et al., 2017) .

The technique of minimizing System average RMS frequency index- $SARFI_X$, which gives a measure of the average number of voltage sags below a pre-specified threshold that has been studied for optimizing the placement of DVR (Bach, 2019) .

CHAPTER THREE: METHODOLOGY

The stepwise methodology followed during the course of the research from the start till its completion has been presented in this chapter. The flow diagram of the methodology developed during the process of the project is shown in Figure 3.1.

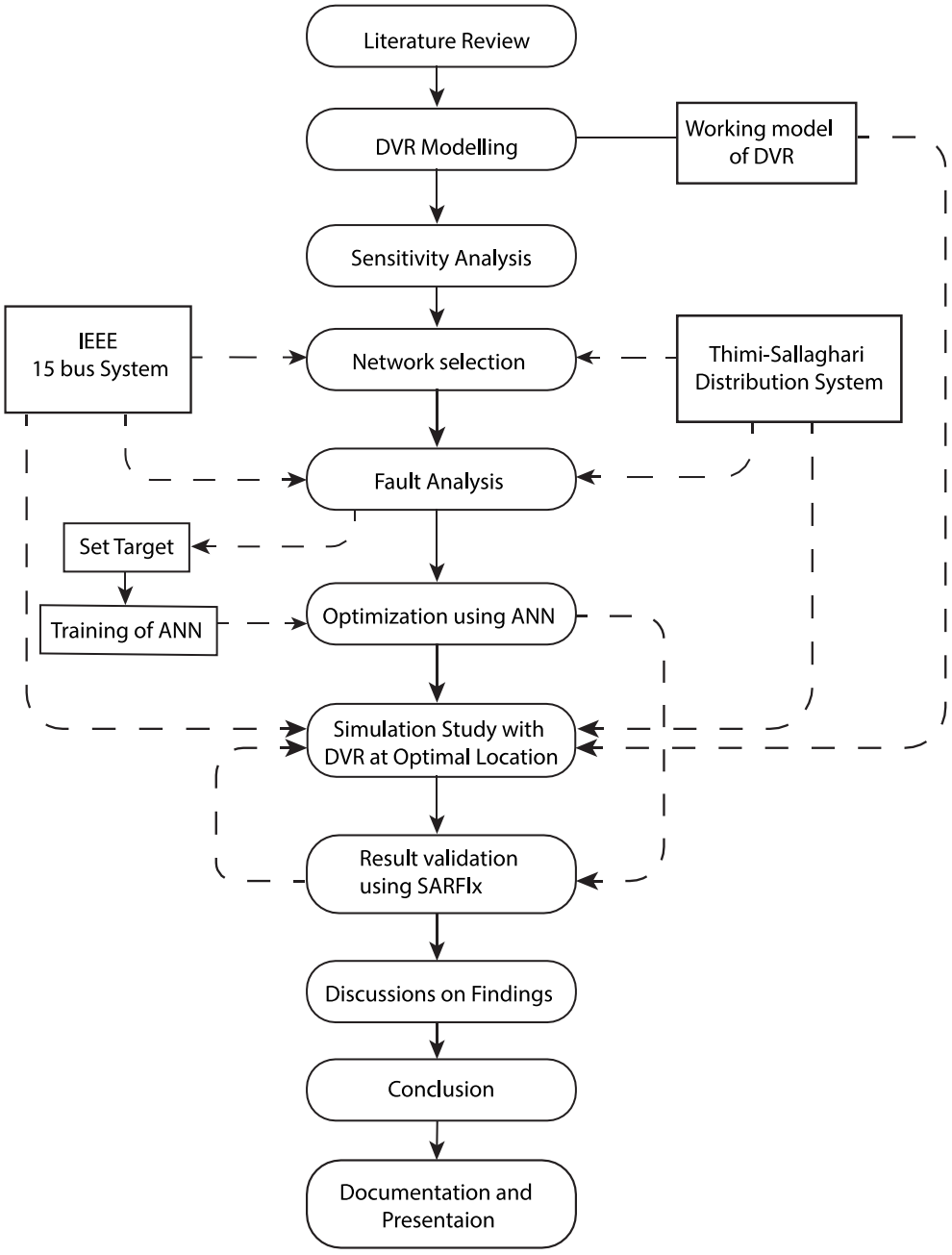

Figure 3.1: Flow diagram of Methodology

3.1 Literature Review

A significant portion of the research was covered by the literature review. Books, journals, papers, articles, and standard regulations were thoroughly studied and

reviewed throughout the project. The literature review mainly focuses on finding out the effect of voltage disturbances on power quality and grid operation as a whole, different types of CPDs, mitigating voltage sag using CPDs, the working mechanism of DVR, and optimization techniques were extremely prioritized to obtain the required background for the study. Moreover, in this process, the required assumptions and theories were noted so that to be used in the project, as explained in Chapter Two.

3.2 DVR Modelling and Sensitivity Analysis

The SIMULINK model of DVR has been developed with the necessary boundary conditions, and parameters were according to the reviewed literature. It has been installed into a simple power system to study performance efficiency.

Furthermore, in order to have an effective response from DVR, it is desired for the change in the developed model is able to operate in a wide range of load power demand and length of the distribution line (l) from DVR interconnection node to the node whose voltage is to be studied. MATLAB sensitivity analyzer toolbox has been used to perform a sensitivity analysis of the DVR connected system to evaluate how the parameters of a model influenced the output voltage and to determine the certainty of load voltage at the nodes following the DVR interconnection point being more than 90% of the normal threshold value. The complete description of DVR modeling and Sensitivity Analysis is presented in Chapter Four.

3.3 Optimal Placement of DVR

The detailed explanation of the procedure for locating DVR optimally to maximize the system performance in the selected systems is presented in Chapter Five

3.3.1 Selection of Network

In order to achieve the objectives of this thesis, IEEE 15 bus distribution system and Thimi-Sallaghari radial feeder have been selected. The data for the standard IEEE 15 bus system and Thimi-Sallaghari radial feeder has been obtained from the literature review, and the required information is shown in Appendix A and Appendix D, respectively.

3.3.2 Modelling and Fault Analysis of Network

Both systems are designed in the MATLAB/ SIMULINK environment where they were simulated and tested for their performance. The developed models were analyzed by conducting fault analysis on it. Different faults LG, LL, LLG, and LLLG faults were created in each bus, and then the simulations were conducted, and the voltage profiles under the fault conditions were tabulated in Appendix B and E.

3.3.3 ANN Formulation and Determination of Optimal Location

An ANN-based approach has been used to find the optimal location for placing DVR. Neural networks have been built using the Neural network fitting tool available in MATLAB. Post fault voltages obtained from fault analysis were considered as train dataset, and target dataset is set as 0 or 1 based in the fault condition, and the developed neural network has been trained using the training function known as trainlm with an objective of minimizing the deviation of calculated output from the desired output, defined as Mean Squared Error (MSE) and computed as:

$$\text{MSE}=\frac{1}{n}\sum_{i}^{n}(y_i-\hat{y}_i)^2 \qquad \text{Equation 3.1}$$

Where,

y_i = desired output

$\hat{y}_i$ = actual output

The objective function is then given by,

$$y = \min f = \text{minimize (MSE)} \qquad \text{Equation 3.2}$$

After training the neural network, error and output matrices have been created which provide the MSE for each bus in the system. The bus having highest MSE is the most vulnerable bus and is therefore taken as the best or optimal location for the placement of DVR. Vulnerable refers to a bus in a system which has maximum contribution towards bringing the system voltage down to the level of total voltage collapse. Thus, placing a DVR at the most vulnerable bus enhances the voltage stability margins.

3.3.4 Validations of Optimal Location

For validating the results, optimal location was determined with the objective of minimization of System Average RMS Frequency Index (SARFI) of the system in the presence of DVR. The objective is given by,

$$SARFI_X = \frac{\sum_{i=1}^{n} n_i x}{n} \qquad \text{Equation 3.3}$$

where,

X=RMS voltage threshold

$n_i x$=number of voltage sags lower than the specified threshold

n= total number of connected loads (with all the buses)

The objective function is then given by,

$$y = \min\left(SARFI_X\right) = min\left(\frac{\sum_{i=1}^{n} n_i . x}{n}\right) \qquad \text{Equation 3.4}$$

The sag threshold X is considered as 0.9 or 90%, which indicates that we compute the system average sag frequency based on the number of buses whose voltages go below 90% of the nominal threshold value during a fault.

3.4 Discussion on Findings

The results on independent operation of DVR, sensitivity analysis, the optimal location of DVR using the ANN approach, and validation of optimal location using the SARFI approach are presented in Chapter Six.

The effectiveness of the developed DVR model has been validated as the model mitigates voltage sags and swells occurring in the load, even when the fault occurs. Sensitivity analysis has shown that the DVR can respond effectively to change in various parameters and maintain a safe voltage level in the network that demonstrates the feasibility of applying DVR to network. The optimal location has been determined using the ANN approach, which is validated by comparing it with the results obtained from the SARFI approach.

3.5 Documentation and Presentation of the Findings

As per the guidelines of IOE, all the findings from the research works have been documented in the form of research papers and a formal thesis report.

CHAPTER FOUR: DVR MODELING AND SENSITIVITY ANALYSIS

4.1 Modeling of DVR

A proposed DVR system is modeled in Simulink environment and tested with a simple network to study the performance efficiency of the DVR and its suggested control to mitigate voltage sag/swell, as shown in Figure 4.1.

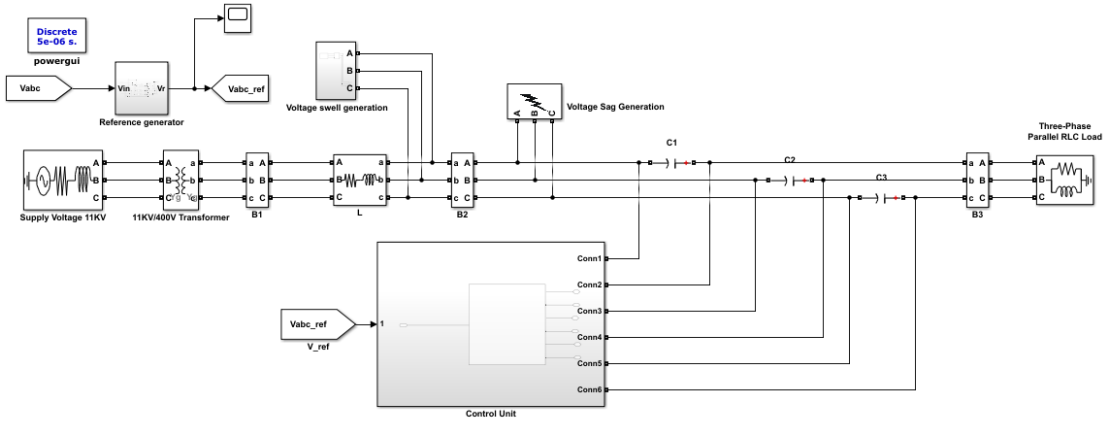

Figure 4.1: Simulink model of DVR connected system

The system has an 11 kV, 50 Hz three-phase source that feeds a line through an 11kV/0.4 kV, Y/Y transformer, which then supplies a three-phase load. The grid voltage is stepped down to 400 V to allow the utilization of low voltage sensitive load, and the system runs at 50 Hz frequency. Voltage sags are generated by simulating different faults between the source, and the load and voltage swell is externally simulated by superimposing three-phase voltages.

4.1.1 Parameters Design of DVR

i. Energy Storage Device

The energy storage device determines the power of the rating of DVR and the amount of voltage sag to be mitigated. The necessity of high voltage energy storage for high voltage systems makes DVR inappropriate for high voltage applications, the reason why DVR is extensively used at medium and low-voltage applications. Since the energy storage device for DVR is one of the most expensive components, it must be chosen with care.

First, the voltage level at which DVR has to be connected has to be considered then the level of mitigation desired for the voltage sag is determined, based on which the

minimum voltage rating for the energy storage device that meets the given requirement is selected. For our design, with a load of rating P=100kW and Q=5kVAR at 400V, an energy storage device of 400V has been selected to meet the requirement that the DVR compensates almost all magnitude of voltage sags possible in the system (ideally).

The load voltage requirement determines the DC voltage requirement for the energy storage of a DVR in a radial distribution network. In a radial distribution feeder operating at 11kV where it has been found that energy storage with a voltage rating of 5kV can effectively mitigate the voltage sag restoring the voltages at the buses above 0.97p.u. (Gupta, et al., 2010). However, this only gives a tentative measure for the sizing of the DC storage. Actual load distribution and system parameters must be considered while selecting the voltage level for the DC storage system. For 11kV systems, we have used a DC storage with a rated voltage of 6kV. For this, voltage sag mitigation by DVR was studied by increasing the voltage level of DC storage systems. For 5kV, 5.5kV and 6kV storage, there voltages were restored to 0.93p.u., 0.96p.u. and 0.99p.u. respectively. While increasing the voltage level to 6.5kV, there was voltage sag with voltage reaching up to 1.05 p.u. for the maximum of the faults simulated in the system. Thus, an optimal size of 6kV was selected for the voltage level of DC energy storage for both the 11kV radial distribution networks under study.

ii. Voltage Source Inverter

The selection of inverter mainly depends upon connection, power quality requirements, cost, gate drive speeds, and compatibility. MOSFET switches are easy to control and have the capability to work within a broad power range, the reason why MOSFET switches have been chosen in the converters. A simple inverter circuit for each phase has been incorporated using 4 MOSFETs, which are switched through a relay.

iii. Injection Transformer

In order to size the turn ratio (n) of a transformer, the desired injection level to the grid and the ability of the inverter to provide that injection level has to be taken into account. The selection of voltage ratings of the transformer must be made carefully underrating the transformer leads to core saturation, while overrating is also undesired because it adds unwanted extra costs. A detailed design of the series injection transformer for DVR applications has been presented in (Sasitharan, et al., 2008).

For our design, each phase has a 10KVA series injection transformer with a 1:1 ratio with each winding rated at 50V, and the windings have a resistance of 0.000002 p.u. and inductance of 0.0000008 p.u, this is for the operation of load at a rated voltage of 400V.

When DVR is operated at an 11kV system, the ratings of the transformer should be selected to meet the current and voltage requirement of both the grid, DC storage, and inverter. For 11kV systems used in the study, the MATLAB model of three single-phase transformers was used, with each transformer rated at 333kVA and with a transformation ratio of 3.46kV/6.35kV. A combination of these three single-phase transformers effectively interfaces the three-phase voltage generated by the combination of three single-phase inverters into the 11kV grid.

iv. Harmonic Filter

LC filters have been used in our model to get rid of high-frequency harmonic components from the voltage injected by the VSC. As a general rule of thumb, for a system where DVR has to be operated, inductor (L) should be selected to provide a high impedance path for high-frequency ripples and offers a low impedance path to the components at fundamental. Capacitance (C) should be chosen such that it behaves like a high pass filter with a cut-off comparable to around half of the inverter switching frequency. For our design requirement, the filters with values of L=1e-7H and C=4700µF were able to effectively filter out the ripples in inverter output, resulting in a sinusoidal output voltage that is fed to the load.

4.1.2 Reference Voltage Generation

The reference voltage generation block compares the desired load voltage with the actual voltage at the load terminal, and based on this; it gives the measure of the voltage to be injected/absorbed by the DVR and using this reference, the control of DVR is carried out to meet the desired level.

The circuit diagram for reference voltage generation for the control of voltage to be injected at all the three phases of DVR is shown in Figure 4.2. First, the information on the phase of the source voltage is taken through a PLL, assuming the frequency to be at 50 Hz. With this information the desired voltage $v_{peak}.\sin(wt)$ is generated for phase A, B and C, the desired voltage will be shifted by 120 degrees from each other.

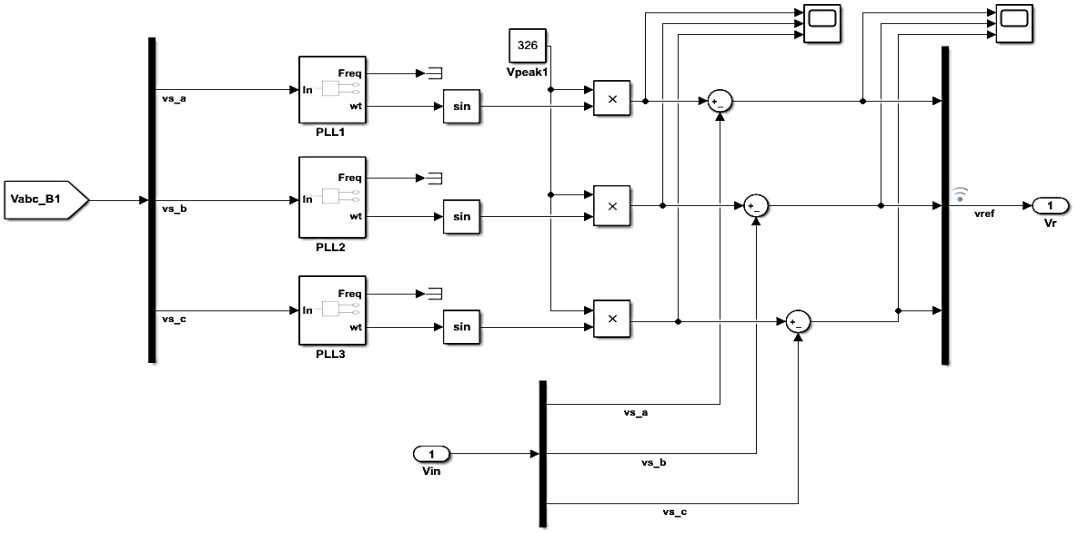

Figure 4.2: Reference generation

The voltage at load terminal, v_{in} is subtracted at each time form the desired voltages of each phase, and a three-phase reference voltage is generated, which is used in the control block. To bring back the voltage to the desired value, this value of reference voltage gives the proportional measure of the voltage to be injected/absorbed by DVR.

4.1.3 DVR Control Scheme

The design of the control system determines the efficacy of the DVR. The basic operational task of the control system in DVR is to detect an event of voltage sag/swell in the system and correspondingly compute the compensating voltage. It is achieved through switching of inverter in a controlled manner through gate pulses, followed by the correction in voltage injection dynamically with provision of complete termination to the injection process through effective switching off of the inverters through gate pulses after the disturbance no longer exists (Wijekoon, et al., 2003). A schematic diagram for controlling one of the phases of a three-phase DVR is shown in Figure 4.3.

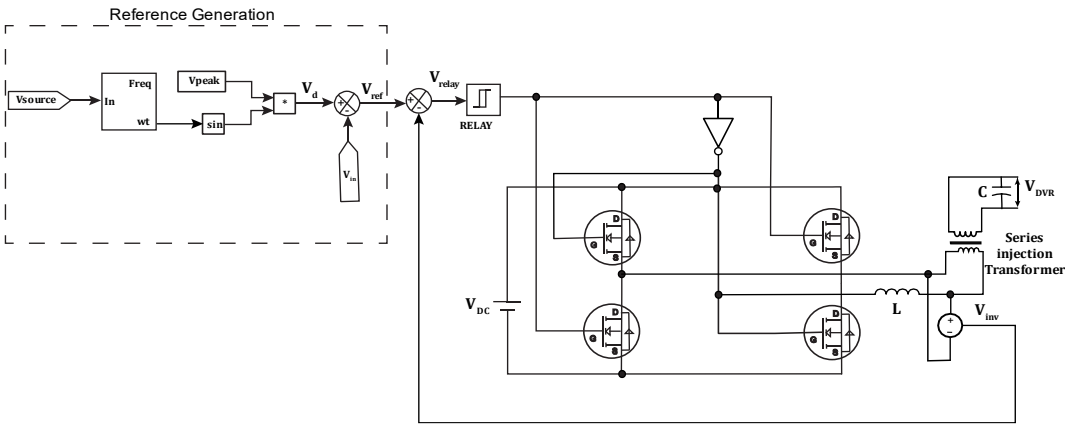

Figure 4.3: DVR Control Scheme

The reference generation block generates a reference signal by comparing the actual instantaneous load voltage with the desired voltage. The desired voltage is taken as the ideal source voltage during normal operating conditions.

If v_{peak} is the peak voltage of the source, then the desired voltage that the DVR tends to maintain at the load side is given by,

$$v_d = v_{peak}.\sin(wt) \qquad \text{Equation 4.1}$$

If v_{in} is the load voltage, then the reference voltage that the DVR uses for control is given by $v_{ref} = v_d - v_{in}$. This reference voltage is then the measure of the amount by which load voltage has sagged and provides information on the amount of power DVR needs to provide to control the load voltage. This v_{ref} is then compared with the voltage injected by the inverter, v_{inv} so that the input that goes to the relay is given by,

$$v_{relay} = v_{ref} - v_{inv} \qquad \text{Equation 4.2}$$

The output of the relay block switches between 1 and 0 depending on the difference $v_{ref} - v_{inv}$, such that,

$$relay\ output = \begin{cases} 1, if\ v_{ref} - v_{inv} \geq 0.1 \\ 0, if\ v_{ref} - v_{inv} < -0.1 \end{cases} \qquad \text{Equation 4.3}$$

This relay output is then used to switch the MOSFETs of the DC-source powered single-phase inverter. During fault on the line between the source and the load, the load voltage, v_{in} will undergo a sag and this sag in voltage gets reflected in the reference voltage as, by an increase in the value previously zero to an amount by which the voltage has undergone sag as $v_{ref} = v_d - v_{in}$ So when vin decreases v_{ref} will decrease. Under such circumstance, the input to the relay v_{relay} will also increase for a constant v_{inv} , and when v_{relay} goes above 0.1, the relay turns on and switches the MOSFETs through gate pulses, such that the inverter injects the voltage to match the reference signal. DVR keeps injecting the voltage until the voltage injected by DVR, restores the voltage v_{in} within a certain specified threshold value.

After the fault has been mitigated, v_{in} increases to its pre-fault value and the reference signal v_{ref} decreases become zero as the load voltage is the same as the desired voltage,

v_d. Under this situation, the input to the relay, v_{relay} decreases below the threshold value of -0.1 and this causes the relay to switch off thereby switching off the MOSFETs through gate pulses, and the DVR no longer injects the voltage into the grid and under this scenario $v_{inv} = 0$. Now both v_{ref} and v_{inv} have become zero, which means after the mitigation of the fault, DVR remains off until the next event when it needs to operate. In this way, the output of the DVR tracks the reference through a simple feedback control method.

4.2 Sensitivity Analysis

To demonstrate the viability of applying DVR to the network for different uncertainties of load and line length, sensitivity analysis has been performed. Sensitivity Analysis is a method to evaluate how the parameters and states of a model influence the output or certain design requirements. A simple process for conducting sensitivity analysis in a system is shown in Figure 4.4.

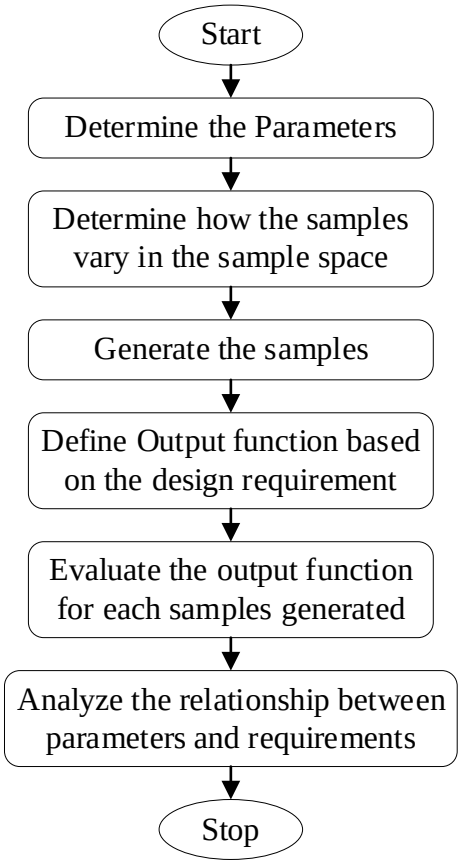

Figure 4.4: Flowchart for Sensitivity Analysis

The circuit diagram for studying the sensitivity analysis is shown in Figure 4.5, which shows DVR interconnected at node 1, which also supplies power to another node, node

2, right after it through a distribution line of length l. Sensitivity analysis for the modeled system, with one more load added after the node at which DVR is connected through a distribution line, has been performed using the MATLAB's sensitivity analyzer toolbox. Sensitivity analysis determines the certainty of the output voltage at node 2 to be maintained above 0.9 p.u. when DVR is installed in node 1 of the network and Monte Carlo based stochastic analysis has been used in order to study if the proposed model of DVR is actually able to improve the voltage profile for different uncertainties in the network.

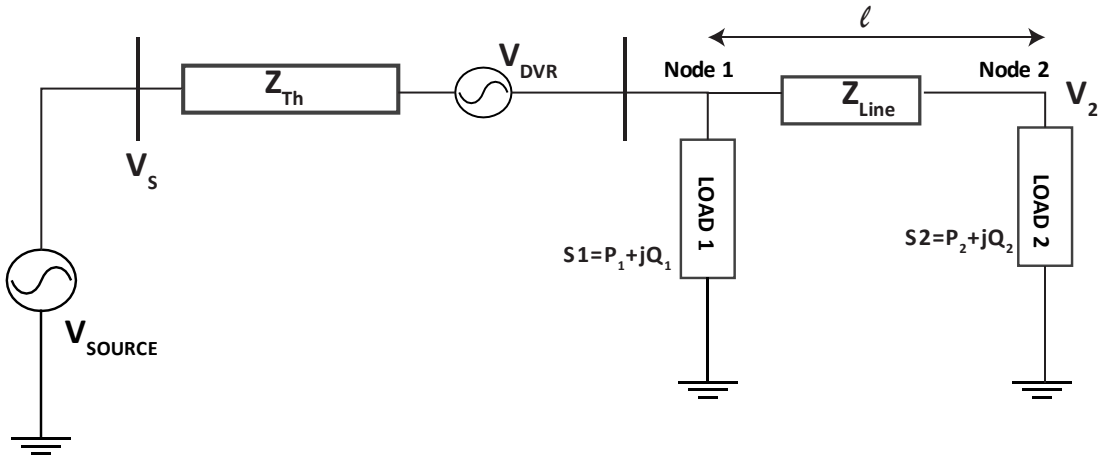

Figure 4.5: DVR connected with multiple loads

It is desired to study how the voltage at node 2, right after the DVR interconnection point, varies with different variations in system parameters. In this analysis, load complex power (S2) and the length of the distribution line (l) connecting the node at which DVR is connected to the node whose voltage is to be studied are taken as the system parameters that are to be varied during each simulation. Output function, which is the voltage at the node after the bus at which DVR is connected, is calculated from MATLAB simulation for these several pairs of randomly generated sample values.

Low voltage and medium voltage radial distribution networks are subjected to large variations in line lengths and load demand, which increases the haphazardness of the network. It is desired to see how the voltage in network behaves when there is random variation in the length of line segments and load demand. Stochastic analysis using MC simulation has been carried out to study this behavior. For the variation of the samples, the random normal distribution has been used for both the parameters to generate several pairs of sample values.

For the normal distribution of S and l , parameters are defined as shown in Table 4.1.

Table 4.1: Parameters for normal distribution

Parameter	Mean	Standard deviation
S (KVA)	140	30
l (m)	350	75

For each trial, the value of expected output voltage at the load terminal is given by:

$$\overline{V_j} = \frac{1}{N}\Sigma_{k=1}^{N} V_k \qquad \text{Equation 4.4}$$

Where, $k = 1,2,3,\cdots\cdots, N$

The variance of the output voltage at the load terminal is given by,

$$Var(V_j) = \frac{1}{N-1}\Sigma_{k=1}^{N}\left(V_k - \overline{V_j}\right)^2 \qquad \text{Equation 4.5}$$

Iterations are carried out until consecutive values of $\overline{V_j}$, $Var(V_j)$ and certainty of output voltage converges within the prespecified tolerance level. With N=10,000, MC simulations were done until the desired threshold was achieved for the convergence of $\overline{V_j}$, $Var(V_j)$ and certainty of output voltage remaining above 0.9p.u. Respective errors in the values of $Var(V_j)$ and certainties are given in the table.

Table 4.2: Convergence of the Monte Carlo Method for different no. of iterations

No. of iterations	2,000	5,000	**10,000**	20,000	30,000
$\overline{V_j}$	0.94	0.93	**0.93**	0.93	0.93
$Var(V_j)$	0.000667	0.00065	**0.000634**	0.000626	0.00063
$Var(V_j)$ % Error	5.157	1.942	**0**	1.191	0.588
Certainty	92.97	91.07	**90.84**	90.751	90.761
Certainty % Error	2.344	0.253	**0**	0.097	0.086

The table depicts that errors in variance and certainty that the voltage remains above 0.9p.u. do not change much even after increasing the sample trials above 10,000, thus N=10,000 was chosen as the stopping criteria.

CHAPTER FIVE: OPTIMAL PLACEMENT OF DVR

5.1 Test System Description

IEEE 15 bus test system

To validate the model of DVR, it is required to have its operation tested in a real test system that is able to replicate the behavior of an actual distribution network. One of the important reasons for using the model in test feeder is to have the proper representation of an actual real-world system so that we can have a much better approximation on how a developed model behaves while operating in the real-world distribution system.

For a distribution network, the following components give descriptive information about the system into consideration.

- Primary Voltage
- Network Length
- Number of loads/ buses
- Transformer size, i.e., maximum diversified demand

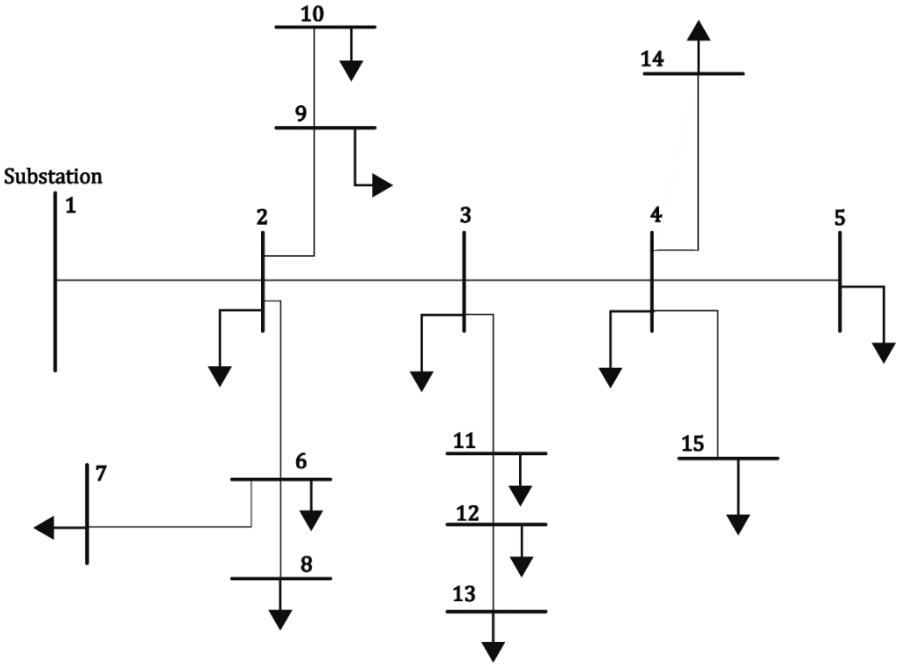

Figure 5.1: SLD of IEEE 15 bus system

For our test system, we have selected IEEE 15 bus test system, which has characteristics that closely align with typical radial distribution existing in Nepal. Operating at a

voltage of 11kV, the 15-bus system represents a highly loaded system with overhead distribution lines such characteristics are typical of distribution lines running in Nepal.

Single Line Diagram (SLD) of the IEEE 15 bus system is shown in figure 5.1, which is composed of 15 buses, including one generator bus and fourteen load buses. The system loads have a total real power demand of 1227kW and reactive power demand of 1251kVAR (Das, et al., 1995). Loads in these test systems are considered as constant PQ loads.

Case Study: Thimi- Sallaghari Radial Distribution System

To study the behavior of the DVR model in a typical Nepalese radial distribution system, a model of Thimi-Sallaghari radial distribution system under operation in Bhaktapur, Nepal, is taken. The distribution system is drawn from the 11/11 KV Thimi switching station.

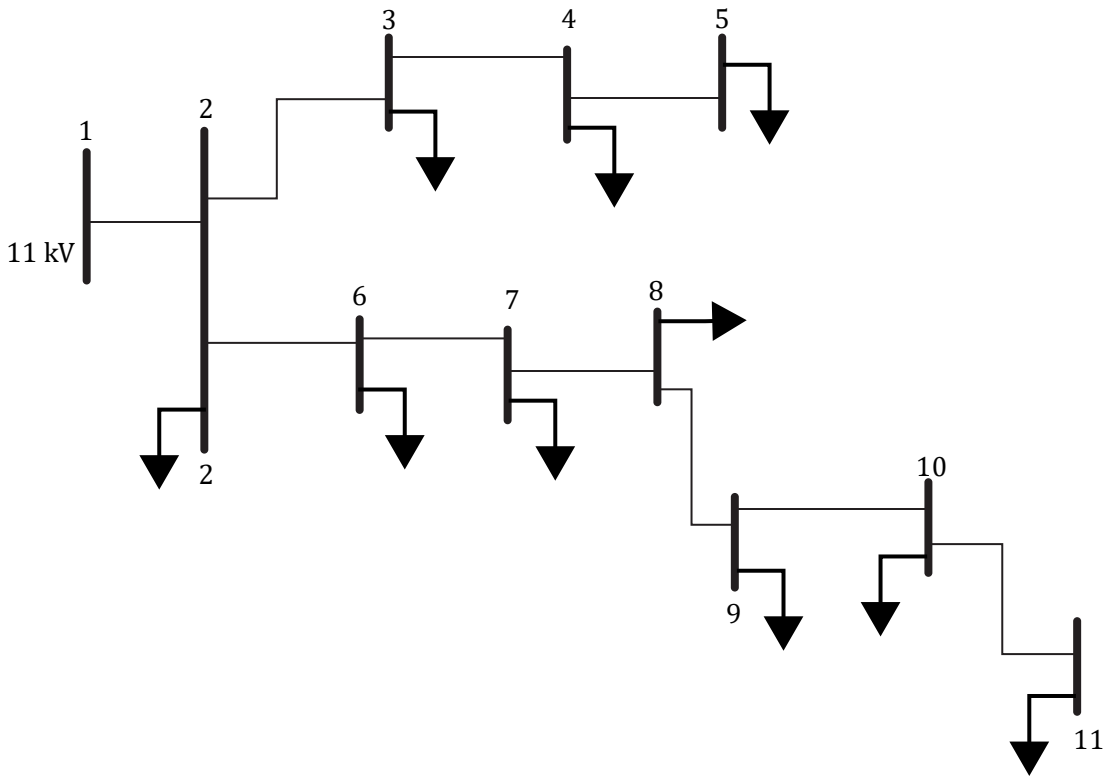

Figure 5.2: SLD of Thimi-Sallaghari distribution system

As seen from the SLD of the distribution system in Figure 5.2, it consists of 11 buses composed of one generator bus and ten load buses. The system has a net real power demand of 1103 kW and reactive power demand of 1116kVAR (Regmi, 2017). For the

purpose of study, all loads are considered to be PQ loads, which remains valid for most of the domestic and industrial load under operation as a high proportion of existing loads are PQ loads in a typical distribution system.

5.2 Modeling and Fault Analysis of Test System

The simulation model for a network has been built, and the short-circuit analysis of the test systems has been performed under various faulted conditions using MATLAB SIMULINK environment. All four types of faults Single Line to Ground (SLG), Line-to-Line (LL), Line to Line to Ground(LLG), and three-phase balanced(3Φ) faults have been simulated in the modeled system with different possible fault resistances to have a comparative study on the bus voltages during the fault and pre-fault condition.

According to the purpose of the study, IEEE 15 bus system and Thimi-Sallaghari radial distribution system have been designed under MATLAB/SIMULINK platform by using the value obtained. The developed models have been analyzed by conducting Fault studies on them, and the time domain simulations have been done. After the system was modeled, tests were carried out by simulating all possible faults at different locations of the system. During a fault, the line currents and voltages are governed by the transient response of an RL circuit where the fault current rises with a dc offset that dies exponentially while the voltages experience transients for up to a few cycles depending on the fault location and fault resistance. Fault resistance was set for 1 ohm, and ground resistance was set for 0.01 ohm for ground faulted trials.

Phase-A of faulted phase in the “three-phase fault” module and “ground fault” has been selected for LG fault. Similarly, both phases, A and B phases of the faulted phase in the “three-phase fault” module have been selected for LL fault, the two phases, A and B phases of the fault phase in the “three-phase fault” module and “Ground Fault” has been selected for LLG fault, and the corresponding A, B and C phases in the “three-phase fault” module and “Ground Fault” has been selected for LLLG fault. Different faults were created in each bus for a duration of 100ms, and the voltage profile of each bus under these faulted conditions was recorded.

The main purpose of this analysis is to have a large set of data on the variation of bus voltages at the event of a fault, which could then be used in the training of neural networks to predict the most vulnerable bus in the system.

5.3 Optimal location based on ANN approach

A neural network fitting tool has been used to build the ANN, which makes it very easy for data selection, creation, training, analysis, and evaluation using mean square error (MSE) (Beale, et al., 2010).

Building of ANN

Feedforward neural network (FFNN) has been built using the input train data set and target data set. During the process of training data development, it is desired that the data represents all possible situations under which ANN has to perform. The magnitudes of after-fault voltages were only considered for all the buses to obtain the input data, and The target data output of ANN was set as 0 or 1 based in the fault condition. For IEEE 15 bus system, the training data and target data is a 14*168 matrix that represents 168 samples of 14 elements, and for the case study of Thimi-Sallaghari radial distribution system, the input and output data both are 10*120 matrices that represent 120 samples of 10 elements.

After determining inputs and target outputs, FFNN was created using input, output, and hidden layers where input data and target outputs are arranged in the layered feed-forward arrangement. Tan sigmoid and purelin functions respectively are used by the hidden layer and output layer. It is important that the samples be categorized into training, testing, and validation samples before the testing.

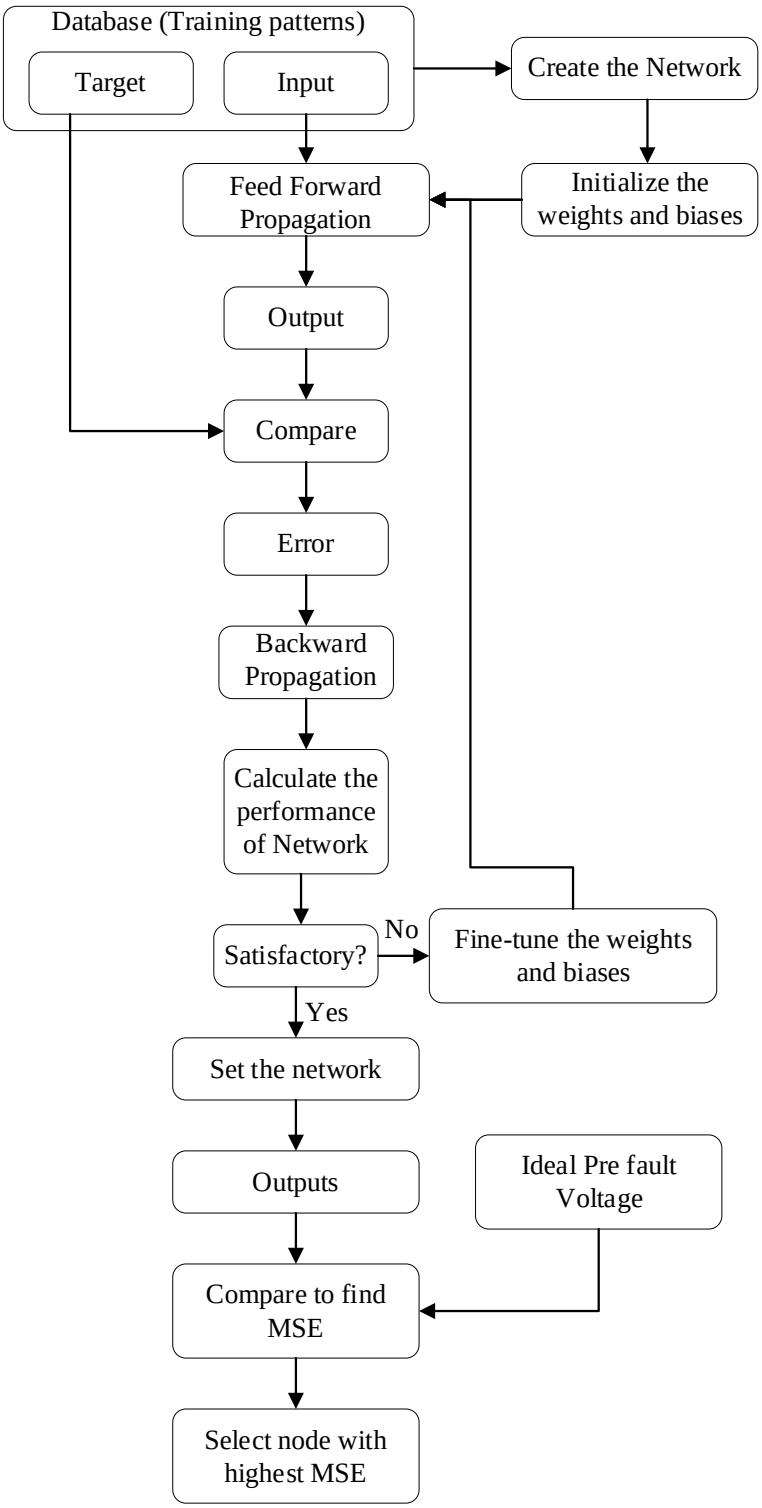

Figure 5.3: Flowchart of ANN implementation

Training of ANN

Training of neural networks requires a large set of data categorized mainly as training dataset and output target dataset, which basically act as input-output pairs that go into the networks. In ANN optimization, the objective function is the mean square error

function. Initially, weights are chosen randomly, and the error rate obtained in the previous iteration determines the tuning of the weights. It is required to have properly tuned weights to ensure lower rates of error, which in turn make the model more reliable and effective. In the present work, one of the fastest backpropagation algorithms—Levenberg Marquardt backpropagation has been used to update the weight and bias on the basis of Levenberg Marquardt based optimization.

The Levenberg-Marquardt algorithm provides high training and computation speed (Beale, et al., 2010). When a performance function has been designed as a sum of squares, the Hessian matrix can be computed as (Zayani, et al., 2008)

$$H=J^T J \qquad \text{Equation 5.1}$$

Then the gradient is given by,

$$g= J^T e \qquad \text{Equation 5.2}$$

In the above equations, J is the Jacobian matrix comprising of terms with derivatives of error with respect to weights and biases. In equation 5.2, e is a vector representing errors.

Similar to how Jacobian behaves in Newton Raphson's method, the Levenberg-Marquardt algorithm also uses the same approximation to Hessian matrix (Beale, et al., 2010)

$$x_{m+1}= x_m - [J^T J + \lambda I]^{-1} J^T e \qquad \text{Equation 5.3}$$

Here, λ, a scalar, plays a significant role in controlling the behavior of the algorithm. With $\lambda = 0$, the algorithm follows Newton's method, while with a higher value of λ the algorithm becomes gradient descent having a small step size. Thus, when performance is reduced, λ has a lower value. However, when a tentative step increases the performance function, λ has a higher value. In this way, performance function is reduced at each epoch.

In order to determine the performance of the Levenberg-Marquardt feedforward network, mean square error (MSE) is calculated as:

$$\text{MSE}=\frac{1}{n}\sum_{i}^{n}(y_i-\hat{y}_i)^2 \qquad \text{Equation 5.4}$$

where y_i and $\hat{y}_i$ are desired output and actual output, respectively.

$$y=\min f=\text{minimize (MSE)} \qquad \text{Equation 5.5}$$

In order to choose the final architecture for the given input and output, training performance has been evaluated.

Table 5.1: Parameters and Performance of ANN model

Parameters	**IEEE-15 bus system**	**Thimi-Sallaghari distribution system**
No. of training data	168 samples	120 samples
No. of hidden neurons	18	13
Learning Algorithm	LM (trainlm)	LM (trainlm)
Performance function	Mean Square Error (MSE)	Mean Square Error (MSE)
Activation function (hidden layer)	tan sigmoid	tan sigmoid
Activation function (output layer)	Purelin	Purelin
Training Performance (MSE)	2.91e-04	1.471e-06

For both cases, satisfactory training performance has been found after the completion of the training of the network, and hence neural network is selected as final architecture. The training of the chosen network gives output matrices. For all the load buses, mean squared deviations of the voltages of various buses from their pre-fault values were calculated, which provides the most vulnerable bus of the system.

5.4 Validation of Optimal location

For the validation of results, optimal location based on the approach of finding the minimum value of SARFI (System Average RMS Frequency Index) of the system in the presence of DVR has been determined. In the test systems we have used—Thimi-Sallaghari radial distribution network and IEEE-15 bus system, the performance of DVR for global sag mitigation will be tested based on SARFI, and the optimal location

will be the one for which SARFI comes out minimum for a different combination of DVR placement along with faults at all possible buses in the system.

With this approach, the objective is to minimize the SARFI for the system, which is given by,

$$SARFI_X = \frac{\sum_{i=1}^{n} n_i x}{n} \qquad \text{Equation 5.6}$$

Where,

X=RMS voltage threshold

$n_i x$=number of voltage sags below a prespecified threshold value

n= total connected loads (assuming all buses in the system)

The objective function is then given by,

$$y = min(SARFI_X) = min\left(\frac{\sum_{i=1}^{n} n_i . x}{n}\right) \qquad \text{Equation 5.7}$$

While finding the optimal location using $SARFI_X$, the cost for power quality investment is neglected along with the assumption that DVR has limited power injection capability.

For our study, we have set the sag threshold X as 0.9 or 90%, which indicates that we compute the system average sag frequency based on the number of buses whose voltages go below 0.9 p.u. or 90% of the nominal threshold value during a fault. Some of the assumption made while carrying out the optimization process are as follows:

- Placement of only one DVR is considered
- A three-phase balanced fault has been considered for all cases
- The fault rate distribution is taken as uniform, and the rate is taken as 1, that is for the period of simulation only one fault occurs in the system

The stepwise process to be followed in the optimization process which involves a large set of simulations with faults simulated at different buses with a different combination of DVR at different locations is shown in the flowchart of Figure 5.4

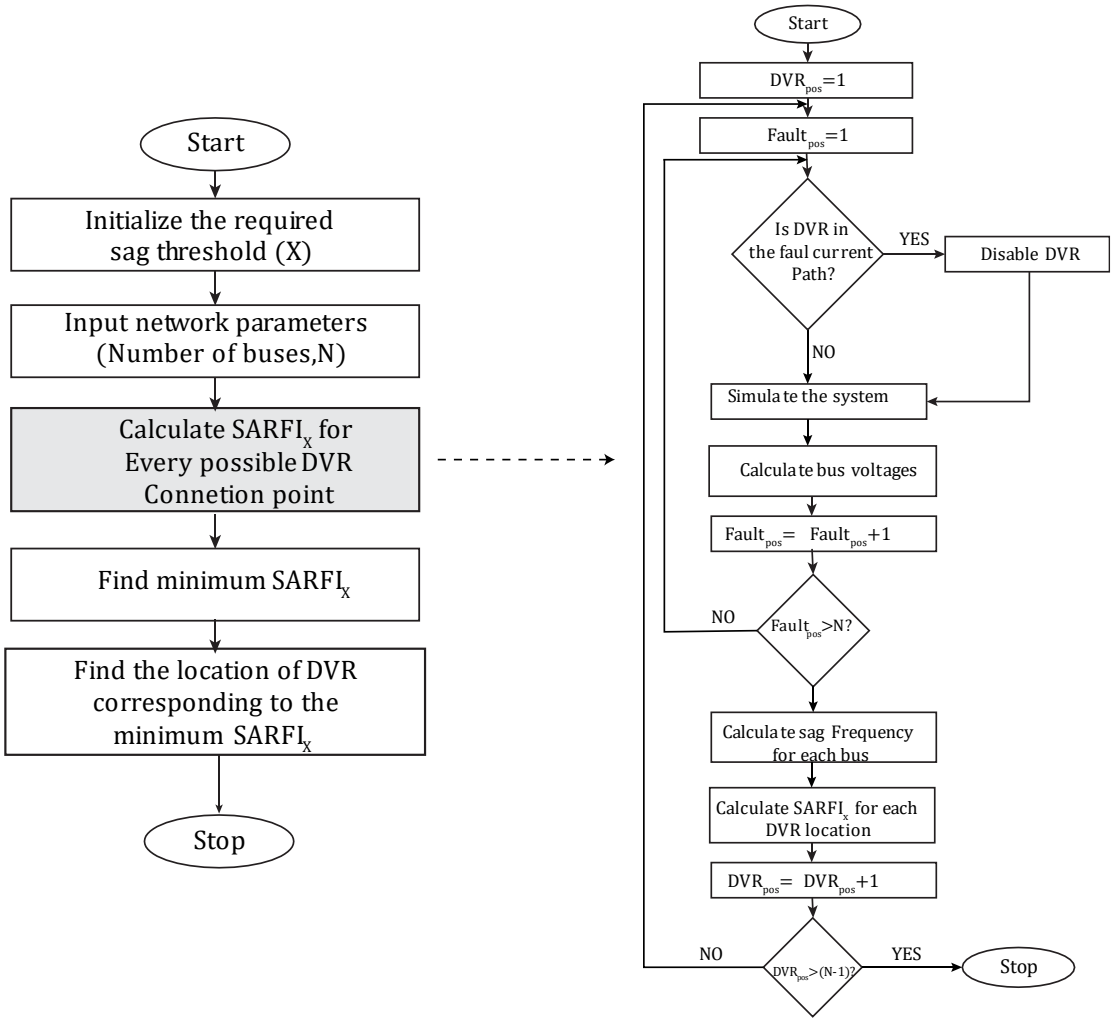

Figure 5.4: Flowchart for the Optimization process using SARFI

The left flowchart shows the stepwise details of the optimization process while the flowchart in the right shows the stepwise process to be followed while computing the SARFI index through by using MATLAB simulation.

CHAPTER SIX: RESULT AND DISCUSSION

6.1 Voltage Sag/ Swell Mitigation by DVR

6.1.1 Compensation of Balanced Voltage Sag and Swell

Independent operation of the developed DVR model was studied by simulating a three-phase balanced fault in the system for a duration of 0.1second from t=0.2 to t=0.3s to simulate voltage sag across the load where the load voltage will be decreased to 70% of its normal as shown in figure 6.1. Voltage swell was also simulated by injecting voltage externally, which is initiated at t=0.4 s up to t=0.5s. And the system voltage during that time rose to 145% of the nominal value.

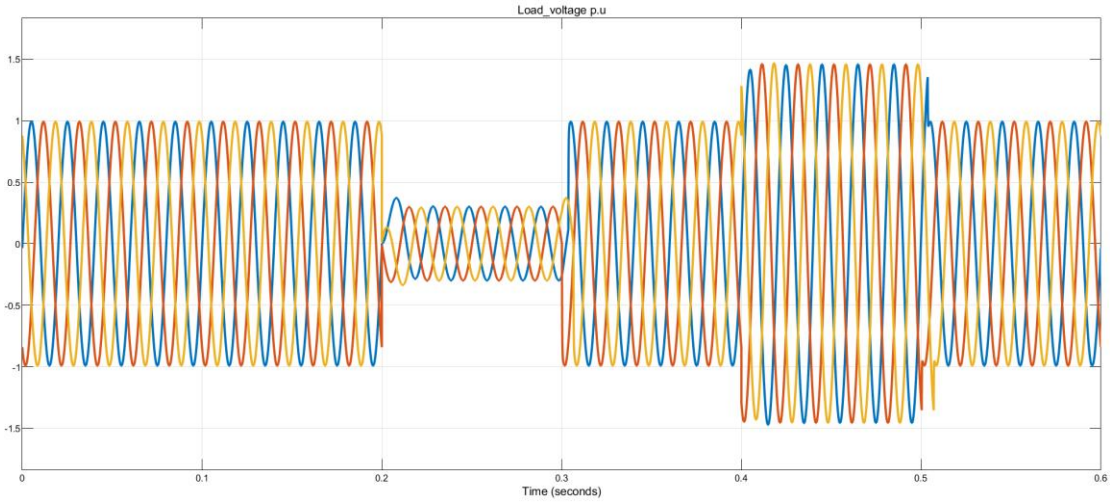

Figure 6.1: Load Voltage (without DVR) for a 3-phase fault

The system was then operated in the presence of DVR in series with a distribution line feeding a load. Figure 6.2 shows the events after the installation of the DVR. The first figure shows the source voltage during a fault (voltage sag), the second figure shows that the load voltage after DVR has compensated the voltage sag. It can be clearly observed that when the source voltage sags from t=0.2 to 0.3 s and swells from t= 0.4 to 0.5 s, DVR has either injected or absorbed the power for a constant voltage across the load terminal. The third figure in Figure 6.2 shows the profile of power injection and absorption by the DVR. From the third figure, it can be seen that the DVR has injected voltage (power) into the load from t=0.2s to t=0.3s for voltage sag whereas, DVR has absorbed the excess voltage from t=0.4s to 0.5s for voltage swell. It is seen that the injected voltage by DVR, during sag/swell varies to bring back the load voltage

to a safe operating level from any deviated values. There is no power exchange between DVR and the load unless there is a sag/swell in the load voltage.

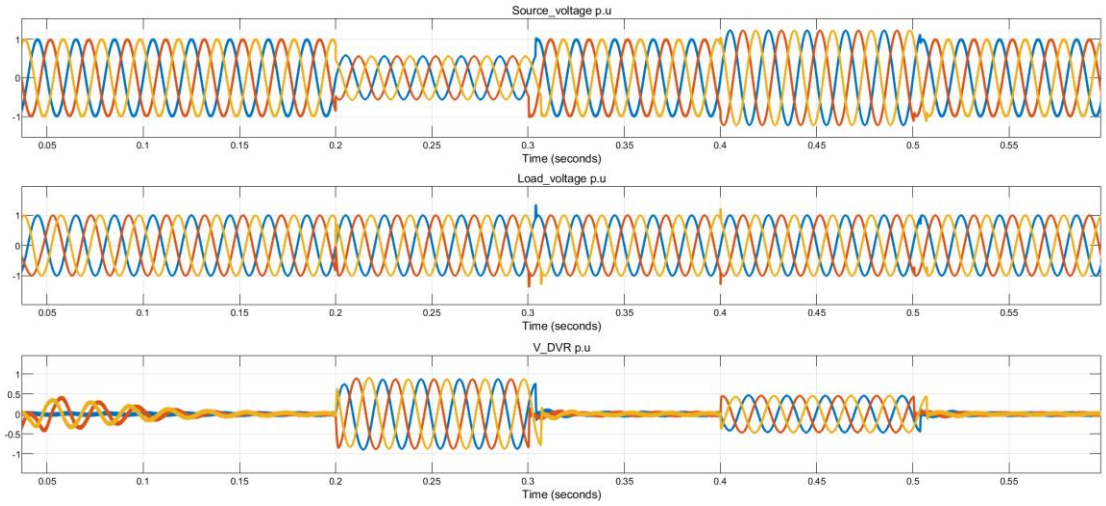

Figure 6.2: Bus Voltage with DVR a) Source Voltage b) Load Voltage c) DVR injected Voltage

It has been shown that the developed DVR model mitigates balanced voltage sags and swells occurring in the load, even when the source side voltage has sagged.

6.1.2 Compensation of Unbalanced Voltage Sag and Swell

Balanced faults are the least occurring events in power systems, with unbalanced fault unbalanced faults occurring for more than 95% of the time. Among different faults, Single Line to Ground (SLG) faults are the most frequent– responsible for almost 80% of the total number of faults. It is important that the modeled DVR is able to compensate for the unbalanced voltage sags during SLG faults occurring in the systems.

For this, an unbalanced fault (SLG) fault has been simulated for the time duration of 0.2 s to 0.3 s, and an unbalanced voltage swell is also simulated by superimposing single-phase voltage into the network for the duration of 0.4 s to 0.5 s. Waveforms of load voltage under this unbalanced fault show that Phase A has decreased to 10% of its normal operating voltage while the phases B and C are still healthy. An unbalanced voltage swell was simulated by superimposing single-phase voltage in one of the phases in the network for the duration of 0.4 to 0.5 s during which phase A voltage swell to 145% of the normal operating voltage.

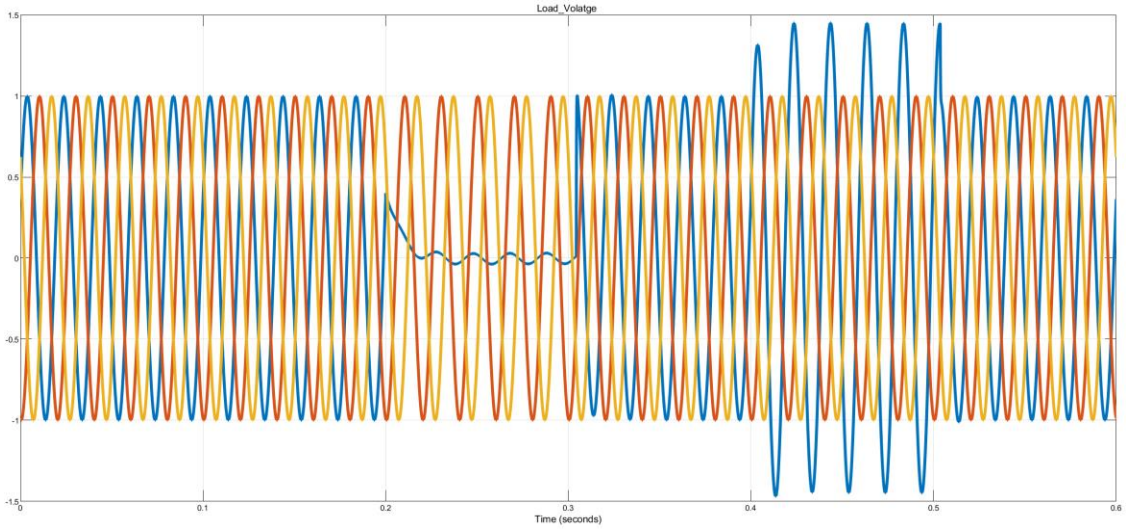

Figure 6.3: Load Voltage (without DVR) for an SLG fault

The second and the third part of Figure 6.4 show the injected voltage by DVR for load voltage compensation and the voltage at the load terminal after compensation from DVR. It can be clearly observed that when the source voltage sags from t=0.2 to 0.3 s and swells from t= 0.4 to 0.5 s, DVR has injected voltage for phase A from t=0.2s to t=0.3s whereas, DVR has absorbed the excess voltage from phase A and B from t=0.4s to 0.5s. It can be seen that the voltage injected by the DVR in phase A during swell is 180 degrees out of phase with the voltage injected by the DVR during the sag period, indicating that the DVR has absorbed the excess voltage from the load during the sag period.

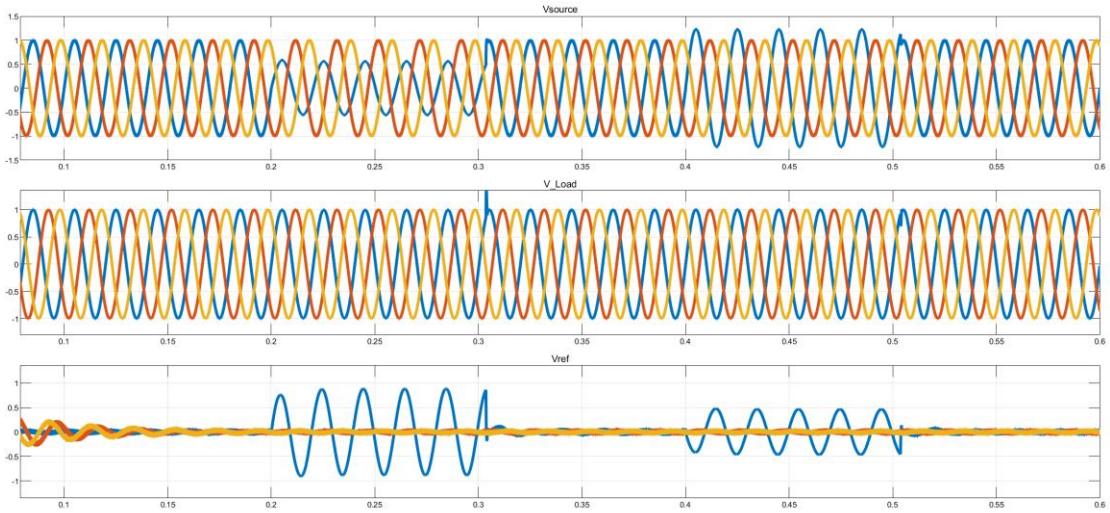

Figure 6.4: Bus Voltage with DVR a) Source Voltage b) Load Voltage c) DVR injected Voltage

It has been shown that the developed DVR model is able to mitigate unbalanced voltage sags and swells occurring in the load, even when the source side voltage has sagged. This model is tested in different radial distribution systems, to effectively restore the voltages in the system buses under certain undesired events.

6.2 Sensitivity Analysis

One of the main ideas behind carrying out sensitivity analysis is to find various system parameters that have the highest impact on the output voltage of the system, this relation between parameters and output is best defined by the correlation coefficient from which we can infer the magnitude and direction of the input-output relationship.

This correlation between the parameters and output voltage can be studied by generating some statistical data from sensitivity analysis. Correlation of input parameters– load power demand (S) and distribution line length (l) was carried out using data from sensitivity analysis. The result of input-output correlation is shown in Figure 6.5, which clearly indicates a negative correlation between the output and both the input parameters, suggesting an obvious fact that the output voltage reduces with increasing load power demand and line length.

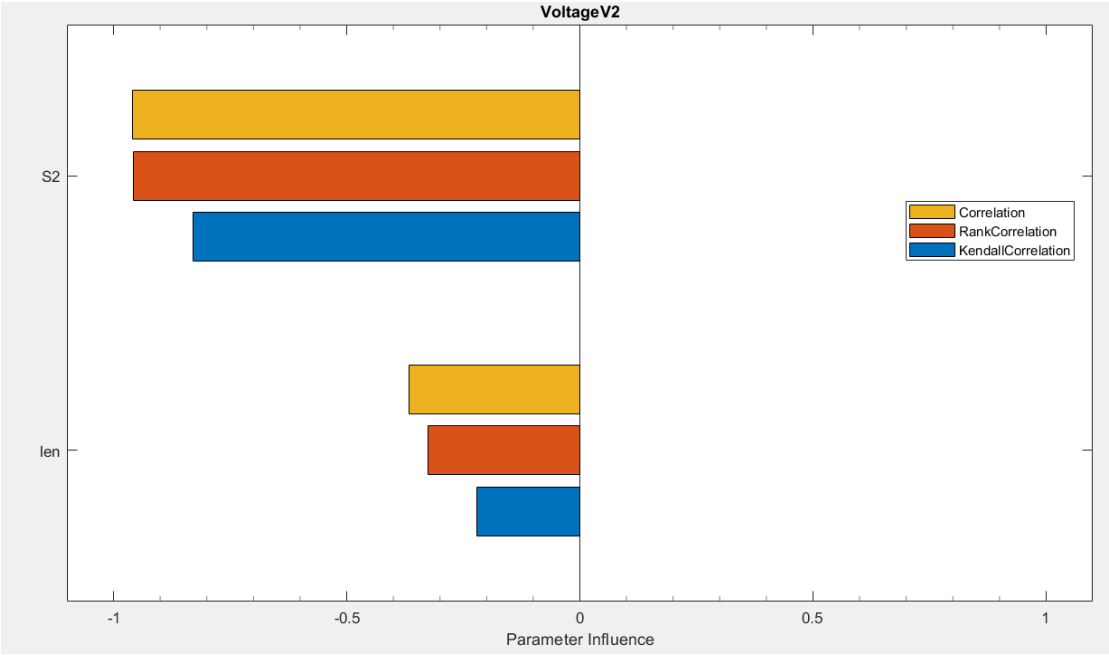

Figure 6.5: Correlation between output voltage and input parameters

Power Demand of the load (S) has a very high correlation coefficient to the output for all three different correlations studied, which is an indication that output voltage (V2)

is most influenced by the load power demand by the load when compared to the line length. The correlation of load power with the output voltage (V2) is around -0.9, while that of line length is around -0.4 to be exact, suggesting that we must be more cautious while altering the load so that the load voltage does not fall below the safe operating range.

After figuring out the parameters that have the most impact on the output, it is desired to see how the developed model behaves under the scenario of random variation of those parameters. The variation of the input parameters over a range was chosen based upon the knowledge of typical values of load demand and line length in an 11kV distribution feeder. MC simulation was run by creating 10000 different samples with parameters as discussed in table 4.1, based on this a probability distribution of the output voltage over the range of variation of those values generated to verify the working of the developed model under different operational variations.

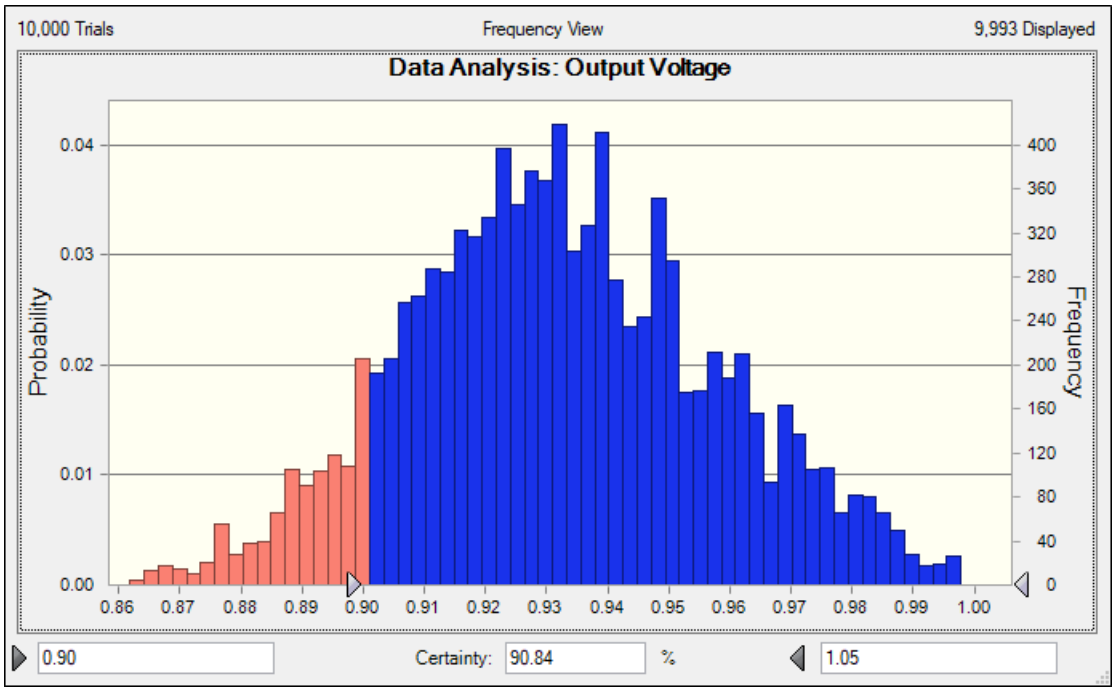

Figure 6.6: Probability distribution of Output Voltage V2

The probability distribution of the evaluated output function is shown in Figure 6.6, which indicates a huge proportion of the sample (more than 90%) having voltage above 0.9 p.u. From the histogram, the probability that the output voltage remains above 0.9 p.u. is 90.84%. Since for most of the randomized sample simulations, the voltage at the node right next to DVR, during the fault period, still remains above 0.9p.u. It can be said that the model of DVR can be used for a different range of loads and distances of

loads from the DVR. It must be noted that the output voltages are taken during the faulted period, and DVR being able to maintain a safe voltage level at the load bus for most of the simulated cases show that the model is well suited for changes in loads and different load distribution in a distribution network.

6.3 Optimal Location of DVR

IEEE 15 bus system and Thimi-Sallaghari radial feeder have been modeled in MATLAB/SIMULINK environment, and the same model has been simulated for different faults scenario and the values of the post fault voltages were measured and were provided to the neural networks as inputs and output target data were considered as 0 or 1 based on fault condition. This developed model was then trained in order to obtain error and output matrices. For all the load buses, average squared deviations of output from the pre-fault value were calculated to have the information about the bus that is most prone to voltage deviations.

IEEE 15 bus test system

Following the procedure of optimization, it was observed that bus-3 had the highest value of MSE, making it the most vulnerable bus. Figure 6.7 shows the distribution of MSE in the buses of the 15-bus system during the state of minimum MSE of the system. It can be clearly seen that, without placement of DVR when the system has minimum MSE, the largest MSE among all the system buses is at bus 3 making bus 3 the most vulnerable. It shows that the DVR has to be connected with the power being injected to bus 3, so that the system will operate with minimum MSE possible for a given operation. However, there exist multiple lines where DVR could be placed with power being injected into bus 3. With simulation studies done with DVR present in all possible lines connected to bus 3 it was observed that the performance of DVR for mitigation of voltage sag was most effective with it being in the line 2-3. As a result, line 2-3, in IEEE 15 bus system was chosen as the optimal location.

The maximum vulnerability of a bus in the system can be attributed to its location in the system along with the load distribution such that for most of the faults in the system, the vulnerable bus lies in the fault current-carrying path as a result has maximum value for its voltage deviation from the rated voltage.

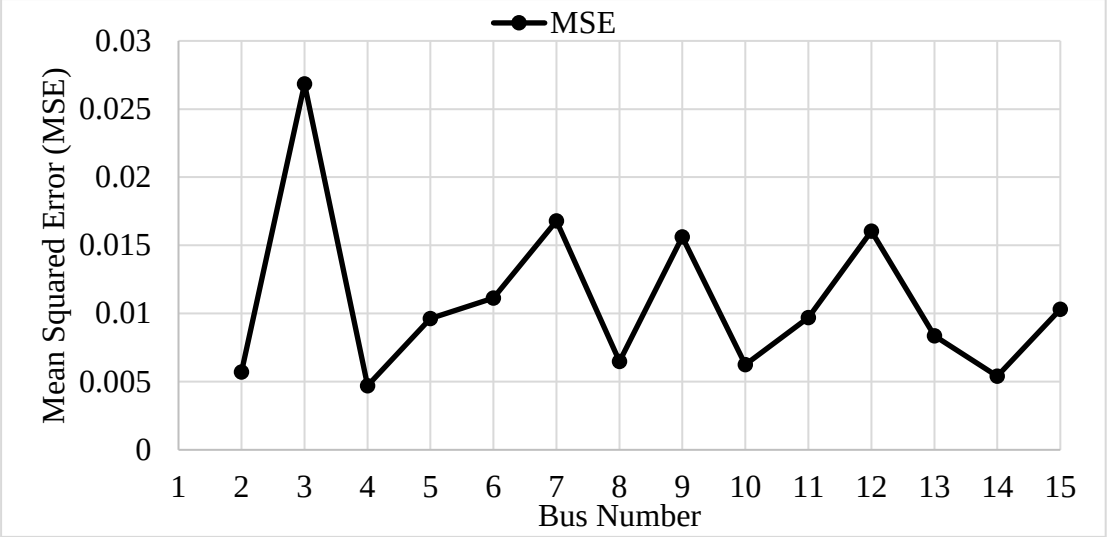

Figure 6.7: MSE at different buses of the IEEE-15 bus system

Case Study: Thimi-Sallaghari radial distribution system

Like the IEEE-15 bus test system, optimization was carried out in Thimi-Sallaghari 11-bus radial distribution network, such with the same procedure. Since the DVR needs to be connected such that it supplies power into the most vulnerable bus, it must be connected in one of the lines connecting bus 6. With simulation studies done with DVR present in all possible lines connected to bus 6 it was observed that the performance of DVR for mitigation of voltage sag was most effective with it being in line 2-6. As a result, line 2-6, in Thimi-Sallaghari radial distribution system, was chosen as the optimal location.

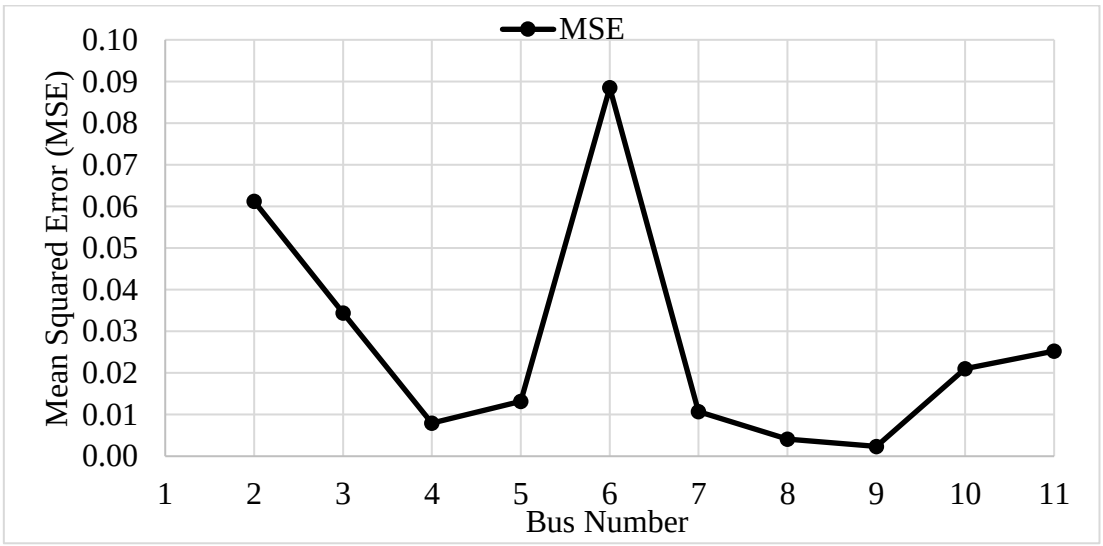

Figure 6.8: MSE at different buses for 11 bus system

Figure 6.8 illustrates the plot of MSE of all the buses in Thimi-Sallaghari 11 bus radial distribution system during the state of minimum MSE of the system. It can be clearly

seen that, without placement of DVR when the system has minimum MSE, the largest MSE among all the system buses is at bus 6, making bus 6 most affected by system voltage deviation. Since the DVR needs to be connected such that it supplies power into the most vulnerable bus, it must be connected in one of the lines connecting bus 6. With simulation studies done with DVR present in all possible lines connected to bus 6 it was observed that the performance of DVR for mitigation of voltage sag was most effective with it being in line 2-6. As a result, line 2-6, in Thimi-Sallaghari radial distribution system, was chosen as the optimal location

6.4 Placement of DVR at Optimal Location

IEEE 15 bus test system

To study the behavior of DVR when placed at the optimal location, and also to verify the result obtained for optimal location, DVR was placed in the line 2-3 and operated under the different faulted scenario. A balanced three-phase fault was simulated, for a period of 0.1s, at bus 2, from t=0.2s to t=0.3s. When a fault occurs in bus 2, the bus voltages in the other healthy buses also undergo sag. It can be seen from Figure 6.10 that all the buses that originate radially from bus-3 have felt the effect of the fault in bus-2, and a significant amount of voltage sag was observed in the buses going radially after bus-3 where the voltage has reduced to less than 0.4 p.u. This voltage level is not acceptable for the operation of loads in those buses and can cause severe malfunctioning of the loads. In order to mitigate this, DVR hast to be placed in the system so that bus voltages can be restored back to a safe operating range during the faulted period. With the placement of DVR at an optimal location, simulations were carried out during the faulted scenario.

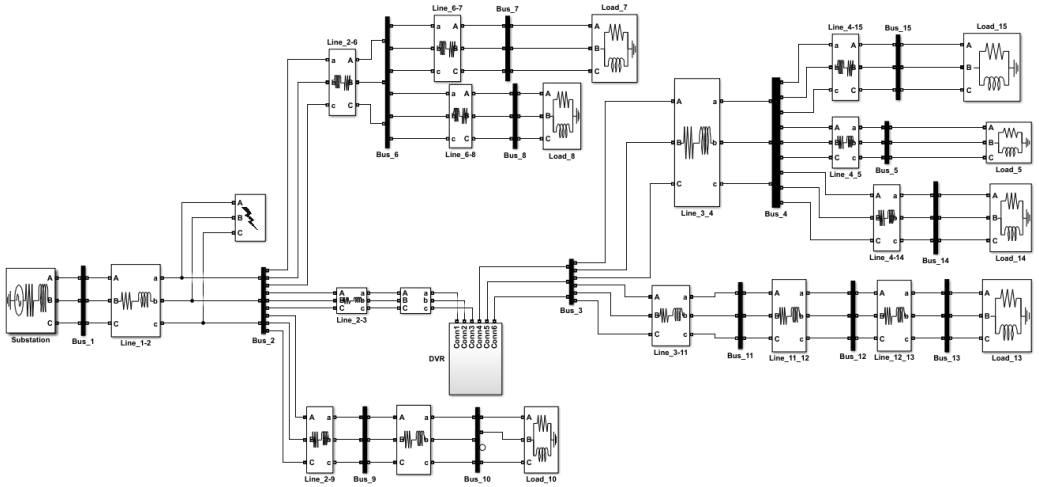

Figure 6.9: Simulink model of IEEE 15bus with DVR at line 2-3

The voltage profiles of the buses, going radially outwards from the line 2-3, where DVR was placed are illustrated in Figure 6.11. Also, from Figure 6.10 and Figure 6.11, it can be seen that, during a faulted scenario in the system, with optimal placement of DVR, bus voltages have been restored to their pre-fault condition.

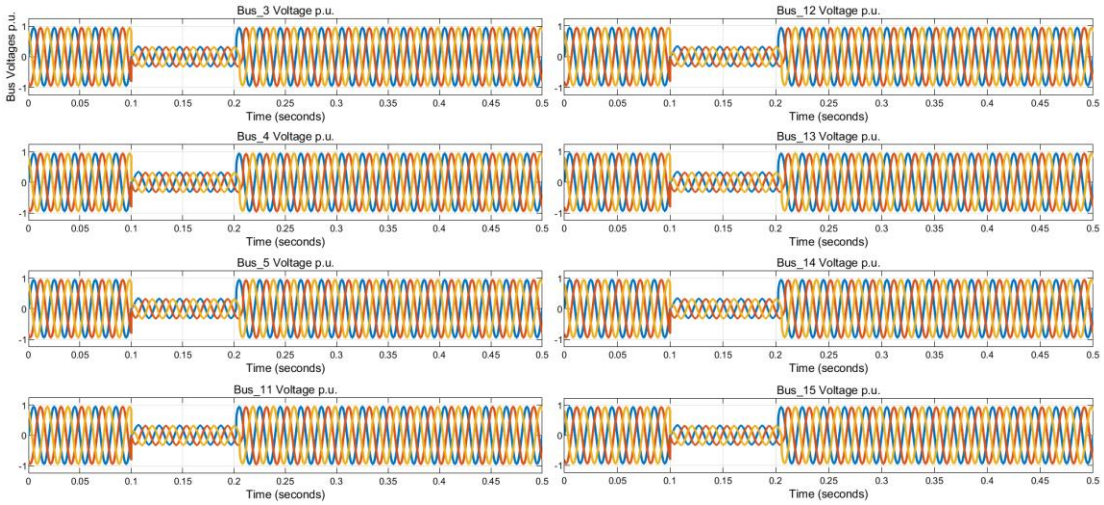

Figure 6.10: Bus voltages in p.u. with fault in bus 2 (without DVR)

In fact, we can also observe that the pre-fault voltages of the buses going radially after bus 3 are in the range of 0.97 p.u in bus-3 and reducing up to 0.94p.u. in bus-5 and bus-14 as expected in a radial distribution system. However, when DVR is at optimal location, not only has the post fault voltage been restored back, but also the pre-fault bus voltages without DVR have also been improved with bus 3 having its voltage almost 1 p.u. and voltage profile at other buses are also improved significantly.

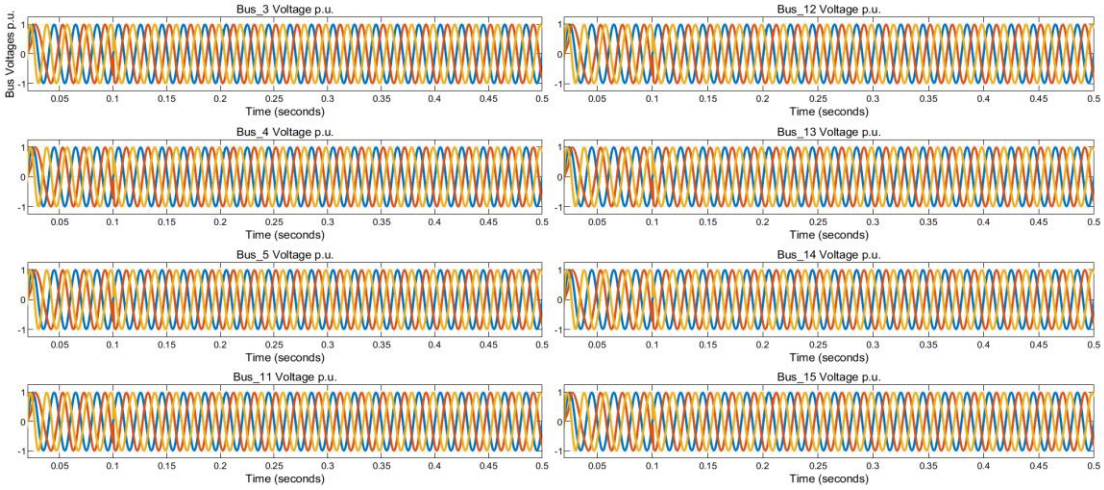

Figure 6.11: Bus voltages in p.u. with fault in bus 2 (with DVR in line 2-3)

The comparison of the pre-fault voltage, fault voltage, and restored voltages in the buses that lie radially outwards of the optimal location in the 15-bus system is depicted in Figure 6.12. It has to be noted that DVR is a series-connected device and has a

unidirectional power flow and hence can mitigate the voltage sags at buses that occur after it in the system. From Figure 6.12, we can observe that voltage profiles of the buses after DVR interconnected node show a significant improvement of voltage profile during a fault in the system with voltages being restored from around 0.35 p.u. to more than 0.95 p.u. even for the bus farthest from the DVR interconnection point.

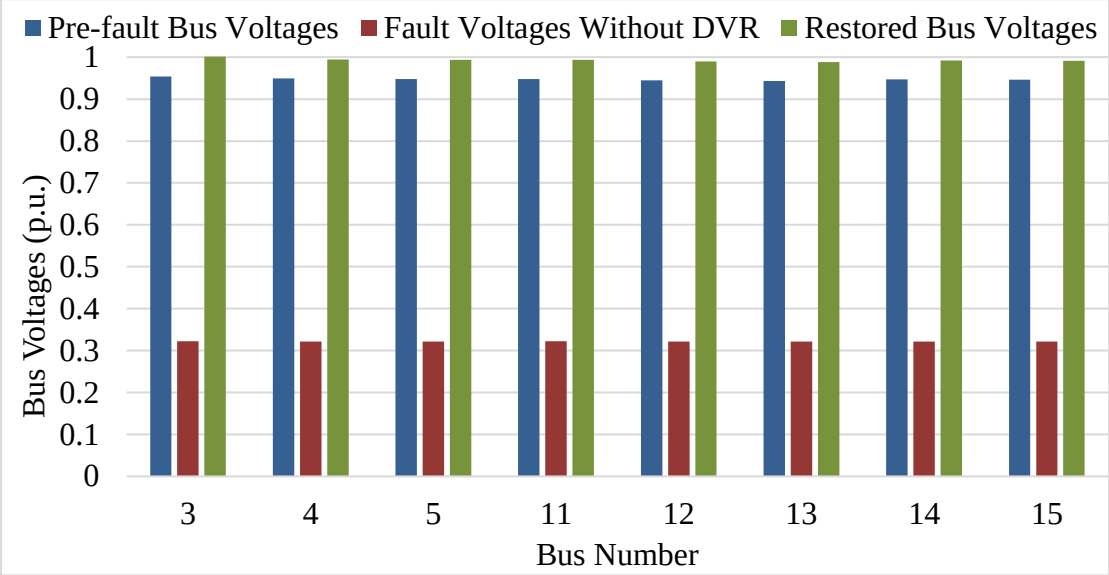

Figure 6.12: Voltage profile of different buses in 15 bus system

Case Study: Thimi-Sallaghari radial distribution system

Like 15 bus system, for the validation of the results obtained for optimal location, DVR was placed in the line 2-6 and operated under different faulted scenario. Simulink model of 11 bus system with DVR at optimal location is shown in Figure 6.13.

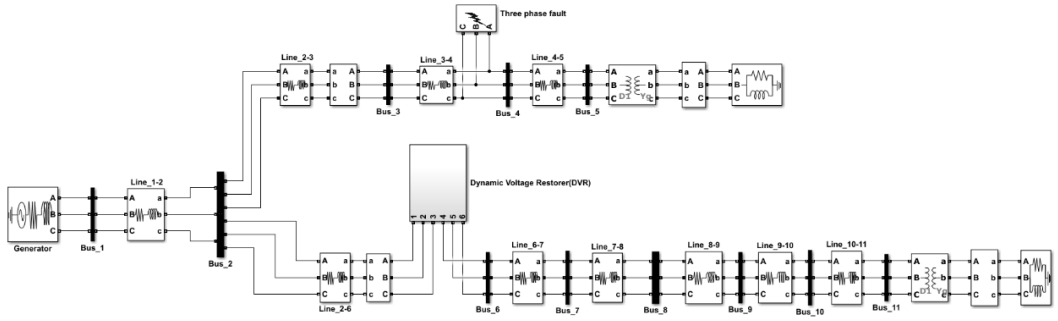

Figure 6.13: Simulink model of Thimi-Sallaghari distribution system with DVR at line 2-6

A balanced three-phase fault was simulated, for a period of 0.1s, at bus 4, from t=0.2s to t=0.3s. When a fault occurs in bus-4, the bus voltages in the other healthy buses also undergo sag. It can be seen from that; all the buses originate radially from bus 6, have felt the effect of the fault in bus 4 and a significant amount of voltage sag was observed in the buses going radially after bus-6, where the voltage has reduced to around 0.6 p.u.

which can be detrimental for any loads operating at those buses. Simulations were run with DVR placed in line 2-6 (optimal location), and the voltage profile in the buses going radially outward from line 2-6, were obtained as shown in Figure 6.15. One can observe from Figure 6.14 and Figure 6.15 that during a faulted scenario in the system, with DVR at an optimal location, it is able to bring back the bus voltages up to their pre-fault values.

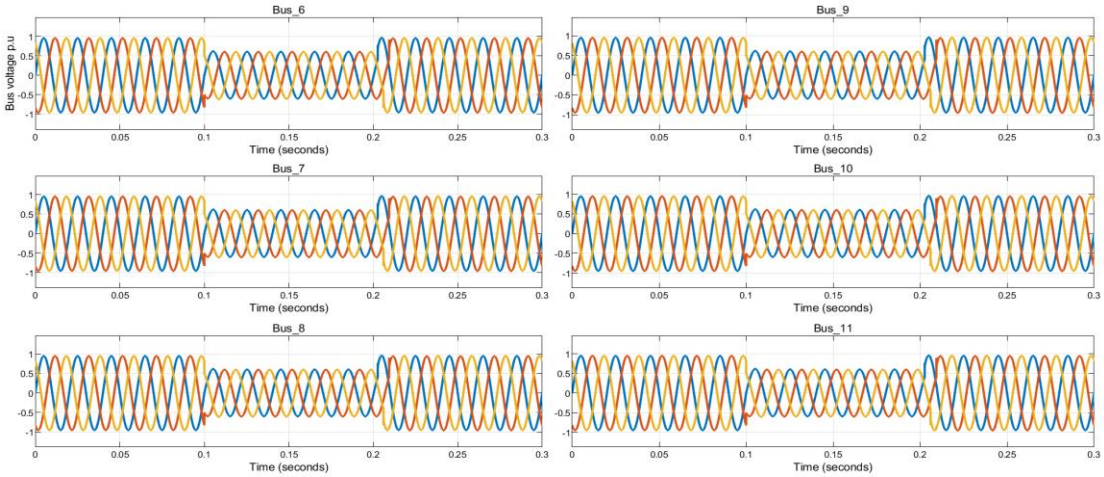

Figure 6.14: Bus voltages in p.u. with fault in bus 4 (without DVR)

It can also be observed that the pre-fault voltages of the buses going radially outwards of bus-6 are in the range of 0.96 p.u. in bus-6 and reducing up to 0.94p.u. in bus 11 as expected in a radial distribution system. However, when DVR is at the optimal location, not only has the post fault voltage been restored back but also the pre-fault voltages without DVR have also been improved with bus-6 having its voltage at almost 1p.u. (pre-fault, and post-fault) and voltage profile at other buses are also improved significantly.

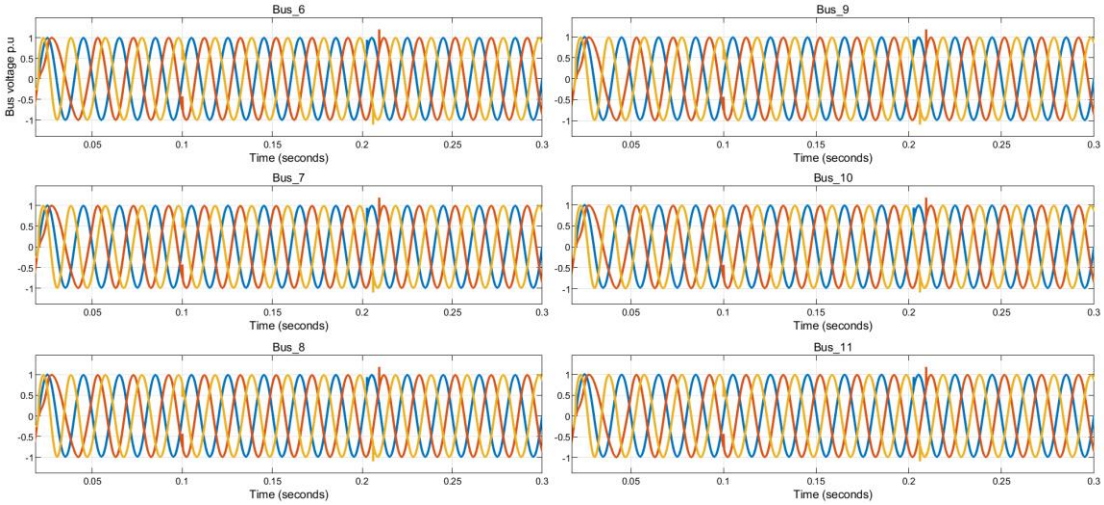

Figure 6.15: Bus voltages in p.u. with a fault in bus 4 (with DVR in line 2-6)

The comparison of the pre-fault voltage, fault voltage and restored voltages of the buses that lie radially outward of the optimal location in the Thimi-Sallaghari radial system is shown in Figure 6.16

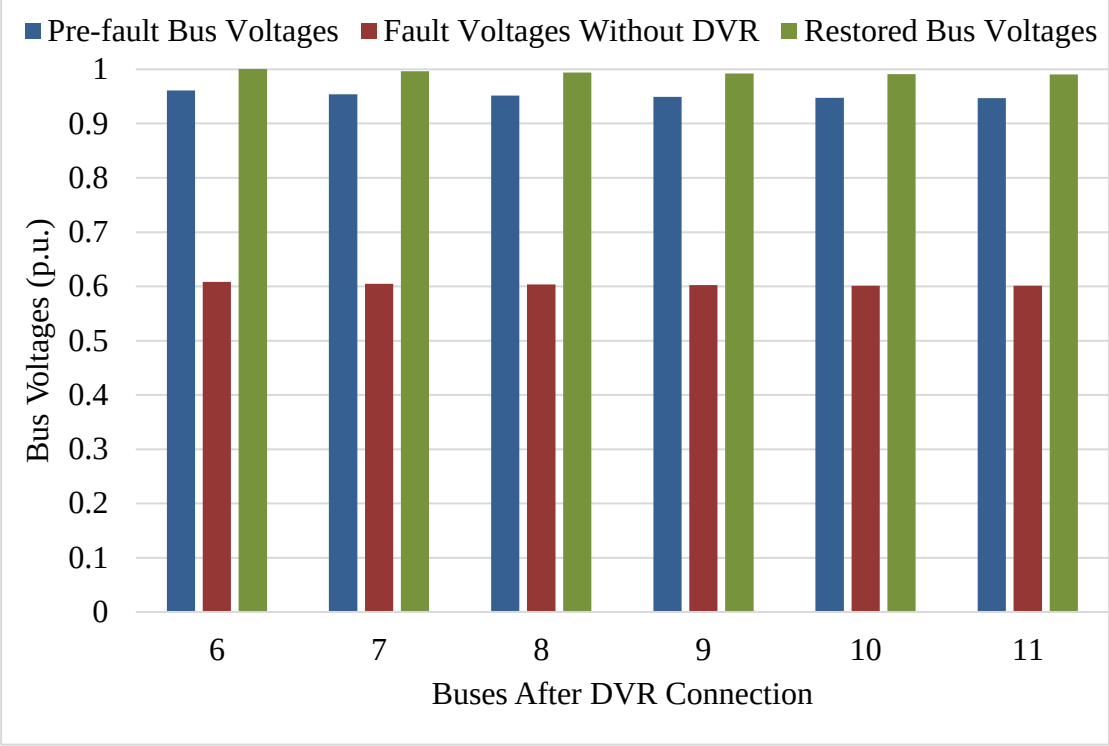

Figure 6.16: Voltage Profile of different buses in Thimi-Sallaghari radial system

Comparing the bus voltages during fault without DVR and after the installation of DVR in the optimal location, a substantial increase in the voltages of the buses that lie behind the DVR connection point is seen. Improvement of the voltage profile of the buses from that of the pre-fault case can also be seen. Since DVR is a device operated in series, it only improves the voltage profile of the buses that lies behind it in the radial distribution system.

6.5 Validations of Results

As explained in earlier sections, we used Artificial Neural Networks (ANN) for determining the location of DVR for which there is a minimum deviation in system bus voltages. For this, we have used the formulation to find the most vulnerable bus in terms of the Mean Squared Error (MSE) form. Using this technique, the optimal location in 11 bus Thimi-Sallaghari radial distribution systems came out to be at line 2-6, and that of the IEEE 15 bus distribution system came out to be at line 2-3, which is the same optimal location obtained by using ANN-based optimization.

Following the steps for the optimization for SARFIx based process, simulations were run for both IEEE 15 bus system and the Thimi-Sallaghari distribution system. Bus voltages at each bus were recorded for every possible fault scenario on the system with DVR at each possible location on the system. Sag frequencies at each bus were calculated, and respective SARFI for each location of DVR was computed. Based on this observation, the optimal location was selected as the location for which the calculated $SARFI_{90}$ had the minimum value of all the possible locations of the DVR.

IEEE-15 bus radial distribution system

Voltages at each bus were recorded for every possible fault scenario on the system with DVR placed in every possible location in the system. The number of times bus voltage goes below 0.9p.u. was counted for each bus, and this sag frequency was used to calculate SARFI for each location of DVR, and the bus for which this value came out to be the minimum was the best/optimal location to place the DVR.

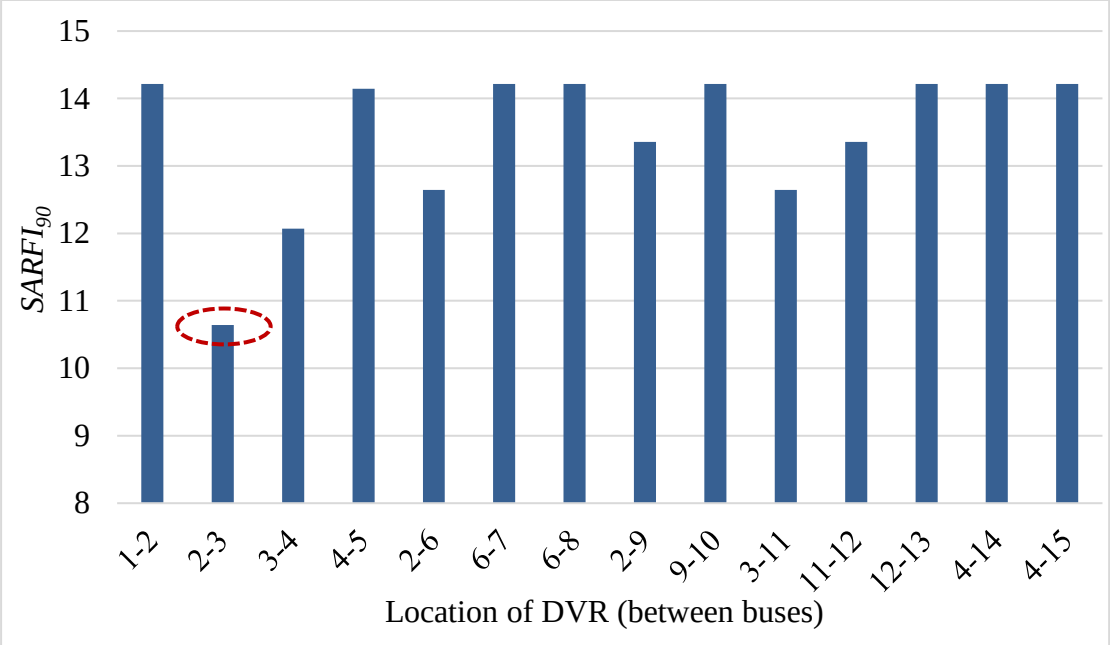

Figure 6.17: $SARFI_{90}$ for different locations of DVR at 15 bus

After the completion of the optimization process, it was noted that for IEEE 15 bus system, the value of $SARFI_{90}$ had a minimum value of 10.64 when DVR was located in the line 2-3 (between buses 2 and 3). Figure 6.17 shows the comparison of $SARFI_{90}$ computed for all different locations of DVR in the system which clearly indicates that the DVR location that corresponds to the minimum $SARFI_{90}$ is between bus 2 and 3, which is the optimal location based on the formulation of the problem. Using the ANN

technique, the same location between bus 2-3 was found to be the optimal location. Since, using both approaches—ANN and SARFI, the optimal location for 15 bus system came out to be the same, we can confidently say that when it is desired to maintain voltage profile of system buses to a certain desired range, the formulation using ANN approach can be correctly used to obtain the optimal location of DVR in radial distribution networks.

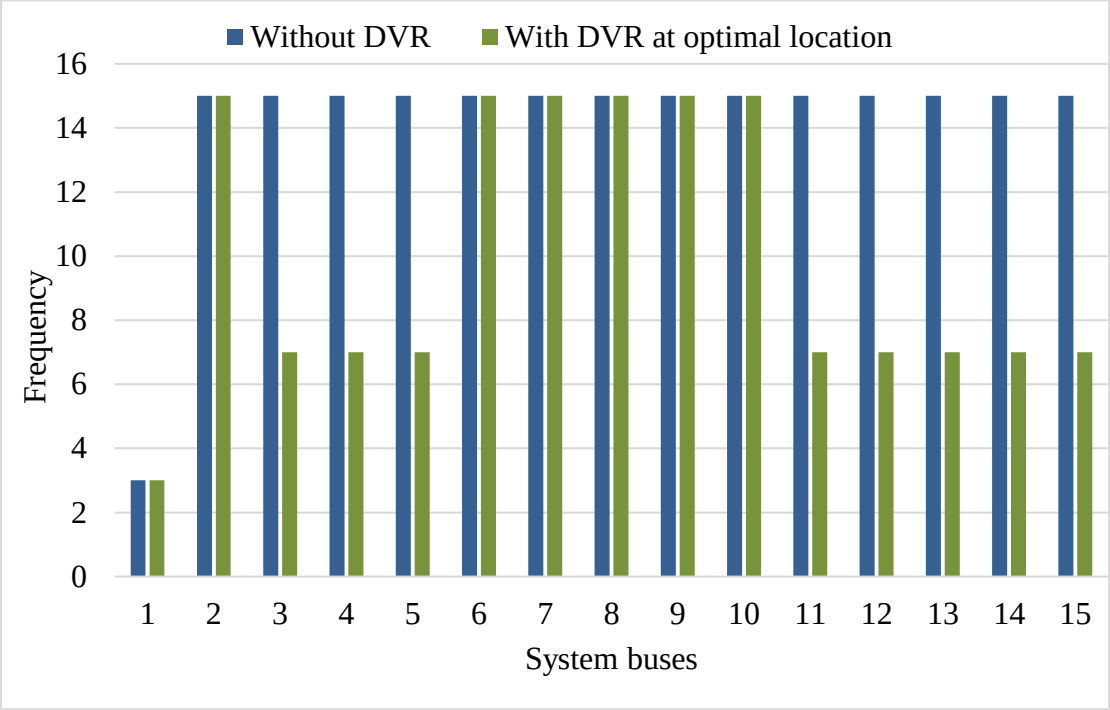

Figure 6.18: Sag Frequency improvement with DVR at the optimal location

It is seen from Figure 6.18 that the sag frequency in the buses after the DVR interconnection point has significantly reduced when compared to their sag frequencies before the installation of DVR. It can be seen that the sag frequency of buses 3,4,5,11,12,13,14, and15 show a significant reduction after the installation of the DVR at the optimal location. These are the buses that go radially outward from bus 3, where DVR is connected. For the other buses, the voltage sag frequency shows no improvement even after DVR interconnection, which is due to the fact that DVR is a series device and does not have the ability to mitigate voltage sags at buses before DVR interconnection node.

Case study: Thimi-Sallaghari radial distribution network

After the completion of the optimization process, it was found that for the 11 bus Thimi-Sallaghari radial distribution system, the value of $SARFI_{90}$ had a minimum value of 7.54 when DVR was located in the line 2-6 between buses(2 and 6).

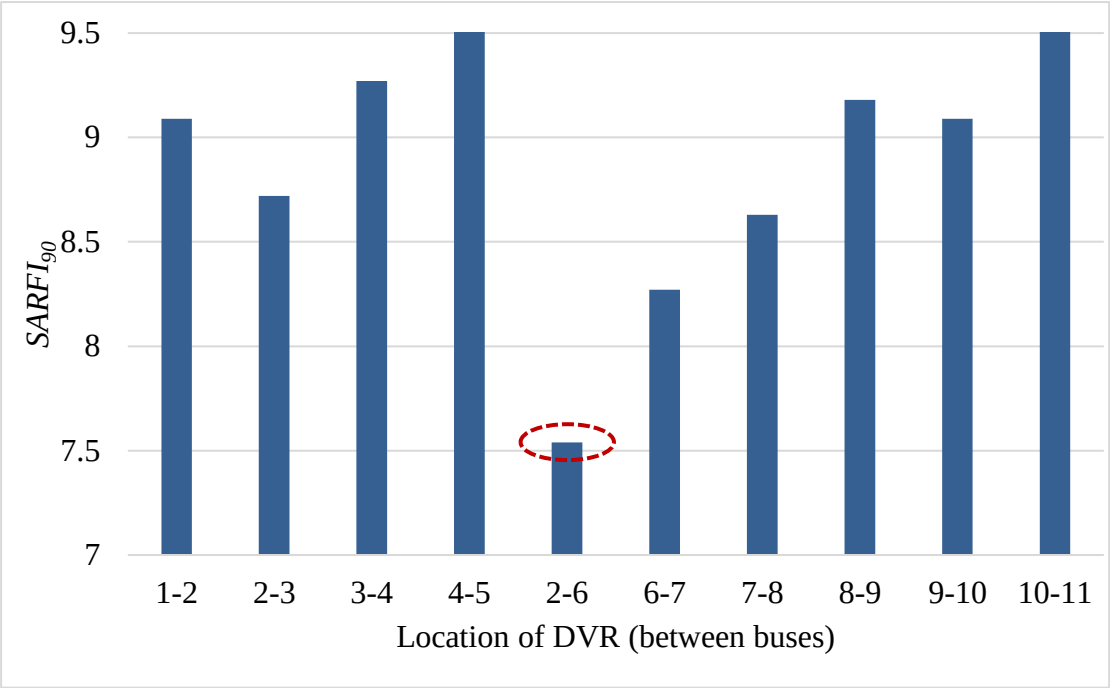

Figure 6.19: $SARFI_{90}$ for different locations of DVR at 11 bus

Figure 6.19 shows the comparison of $SARFI_{90}$ computed for all different locations of the DVR in the system, clearly indicating the minimum $SARFI_{90}$ at the location between bus 2-6. Using ANN technique, optimal location was obtained at the same location in the line between bue 2 and 6 and the value of $SARFI_{90}$ being minimum for the same location using the discussed optimization process validates our result obtained with ANN approach.

Furthermore, Figure 6.20 depicts the improvement in sag frequencies in the system buses after DVR has been connected at the optimal location from the case when the system operates without any DVR. It can be clearly seen that the sag frequency in the buses after the DVR interconnection point has significantly reduced when compared to their sag frequencies before the installation of DVR.

It has already been discussed that DVR is placed in series between the source and load, and it does not improve the voltage profiles at buses before the DVR interconnection

point, which can be seen from above Figure 6.20—buses 1,2,3,4 and 5 show no improvement in voltage sag frequency.

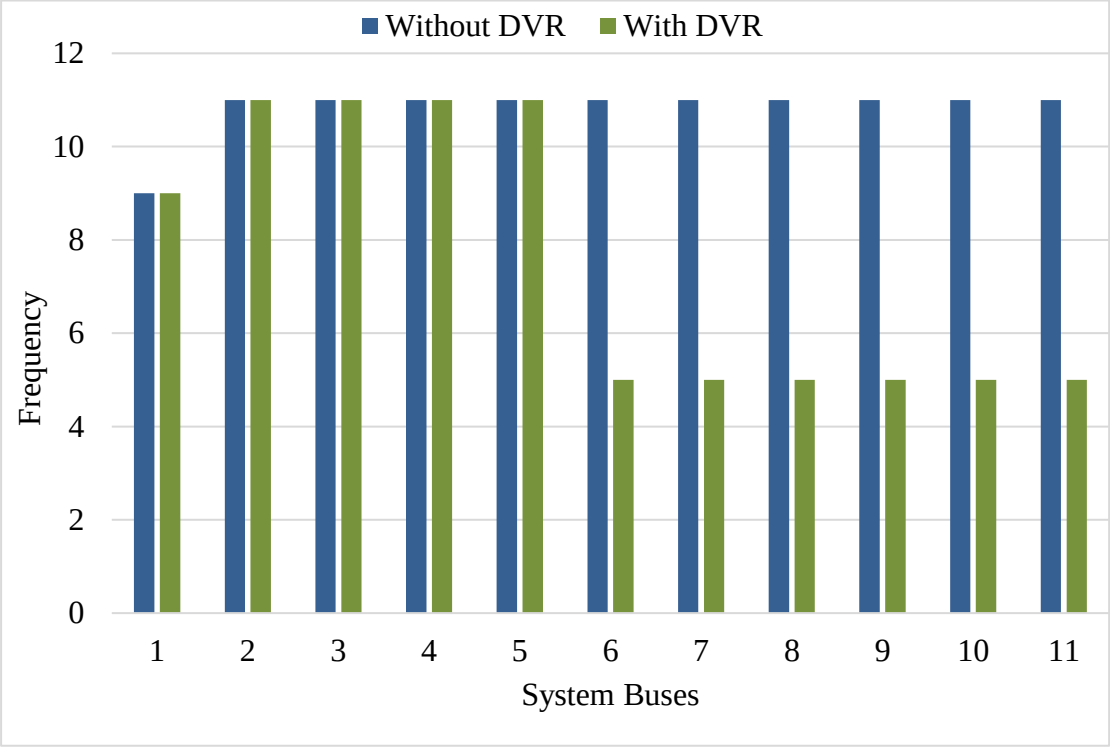

Figure 6.20: Sag frequency improvement with DVR at optimal location

Since the optimal location came out to be the same using ANN approach and by using the formulation for minimizing SARFI, and the fact that the method using SARFI can reliably be used to locate the optimal place in a radial distribution network shows that our results for optimal location obtained using ANN are correct.

CHAPTER SEVEN: CONCLUSIONS AND RECOMMENDATIONS

Conclusions

The following conclusions can be deduced from the findings:

- Simulink model of DVR has been modelled with essential controls in MATLAB/SIMULINK environment and tested with a modelled system comprising of a single source modelled as a negative PQ load that feeds a load of rating P=100kW and Q=5kVAR through a distribution line and transformers. During voltage sag, load voltage dropped down to 0.3 p.u. that is by 70% of its normal voltage, and during the event of voltage swell, voltage rose to 145% of the nominal rated voltage. The integration of the DVR model resulted in the restoration of bus voltage from 0.3p.u. to 0.97p.u. during voltage sag and restoration of voltage from 1.45p.u. to 0.98p.u. during voltage swell. During sag/swell, DVR injected/absorbed the power into/from the load. Thus, a completely working model of DVR capable of operating during both sag and swell has been designed and modelled.

- Sensitivity analysis was performed for the developed model of DVR with a simple test system with two nodes where DVR was connected to the first node, and the voltage at the other node was observed during fault for a different combination of load demand and line length. Monte Carlo Simulation, done with the number of random trials chosen as N=10,000, showed that the DVR model was able to mitigate voltage sag under a wide range of load demand and line lengths. From the study of the correlation between the input variables and (load demand and line length) and the voltage at the second node during a fault, it was found that load power demand has a substantial contribution to the voltage drop than the line length. Stochastic study of the results from MC simulation suggested that the certainty of the output voltage at the second node to remain above 0.9 p.u. was 90.84%, and under no circumstances, the voltage dropped below 0.86 p.u. during the fault. This led to the conclusion that the DVR model can operate over a wide range of variations of load and line lengths, which are subject to variation in a radial distribution system.

- An ANN-based optimization problem was formulated, and the optimization was carried out to locate the optimal place for DVR in IEEE 15 bus system and in Thimi-Sallaghari radial distribution system. The building and training of ANN provided information about the MSE of buses, and the bus with the highest MSE was considered as the most vulnerable bus. The location of the optimal place for DVR was found out to be at line 2-3 for the IEEE 15 bus system with the highest MSE of 0.02684 at bus 3 and line 2-6 for Thimi-Sallaghari radial distribution system with highest MSE of 0.0885 at bus 6. A simulation study with DVR placed in optimal location showed significant restoration of bus voltages for the buses that lie radially outward from the DVR interconnection point. In both cases, DVR at the optimal location was able to restore the voltage above 0.95 p.u. from a very low voltage of around 0.35 p.u. even at the bus farthest from the DVR.
- In order to validate the optimization results obtained using ANN, another procedure was used to locate the optimal place for DVR in both systems which were based on finding the minimum value of SARFI (System Average RMS Frequency Index) of the system in the presence of DVR during the event of voltage sag. With this optimization process, the optimal location for DVR in IEEE 15 bus system was found out to be in line 2-3— this location had minimum SARFI of 10.64 among all other possible locations. Similarly, the optimal location corresponding to the location for which SARFI was minimum in the Thimi-Sallaghari distribution system was found out to be in line 2-6. With DVR located in the line 2-6, SARFI had a minimum value of 7.54 when compared to all other location. Using this Optimization technique based on SARFI, the optimal location for DVR, for two test systems, was found to be the same as those obtained in the ANN approach.

Recommendations

- In more complex and interconnected distribution systems, a large number of such DVRs need to be placed, and the formulation of more complex optimization problems has to be carried out to perform decentralized voltage restoration. In such scenario training, the ANN and control of DVR will have to be improvised based on the system and operational requirements.

- Power-sharing among one or more DVRs during the event of voltage sag/swell using droop control so that they share active/reactive power proportionally based on their capacity for better co-ordination should be studied
- With radial distribution being the most prevalent distribution system, voltage control in these networks is of more significant concern to researchers around the globe, especially with the proliferation of smart grids and integration of Inverter Based Resources (IBRs) in the systems. Operation of DVRs in systems in the presence of DERs and Inverters and their coordinated control among themselves and with other devices is another aspect to look into while moving forward with using DVR in modern, smart distribution systems.
- In this study, we have taken voltage sag to see the most vulnerable bus and optimally place the DVR; however, the same procedure can be repeated for voltage swell also, and the optimization can be carried out using ANN by simple changes in the formulation and implementation.

REFERENCES

Bach, K., 2019. A novel method for global voltage sag compensation in IEEE 69 bus distribution system by Dynamic Voltage Restorers. *Journal of Engineering Science and Technology,Vol. 14, No. 4,* pp. 1893-1911.

Beale, M., Hagan, M. & Demuth, H., 2010. MATLAB Neural Network Toolbox™ User's Guide. *The Mathworks, Version 8, no. 1.*

Bhonde, S., Jadhao, S. & Pote, R., 2017. *Enhancement of Voltage Quality in Power System through Series Compensation using DVR.* Mysore, s.n., pp. 826-830, doi: 10.1109/CTCEEC.2017.8455101..

Das, D., Kothari, D. & Kalam, A., 1995. Simple and efficient method for load flow solution of radial distribution networks. *International Journal of Electrical Power & Energy Systems; Volume 17; Issue 5*, pp. 335-346.

Edomah, N., 2009. *Effects of voltage sags, swell and other disturbances on electrical equipment and their economic implications.* Prague, Czech Republic, IEEE, pp. 1-4, doi: 10.1049/cp.2009.0502..

Ghosh, A. & Ledwich, G., 2001. *Structures and control of a dynamic voltage regulator (DVR).* Columbus, OH, USA, IEEE, pp. 1027-1032 vol.3.

Gupta, S. K., Tiwari, H. & Pachar , R., 2010. Estimation of DC Voltage Storage Requirements for Dynamic Voltage Compensation on Distribution Network using DVR. *International Journal of Engineering and Technology,* 2(1), pp. 124-131.

Haque, M., 2001. Voltage Sag Correction by Dynamic Voltage Restorer with Minimum Power Injection. *IEEE Power Engineering Review, vol. 21, no. 5*, pp. 56-58.

Husain, S. .. & Subbaramiah, M., 2013. *An analytical approach for optimal location of DSTATCOM in radial distribution system.* Nagercoil, IEEE, pp. pp. 1365-1369.

IEEE, 1994. IEEE Recommended Practice for Electric Power Distribution for Industrial Plants. *IEEE Std 141-1993,* pp. 1-768,doi: 10.1109/IEEESTD.1994.121642..

Leon, J. A. D. d. & Taylor, C. W., 2002. *Understanding and solving short-term voltage stability problems.* Chicago, IL, USA,, IEEE, pp. 745-752.

McGranaghan, M. F., Mueller, D. & Samotyj, M., 1993. Voltage sags in industrial systems. *IEEE Transactions on Industry Applications, vol. 29, no. 2,*, pp. 397-403.

Milanovic, J. & Zhang, Y., 2010. Modeling of FACTS Devices for Voltage Sag Mitigation Studies in Large Power Systems. *IEEE Transactions on Power Delivery,vol. 25, no. 4,* pp. 3044-3052.

Mohammadi, M., 2013. Voltage Dip Rating Reduction Based Optimal Location of DVR for relaibility improvement of electrical distribution system. *International Research Journal of Applied and Basics Sciences,* pp. 3493-3500.

Ogunboyo, P., Tiako, R. & Davidson, I., 2018. Effectiveness of Dynamic Voltage Restorer for Unbalance Voltage Mitigation and Voltage Profile Improvement in Secondary Distribution System. *Canadian Journal of Electrical and Computer Engineering, vol. 41, no. 2,* pp. pp. 105-115, doi: 10.1109/CJECE.2018.2858841..

Reddy, A. V. S., Reddy, D. & Vinoda, N., 2017. Optimal Placement of Dynamic Voltage Restorer in Distribution Systems for Voltage Improvement Using Particle Swarm Optimization. *Int. Journal of Engineering Research and Application, Vol. 7, Issue 3, (Part -1),* pp. 29-33.

Regmi, T., 2017. *Optimal Allocation of Capacitor Bank for Loss Minimization and Voltage Improvement Using Analytical Method,* Nepal: Department of Electrical and Electronics Engineering, Kathmandu University.

Remya, V., Parthiban, P., Ansal, V. & Babu, B., 2018. Dynamic Voltage Restorer (DVR) – A Review. *Journal of Green Engineering, volume: 8, no:4,* pp. 519-572.

Renders, B., Degroote, L., Driesen, J. & Vandevelde, L., 2007. Profits of power-quality improvement by residential distributed generation. *Renders, B., Degroote, L., Driesen, J., & Vandevelde, L. (2007). Profits of power- 42nd International Universities, Power Engineering Conference.,* pp. 377-381.

Reynaldi, A., Lukas, S. & Margaretha, H., 2012. *Backpropagation and Levenberg-Marquardt Algorithm for Training Finite Element Neural Network.* Valetta, Malta, IEEE, pp. 89-94.

SARI/Energy, N., 2003. *Economic Impact of Poor Power Quality on Industry Nepal,* s.l.: USAID-SARI/Energy Program.

Sasitharan, S., Mishra, M., Kumar, B. & Jayashankar, V., 2008. *Rating and design issues of DVR injection transformer.* Austin, TX,USA, IEEE, pp. 449-455.

Singh, B., Verma, M. K., Mehrotra, O. N. & Tanti, D. K., 2011. AN ANN BASED APPROACH FOR OPTIMAL PLACEMENT OF DSTATCOM FOR VOLTAGE SAG MITIGATION. *International Journal of Engineering Science and Technology Vol. 3 No. 2,* pp. 827-835.

Singh, T. & Singh, L., 2015. Comparative Analysis of Custom Power Devices for Power Quality Improvement in Non-linear Loads. *International Conference on Recent Advances in Engineering & Computational Sciences* , pp. 1-5.

Soni, J. S., Agrawal, H. P. & Gupta, D. R., 2013. Potentials and Capabilities of FACTS Controllers for Quality and Performance Enhancement of Power System. *International Journal of Innovative Technology and Exploring Engineering (IJITEE), , Volume-2, Issue-4,* pp. 106-111.

Tagliarini, G. & Christ, J., 1991. Optimization Using Neural Networks. *IEEE Transactions on Computers, vol. 40, no. 12,* pp. 1347-1358.

Tamjis, M. R. & Lau, S. L., 2006. The economies of power quality. *IET Power Engineer Volume 20, Issue 6,* pp. 38-41.

Wijekoon, H. M., Vilathgamuwa, D. M. & Choi, S. S., 2003. Interline dynamic voltage restorer: an economical way to improve interline power quality. *IEE Proceedings - Generation, Transmission and Distribution, vol. 150, no. 5, doi: 10.1049/ip-gtd:20030800.,* pp. 513-520.

Wilamowski, B., 2009. Neural network architectures and learning algorithms. *IEEE Industrial Electronics Magazine, vol. 3, no. 4,* pp. 56-63.

Y.K, B. & G.K, P., 2015. Power Quality Enhancement using ANN-based Optimal Placement of D-STATCOM in a Radial Distribution System. *International Science Community Association,* pp. 150-153.

Zayani, R., Bouallegue, R. & Roviras, D., 2008. *Levenberg-Marquardt learning neural network for adaptive predistortion for time-varying HPA with memory in OFDM systems.* Lausanne, Switzerland, IEEE, pp. 1-5.

PUBLICATION

Ghimire, A., Bhattarai, N. & Motra, L., 2020. *Optimal placement of Dynamic Voltage Restorer in Radial Distribution System using Artificial Neural Network Approach.* International Research Journal of Engineering and Technology (IRJET), May.07(05).

APPENDIX A: LINE AND LOAD DATA OF IEEE-15 BUS SYSTEM

Bus No.	Load Data	
	Active Power (kW)	Reactive Power (kVAR)
1	0	0
2	44.099998	44.990997
3	70	71.414284
4	140	142.828568
5	44.099998	44.990997
6	140	142.828568
7	140	142.828568
8	70	71.414284
9	70	71.414284
10	44.099998	44.990997
11	140	142.828568
12	70	71.414284
13	44.099998	44.990997
14	70	71.414284
15	140	142.828568

Bus No.		Line Data	
From	To	R(Ohm)	X(Ohm)
1	2	1.35309	1.32349
2	3	1.17024	1.14464
3	4	0.84111	0.82271
4	5	1.52348	1.0276
2	6	2.55727	1.7249
6	7	1.0882	0.734
6	8	1.25143	0.8441
2	9	2.01317	1.3579
9	10	1.68671	1.1377
3	11	1.79553	1.2111
11	12	2.44845	1.6515
12	13	2.01317	1.3579
4	14	2.23081	1.5047
4	15	1.19702	0.8074

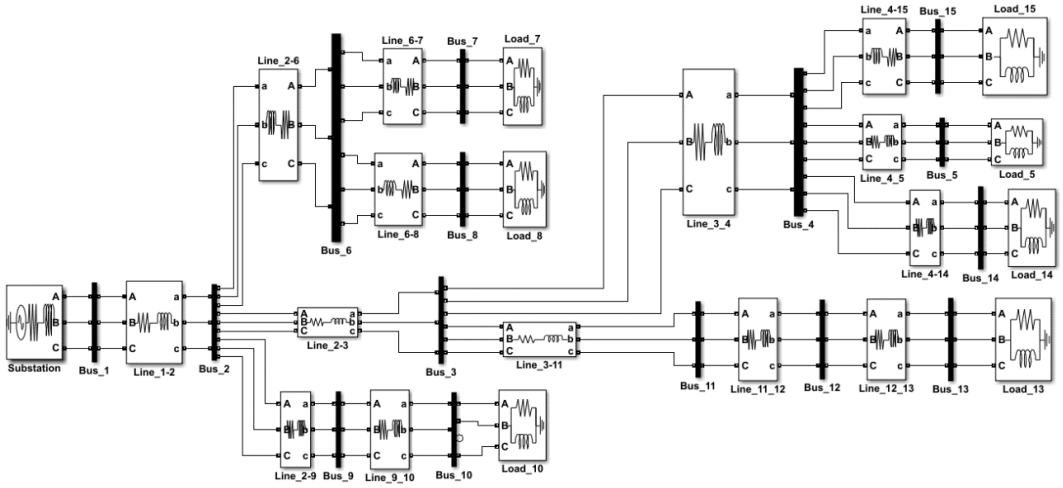

Figure A-1: Simulink Model of IEEE 15 bus

APPENDIX B: IEEE-15 BUS TRAIN DATA SAMPLES FOR ANN

Train data samples: 14 × 168 matrix where 14 rows represent the load buses and 168 columns represent the 14 load buses × 3 phases × 4 faults. Column 1 to 3: L-G fault voltage, Column 4 to 6: LL fault voltage, Column 7 to 9: LLG fault voltage, Column 10 to 12: LLLG fault voltage for bus 2. Similarly, other columns represent the voltage values for faults for other remaining buses 3-15 as in bus 2

Column 1 through 18

0.326	0.967	0.967	0.692	0.384	0.967	0.325	0.323	0.967	0.323	0.322	0.322	0.519	0.967	0.967	0.727	0.585	0.967
0.325	0.954	0.954	0.685	0.381	0.954	0.324	0.320	0.954	0.322	0.319	0.319	0.214	0.954	0.954	0.612	0.389	0.954
0.324	0.949	0.949	0.683	0.380	0.949	0.324	0.319	0.949	0.322	0.318	0.318	0.215	0.949	0.949	0.610	0.388	0.949
0.324	0.948	0.948	0.682	0.380	0.948	0.324	0.319	0.948	0.322	0.318	0.318	0.215	0.948	0.948	0.610	0.388	0.948
0.325	0.955	0.955	0.687	0.382	0.955	0.325	0.320	0.955	0.323	0.320	0.320	0.515	0.955	0.955	0.720	0.580	0.955
0.325	0.953	0.953	0.686	0.381	0.953	0.325	0.320	0.953	0.323	0.320	0.320	0.514	0.953	0.953	0.719	0.579	0.953
0.325	0.954	0.954	0.686	0.382	0.954	0.325	0.320	0.954	0.323	0.320	0.320	0.515	0.954	0.954	0.719	0.580	0.954
0.326	0.964	0.964	0.691	0.383	0.964	0.325	0.322	0.964	0.323	0.322	0.322	0.518	0.964	0.964	0.725	0.584	0.964
0.326	0.963	0.963	0.690	0.383	0.963	0.325	0.322	0.963	0.323	0.321	0.321	0.518	0.963	0.963	0.725	0.584	0.963
0.324	0.948	0.948	0.682	0.380	0.948	0.324	0.319	0.948	0.322	0.318	0.318	0.215	0.948	0.948	0.610	0.388	0.948
0.324	0.944	0.944	0.681	0.379	0.944	0.324	0.318	0.944	0.322	0.317	0.318	0.216	0.944	0.944	0.609	0.387	0.944
0.324	0.943	0.943	0.680	0.379	0.943	0.324	0.318	0.943	0.322	0.317	0.317	0.216	0.943	0.943	0.608	0.387	0.943
0.324	0.947	0.947	0.682	0.380	0.947	0.324	0.318	0.947	0.322	0.318	0.318	0.215	0.947	0.947	0.609	0.387	0.947
0.324	0.946	0.946	0.681	0.380	0.946	0.324	0.318	0.946	0.322	0.318	0.318	0.215	0.946	0.946	0.609	0.387	0.946

Column 19 through 36

0.518	0.517	0.967	0.518	0.517	0.517	0.607	0.967	0.967	0.761	0.664	0.967	0.606	0.606	0.967	0.606	0.605	0.605
0.213	0.211	0.954	0.212	0.211	0.211	0.342	0.954	0.954	0.630	0.484	0.954	0.341	0.340	0.954	0.341	0.339	0.339
0.214	0.211	0.949	0.213	0.210	0.210	0.171	0.949	0.949	0.582	0.397	0.949	0.171	0.169	0.949	0.170	0.168	0.168
0.214	0.211	0.948	0.213	0.210	0.210	0.171	0.948	0.948	0.581	0.397	0.948	0.171	0.169	0.948	0.170	0.168	0.168
0.514	0.512	0.955	0.514	0.512	0.512	0.601	0.955	0.955	0.753	0.657	0.955	0.601	0.599	0.955	0.601	0.598	0.599
0.514	0.511	0.953	0.513	0.511	0.511	0.600	0.953	0.953	0.752	0.656	0.953	0.600	0.598	0.953	0.600	0.597	0.597
0.514	0.512	0.954	0.514	0.511	0.511	0.601	0.954	0.954	0.752	0.656	0.954	0.600	0.598	0.954	0.600	0.598	0.598
0.517	0.516	0.964	0.517	0.515	0.515	0.605	0.964	0.964	0.759	0.662	0.964	0.605	0.604	0.964	0.605	0.603	0.603
0.517	0.516	0.963	0.517	0.515	0.515	0.605	0.963	0.963	0.758	0.661	0.963	0.604	0.603	0.963	0.604	0.603	0.603
0.214	0.211	0.948	0.213	0.211	0.211	0.341	0.948	0.948	0.627	0.483	0.948	0.341	0.338	0.948	0.340	0.338	0.338
0.215	0.211	0.944	0.214	0.210	0.210	0.341	0.944	0.944	0.626	0.482	0.944	0.340	0.338	0.944	0.340	0.337	0.337
0.215	0.211	0.943	0.214	0.210	0.210	0.341	0.943	0.943	0.625	0.481	0.943	0.340	0.337	0.943	0.340	0.337	0.337
0.214	0.211	0.947	0.213	0.210	0.210	0.172	0.947	0.947	0.581	0.397	0.947	0.171	0.169	0.947	0.170	0.168	0.168
0.215	0.211	0.946	0.214	0.210	0.210	0.172	0.946	0.946	0.581	0.397	0.946	0.172	0.169	0.946	0.171	0.168	0.168

Column 37 through 54

0.697	0.967	0.967	0.811	0.734	0.967	0.696	0.695	0.967	0.696	0.695	0.695	0.634	0.967	0.967	0.792	0.665	0.967
0.492	0.954	0.954	0.695	0.580	0.954	0.491	0.490	0.954	0.491	0.489	0.489	0.627	0.954	0.954	0.783	0.657	0.954
0.350	0.949	0.949	0.633	0.484	0.949	0.349	0.347	0.949	0.349	0.347	0.347	0.624	0.949	0.949	0.779	0.654	0.949
0.129	0.948	0.948	0.551	0.415	0.948	0.129	0.127	0.948	0.128	0.127	0.127	0.623	0.948	0.948	0.778	0.653	0.948
0.689	0.955	0.955	0.802	0.726	0.955	0.689	0.687	0.955	0.689	0.687	0.687	0.163	0.955	0.955	0.571	0.414	0.955
0.688	0.953	0.953	0.800	0.724	0.953	0.688	0.686	0.953	0.688	0.686	0.686	0.163	0.953	0.953	0.571	0.413	0.953
0.689	0.954	0.954	0.801	0.725	0.954	0.688	0.687	0.954	0.688	0.686	0.686	0.163	0.954	0.954	0.571	0.413	0.954
0.695	0.964	0.964	0.808	0.732	0.964	0.695	0.693	0.964	0.694	0.693	0.693	0.632	0.964	0.964	0.790	0.663	0.964
0.694	0.963	0.963	0.808	0.731	0.963	0.694	0.693	0.963	0.694	0.692	0.692	0.632	0.963	0.963	0.789	0.662	0.963
0.490	0.948	0.948	0.691	0.577	0.948	0.489	0.487	0.948	0.489	0.487	0.487	0.623	0.948	0.948	0.778	0.653	0.948
0.489	0.944	0.944	0.689	0.575	0.944	0.488	0.486	0.944	0.488	0.485	0.485	0.622	0.944	0.944	0.776	0.651	0.944
0.488	0.943	0.943	0.689	0.575	0.943	0.488	0.485	0.943	0.488	0.485	0.485	0.621	0.943	0.943	0.775	0.650	0.943
0.349	0.947	0.947	0.633	0.483	0.947	0.349	0.347	0.947	0.349	0.346	0.346	0.623	0.947	0.947	0.777	0.652	0.947
0.350	0.946	0.946	0.632	0.483	0.946	0.349	0.347	0.946	0.349	0.346	0.346	0.622	0.946	0.946	0.777	0.652	0.946

Column 55 through 72

0.633	0.632	0.967	0.633	0.632	0.632	0.693	0.967	0.967	0.820	0.718	0.967	0.693	0.692	0.967	0.692	0.691	0.691
0.626	0.624	0.954	0.626	0.624	0.624	0.685	0.954	0.954	0.809	0.709	0.954	0.684	0.683	0.954	0.684	0.683	0.683
0.623	0.621	0.949	0.623	0.621	0.621	0.681	0.949	0.949	0.805	0.706	0.949	0.681	0.679	0.949	0.681	0.679	0.679
0.623	0.621	0.948	0.623	0.620	0.621	0.681	0.948	0.948	0.805	0.705	0.948	0.681	0.679	0.948	0.680	0.678	0.678
0.162	0.161	0.955	0.161	0.160	0.160	0.293	0.955	0.955	0.601	0.475	0.955	0.293	0.292	0.955	0.292	0.291	0.291
0.163	0.161	0.953	0.162	0.160	0.160	0.134	0.953	0.953	0.552	0.422	0.953	0.133	0.132	0.953	0.133	0.132	0.132
0.163	0.161	0.954	0.162	0.160	0.160	0.293	0.954	0.954	0.600	0.475	0.954	0.293	0.292	0.954	0.292	0.291	0.291
0.632	0.630	0.964	0.631	0.630	0.630	0.691	0.964	0.964	0.817	0.716	0.964	0.691	0.689	0.964	0.690	0.689	0.689
0.631	0.630	0.963	0.631	0.629	0.630	0.690	0.963	0.963	0.816	0.715	0.963	0.690	0.689	0.963	0.690	0.689	0.689
0.623	0.621	0.948	0.623	0.621	0.621	0.681	0.948	0.948	0.805	0.705	0.948	0.681	0.679	0.948	0.681	0.679	0.679
0.621	0.619	0.944	0.621	0.618	0.618	0.679	0.944	0.944	0.802	0.703	0.944	0.678	0.676	0.944	0.678	0.676	0.676
0.621	0.618	0.943	0.620	0.618	0.618	0.678	0.943	0.943	0.801	0.702	0.943	0.678	0.676	0.943	0.678	0.675	0.675
0.622	0.620	0.947	0.622	0.620	0.620	0.680	0.947	0.947	0.804	0.704	0.947	0.680	0.678	0.947	0.680	0.678	0.678
0.622	0.620	0.946	0.622	0.619	0.619	0.680	0.946	0.946	0.803	0.704	0.946	0.679	0.677	0.946	0.679	0.677	0.677

Column 73 through 90

0.700	0.967	0.967	0.823	0.725	0.967	0.700	0.699	0.967	0.699	0.698	0.698	0.592	0.967	0.967	0.774	0.627	0.967
0.691	0.954	0.954	0.813	0.716	0.954	0.691	0.690	0.954	0.691	0.689	0.689	0.585	0.954	0.954	0.765	0.620	0.954
0.688	0.949	0.949	0.808	0.712	0.949	0.688	0.686	0.949	0.688	0.686	0.686	0.583	0.949	0.949	0.761	0.617	0.949
0.688	0.948	0.948	0.808	0.712	0.948	0.687	0.686	0.948	0.687	0.685	0.685	0.582	0.948	0.948	0.760	0.617	0.948
0.310	0.955	0.955	0.606	0.484	0.955	0.309	0.308	0.955	0.309	0.308	0.308	0.586	0.955	0.955	0.766	0.621	0.955
0.310	0.953	0.953	0.605	0.484	0.953	0.309	0.308	0.953	0.309	0.307	0.307	0.585	0.953	0.953	0.764	0.620	0.953
0.130	0.954	0.954	0.550	0.424	0.954	0.129	0.129	0.954	0.129	0.128	0.128	0.586	0.954	0.954	0.765	0.621	0.954
0.698	0.964	0.964	0.820	0.722	0.964	0.698	0.696	0.964	0.697	0.696	0.696	0.181	0.964	0.964	0.587	0.411	0.964
0.697	0.963	0.963	0.820	0.722	0.963	0.697	0.696	0.963	0.697	0.696	0.696	0.181	0.963	0.963	0.587	0.411	0.963
0.688	0.948	0.948	0.808	0.712	0.948	0.688	0.686	0.948	0.687	0.685	0.685	0.583	0.948	0.948	0.760	0.617	0.948
0.685	0.944	0.944	0.805	0.709	0.944	0.685	0.683	0.944	0.685	0.683	0.683	0.581	0.944	0.944	0.758	0.615	0.944
0.685	0.943	0.943	0.804	0.708	0.943	0.685	0.682	0.943	0.684	0.682	0.682	0.580	0.943	0.943	0.757	0.614	0.943
0.687	0.947	0.947	0.807	0.711	0.947	0.687	0.685	0.947	0.687	0.685	0.685	0.582	0.947	0.947	0.760	0.616	0.947
0.686	0.946	0.946	0.806	0.710	0.946	0.686	0.684	0.946	0.686	0.684	0.684	0.582	0.946	0.946	0.759	0.616	0.946

Column 91 through 108

0.591	0.590	0.967	0.591	0.590	0.590	0.692	0.967	0.967	0.819	0.718	0.967	0.692	0.691	0.967	0.692	0.691	0.691
0.585	0.583	0.954	0.585	0.583	0.583	0.684	0.954	0.954	0.808	0.710	0.954	0.684	0.682	0.954	0.684	0.682	0.682
0.582	0.580	0.949	0.582	0.580	0.580	0.681	0.949	0.949	0.804	0.706	0.949	0.681	0.679	0.949	0.680	0.679	0.679
0.582	0.580	0.948	0.582	0.579	0.579	0.680	0.948	0.948	0.804	0.705	0.948	0.680	0.678	0.948	0.680	0.678	0.678
0.586	0.584	0.955	0.586	0.583	0.583	0.685	0.955	0.955	0.810	0.711	0.955	0.685	0.683	0.955	0.685	0.683	0.683
0.585	0.583	0.953	0.585	0.582	0.582	0.684	0.953	0.953	0.808	0.709	0.953	0.684	0.682	0.953	0.683	0.682	0.682
0.585	0.583	0.954	0.585	0.583	0.583	0.684	0.954	0.954	0.809	0.710	0.954	0.684	0.682	0.954	0.684	0.682	0.682
0.180	0.179	0.964	0.179	0.179	0.179	0.380	0.964	0.964	0.641	0.521	0.964	0.380	0.379	0.964	0.379	0.379	0.379
0.180	0.179	0.963	0.180	0.179	0.179	0.131	0.963	0.963	0.555	0.427	0.963	0.131	0.130	0.963	0.130	0.130	0.130
0.582	0.580	0.948	0.582	0.579	0.579	0.680	0.948	0.948	0.804	0.706	0.948	0.680	0.678	0.948	0.680	0.678	0.678
0.580	0.578	0.944	0.580	0.577	0.577	0.678	0.944	0.944	0.801	0.703	0.944	0.678	0.676	0.944	0.678	0.676	0.676
0.580	0.577	0.943	0.580	0.577	0.577	0.677	0.943	0.943	0.800	0.702	0.943	0.677	0.675	0.943	0.677	0.675	0.675
0.582	0.579	0.947	0.581	0.579	0.579	0.680	0.947	0.947	0.803	0.705	0.947	0.679	0.677	0.947	0.679	0.677	0.677
0.581	0.579	0.946	0.581	0.578	0.578	0.679	0.946	0.946	0.802	0.704	0.946	0.679	0.677	0.946	0.679	0.677	0.677

Column 109 through 126

0.665	0.967	0.967	0.799	0.702	0.967	0.664	0.663	0.967	0.664	0.663	0.663	0.759	0.967	0.967	0.848	0.782	0.967
0.439	0.954	0.954	0.681	0.530	0.954	0.438	0.437	0.954	0.438	0.436	0.436	0.596	0.954	0.954	0.752	0.651	0.954
0.438	0.949	0.949	0.678	0.528	0.949	0.437	0.435	0.949	0.437	0.434	0.434	0.594	0.949	0.949	0.748	0.648	0.949
0.437	0.948	0.948	0.678	0.527	0.948	0.437	0.435	0.948	0.437	0.434	0.434	0.593	0.948	0.948	0.747	0.648	0.948
0.658	0.955	0.955	0.790	0.695	0.955	0.658	0.656	0.955	0.658	0.656	0.656	0.750	0.955	0.955	0.839	0.773	0.955
0.657	0.953	0.953	0.788	0.693	0.953	0.657	0.655	0.953	0.657	0.654	0.654	0.749	0.953	0.953	0.837	0.771	0.953
0.657	0.954	0.954	0.789	0.694	0.954	0.657	0.655	0.954	0.657	0.655	0.655	0.749	0.954	0.954	0.838	0.772	0.954
0.663	0.964	0.964	0.796	0.700	0.964	0.663	0.661	0.964	0.663	0.661	0.661	0.756	0.964	0.964	0.846	0.779	0.964
0.662	0.963	0.963	0.795	0.699	0.963	0.662	0.661	0.963	0.662	0.660	0.661	0.756	0.963	0.963	0.845	0.779	0.963
0.146	0.948	0.948	0.560	0.411	0.948	0.145	0.144	0.948	0.145	0.144	0.144	0.382	0.948	0.948	0.629	0.523	0.948
0.147	0.944	0.944	0.560	0.411	0.944	0.147	0.144	0.944	0.146	0.144	0.144	0.101	0.944	0.944	0.529	0.427	0.944
0.147	0.943	0.943	0.559	0.411	0.943	0.147	0.144	0.943	0.146	0.144	0.144	0.102	0.943	0.943	0.529	0.427	0.943
0.437	0.947	0.947	0.677	0.527	0.947	0.437	0.434	0.947	0.436	0.434	0.434	0.593	0.947	0.947	0.747	0.647	0.947
0.437	0.946	0.946	0.677	0.527	0.946	0.437	0.434	0.946	0.436	0.434	0.434	0.593	0.946	0.946	0.746	0.647	0.946

Column 127 through 144

0.758	0.757	0.967	0.758	0.757	0.757	0.801	0.967	0.967	0.872	0.819	0.967	0.801	0.800	0.967	0.801	0.800	0.800
0.596	0.595	0.954	0.596	0.594	0.594	0.669	0.954	0.954	0.789	0.710	0.954	0.669	0.667	0.954	0.669	0.667	0.667
0.594	0.592	0.949	0.593	0.591	0.591	0.666	0.949	0.949	0.785	0.707	0.949	0.666	0.664	0.949	0.666	0.664	0.664
0.593	0.591	0.948	0.593	0.591	0.591	0.665	0.948	0.948	0.784	0.706	0.948	0.665	0.663	0.948	0.665	0.663	0.663
0.750	0.749	0.955	0.750	0.748	0.749	0.792	0.955	0.955	0.862	0.809	0.955	0.792	0.791	0.955	0.792	0.791	0.791
0.749	0.747	0.953	0.749	0.747	0.747	0.791	0.953	0.953	0.860	0.808	0.953	0.791	0.789	0.953	0.790	0.789	0.789
0.749	0.748	0.954	0.749	0.748	0.748	0.791	0.954	0.954	0.861	0.808	0.954	0.791	0.790	0.954	0.791	0.790	0.790
0.756	0.755	0.964	0.756	0.755	0.755	0.799	0.964	0.964	0.869	0.816	0.964	0.799	0.798	0.964	0.799	0.798	0.798
0.756	0.754	0.963	0.755	0.754	0.754	0.798	0.963	0.963	0.868	0.816	0.963	0.798	0.797	0.963	0.798	0.797	0.797
0.382	0.380	0.948	0.382	0.380	0.380	0.497	0.948	0.948	0.680	0.598	0.948	0.496	0.495	0.948	0.496	0.495	0.495
0.101	0.100	0.944	0.100	0.100	0.100	0.264	0.944	0.944	0.566	0.481	0.944	0.263	0.263	0.944	0.263	0.262	0.262
0.101	0.100	0.943	0.101	0.100	0.100	0.081	0.943	0.943	0.516	0.435	0.943	0.080	0.080	0.943	0.080	0.079	0.079
0.593	0.591	0.947	0.593	0.590	0.590	0.665	0.947	0.947	0.783	0.706	0.947	0.664	0.663	0.947	0.664	0.663	0.663
0.592	0.590	0.946	0.592	0.590	0.590	0.664	0.946	0.946	0.783	0.705	0.946	0.664	0.662	0.946	0.664	0.662	0.662

Column 145 through 162

0.725	0.967	0.967	0.826	0.756	0.967	0.724	0.723	0.967	0.724	0.723	0.723	0.710	0.967	0.967	0.827	0.736	0.967
0.539	0.954	0.954	0.717	0.614	0.954	0.538	0.537	0.954	0.538	0.536	0.536	0.515	0.954	0.954	0.722	0.577	0.954
0.409	0.949	0.949	0.656	0.522	0.949	0.409	0.407	0.949	0.409	0.407	0.407	0.383	0.949	0.949	0.668	0.475	0.949
0.409	0.948	0.948	0.656	0.521	0.948	0.409	0.407	0.948	0.408	0.406	0.406	0.383	0.948	0.948	0.667	0.474	0.948
0.717	0.955	0.955	0.817	0.748	0.955	0.717	0.715	0.955	0.717	0.715	0.715	0.703	0.955	0.955	0.817	0.728	0.955
0.715	0.953	0.953	0.816	0.747	0.953	0.715	0.714	0.953	0.715	0.713	0.713	0.702	0.953	0.953	0.816	0.726	0.953
0.716	0.954	0.954	0.816	0.747	0.954	0.716	0.714	0.954	0.716	0.714	0.714	0.702	0.954	0.954	0.817	0.727	0.954
0.723	0.964	0.964	0.824	0.754	0.964	0.722	0.721	0.964	0.722	0.721	0.721	0.708	0.964	0.964	0.824	0.734	0.964
0.722	0.963	0.963	0.823	0.753	0.963	0.722	0.720	0.963	0.722	0.720	0.720	0.708	0.963	0.963	0.823	0.733	0.963
0.536	0.948	0.948	0.714	0.611	0.948	0.536	0.534	0.948	0.536	0.534	0.534	0.513	0.948	0.948	0.718	0.575	0.948
0.535	0.944	0.944	0.711	0.609	0.944	0.535	0.532	0.944	0.535	0.532	0.532	0.512	0.944	0.944	0.716	0.573	0.944
0.535	0.943	0.943	0.711	0.608	0.943	0.534	0.532	0.943	0.534	0.531	0.531	0.512	0.943	0.943	0.715	0.572	0.943
0.116	0.947	0.947	0.542	0.420	0.947	0.116	0.115	0.947	0.115	0.114	0.114	0.383	0.947	0.947	0.667	0.474	0.947
0.409	0.946	0.946	0.655	0.521	0.946	0.408	0.406	0.946	0.408	0.406	0.406	0.126	0.946	0.946	0.544	0.421	0.946

Column 163 through 168

0.710	0.709	0.967	0.710	0.709	0.709
0.515	0.513	0.954	0.515	0.513	0.513
0.383	0.381	0.949	0.382	0.380	0.380
0.382	0.381	0.948	0.382	0.380	0.380
0.703	0.701	0.955	0.703	0.701	0.701
0.701	0.700	0.953	0.701	0.699	0.699
0.702	0.700	0.954	0.702	0.700	0.700
0.708	0.707	0.964	0.708	0.707	0.707
0.708	0.706	0.963	0.707	0.706	0.706
0.513	0.511	0.948	0.513	0.510	0.510
0.512	0.509	0.944	0.511	0.509	0.509
0.511	0.509	0.943	0.511	0.508	0.508
0.382	0.380	0.947	0.382	0.380	0.380
0.125	0.124	0.946	0.125	0.124	0.124

APPENDIX C: IEEE-15 BUS TEST DATA SAMPLES FOR ANN

Column 1 through 45

0	1	1	1	1	1	0	0	1	0	0	0	1	1	1	1	1	1	1	1	1	1	1	1	1	1	1	1	1	1	1	1	1	1	1	1	1	1	1	1	1	1	1	1	1
1	1	1	1	1	1	1	1	1	1	1	1	0	1	1	1	1	1	0	0	1	0	0	0	1	1	1	1	1	1	1	1	1	1	1	1	1	1	1	1	1	1	1	1	1
1	1	1	1	1	1	1	1	1	1	1	1	1	1	1	1	1	1	1	1	1	1	1	1	0	1	1	1	1	1	0	0	1	0	0	0	1	1	1	1	1	1	1	1	1
1	1	1	1	1	1	1	1	1	1	1	1	1	1	1	1	1	1	1	1	1	1	1	1	1	1	1	1	1	1	1	1	1	1	1	1	0	1	1	1	1	1	0	0	1
1	1	1	1	1	1	1	1	1	1	1	1	1	1	1	1	1	1	1	1	1	1	1	1	1	1	1	1	1	1	1	1	1	1	1	1	1	1	1	1	1	1	1	1	1
1	1	1	1	1	1	1	1	1	1	1	1	1	1	1	1	1	1	1	1	1	1	1	1	1	1	1	1	1	1	1	1	1	1	1	1	1	1	1	1	1	1	1	1	1
1	1	1	1	1	1	1	1	1	1	1	1	1	1	1	1	1	1	1	1	1	1	1	1	1	1	1	1	1	1	1	1	1	1	1	1	1	1	1	1	1	1	1	1	1
1	1	1	1	1	1	1	1	1	1	1	1	1	1	1	1	1	1	1	1	1	1	1	1	1	1	1	1	1	1	1	1	1	1	1	1	1	1	1	1	1	1	1	1	1
1	1	1	1	1	1	1	1	1	1	1	1	1	1	1	1	1	1	1	1	1	1	1	1	1	1	1	1	1	1	1	1	1	1	1	1	1	1	1	1	1	1	1	1	1
1	1	1	1	1	1	1	1	1	1	1	1	1	1	1	1	1	1	1	1	1	1	1	1	1	1	1	1	1	1	1	1	1	1	1	1	1	1	1	1	1	1	1	1	1
1	1	1	1	1	1	1	1	1	1	1	1	1	1	1	1	1	1	1	1	1	1	1	1	1	1	1	1	1	1	1	1	1	1	1	1	1	1	1	1	1	1	1	1	1
1	1	1	1	1	1	1	1	1	1	1	1	1	1	1	1	1	1	1	1	1	1	1	1	1	1	1	1	1	1	1	1	1	1	1	1	1	1	1	1	1	1	1	1	1
1	1	1	1	1	1	1	1	1	1	1	1	1	1	1	1	1	1	1	1	1	1	1	1	1	1	1	1	1	1	1	1	1	1	1	1	1	1	1	1	1	1	1	1	1
1	1	1	1	1	1	1	1	1	1	1	1	1	1	1	1	1	1	1	1	1	1	1	1	1	1	1	1	1	1	1	1	1	1	1	1	1	1	1	1	1	1	1	1	1

Column 46 through 90

1	1	1	1	1	1	1	1	1	1	1	1	1	1	1	1	1	1	1	1	1	1	1	1	1	1	1	1	1	1	1	1	1	1	1	1	1	1	1	1	1	1	1	1	1
1	1	1	1	1	1	1	1	1	1	1	1	1	1	1	1	1	1	1	1	1	1	1	1	1	1	1	1	1	1	1	1	1	1	1	1	1	1	1	1	1	1	1	1	1
1	1	1	1	1	1	1	1	1	1	1	1	1	1	1	1	1	1	1	1	1	1	1	1	1	1	1	1	1	1	1	1	1	1	1	1	1	1	1	1	1	1	1	1	1
0	0	0	1	1	1	1	1	1	1	1	1	1	1	1	1	1	1	1	1	1	1	1	1	1	1	1	1	1	1	1	1	1	1	1	1	1	1	1	1	1	1	1	1	1
1	1	1	0	1	1	1	1	1	0	0	1	0	0	0	1	1	1	1	1	1	1	1	1	1	1	1	1	1	1	1	1	1	1	1	1	1	1	1	1	1	1	1	1	1
1	1	1	1	1	1	1	1	1	1	1	1	1	1	0	1	1	1	1	1	0	0	1	0	0	0	1	1	1	1	1	1	1	1	1	1	1	1	1	1	1	1	1	1	1
1	1	1	1	1	1	1	1	1	1	1	1	1	1	1	1	1	1	1	1	1	1	1	1	1	1	0	1	1	1	1	1	0	0	1	0	0	0	1	1	1	1	1	1	1
1	1	1	1	1	1	1	1	1	1	1	1	1	1	1	1	1	1	1	1	1	1	1	1	1	1	1	1	1	1	1	1	1	1	1	1	1	1	1	0	1	1	1	1	1
1	1	1	1	1	1	1	1	1	1	1	1	1	1	1	1	1	1	1	1	1	1	1	1	1	1	1	1	1	1	1	1	1	1	1	1	1	1	1	1	1	1	1	1	1
1	1	1	1	1	1	1	1	1	1	1	1	1	1	1	1	1	1	1	1	1	1	1	1	1	1	1	1	1	1	1	1	1	1	1	1	1	1	1	1	1	1	1	1	1
1	1	1	1	1	1	1	1	1	1	1	1	1	1	1	1	1	1	1	1	1	1	1	1	1	1	1	1	1	1	1	1	1	1	1	1	1	1	1	1	1	1	1	1	1
1	1	1	1	1	1	1	1	1	1	1	1	1	1	1	1	1	1	1	1	1	1	1	1	1	1	1	1	1	1	1	1	1	1	1	1	1	1	1	1	1	1	1	1	1
1	1	1	1	1	1	1	1	1	1	1	1	1	1	1	1	1	1	1	1	1	1	1	1	1	1	1	1	1	1	1	1	1	1	1	1	1	1	1	1	1	1	1	1	1
1	1	1	1	1	1	1	1	1	1	1	1	1	1	1	1	1	1	1	1	1	1	1	1	1	1	1	1	1	1	1	1	1	1	1	1	1	1	1	1	1	1	1	1	1

Column 91 through 135

1	1	1	1	1	1	1	1	1	1	1	1	1	1	1	1	1	1	1	1	1	1	1	1	1	1	1	1	1	1	1	1	1	1	1	1	1	1	1	1	1	1	1	1	1
1	1	1	1	1	1	1	1	1	1	1	1	1	1	1	1	1	1	1	1	1	1	1	1	1	1	1	1	1	1	1	1	1	1	1	1	1	1	1	1	1	1	1	1	1
1	1	1	1	1	1	1	1	1	1	1	1	1	1	1	1	1	1	1	1	1	1	1	1	1	1	1	1	1	1	1	1	1	1	1	1	1	1	1	1	1	1	1	1	1
1	1	1	1	1	1	1	1	1	1	1	1	1	1	1	1	1	1	1	1	1	1	1	1	1	1	1	1	1	1	1	1	1	1	1	1	1	1	1	1	1	1	1	1	1
1	1	1	1	1	1	1	1	1	1	1	1	1	1	1	1	1	1	1	1	1	1	1	1	1	1	1	1	1	1	1	1	1	1	1	1	1	1	1	1	1	1	1	1	1
1	1	1	1	1	1	1	1	1	1	1	1	1	1	1	1	1	1	1	1	1	1	1	1	1	1	1	1	1	1	1	1	1	1	1	1	1	1	1	1	1	1	1	1	1
1	1	1	1	1	1	1	1	1	1	1	1	1	1	1	1	1	1	1	1	1	1	1	1	1	1	1	1	1	1	1	1	1	1	1	1	1	1	1	1	1	1	1	1	1
0	0	1	0	0	0	1	1	1	1	1	1	1	1	1	1	1	1	1	1	1	1	1	1	1	1	1	1	1	1	1	1	1	1	1	1	1	1	1	1	1	1	1	1	1
1	1	1	1	1	1	0	1	1	1	1	1	0	0	1	0	0	0	1	1	1	1	1	1	1	1	1	1	1	1	1	1	1	1	1	1	1	1	1	1	1	1	1	1	1
1	1	1	1	1	1	1	1	1	1	1	1	1	1	1	1	1	1	0	1	1	1	1	1	0	0	1	0	0	0	1	1	1	1	1	1	1	1	1	1	1	1	1	1	1
1	1	1	1	1	1	1	1	1	1	1	1	1	1	1	1	1	1	1	1	1	1	1	1	1	1	1	1	1	1	0	1	1	1	1	1	0	0	1	0	0	0	1	1	1
1	1	1	1	1	1	1	1	1	1	1	1	1	1	1	1	1	1	1	1	1	1	1	1	1	1	1	1	1	1	1	1	1	1	1	1	1	1	1	1	1	1	0	1	1
1	1	1	1	1	1	1	1	1	1	1	1	1	1	1	1	1	1	1	1	1	1	1	1	1	1	1	1	1	1	1	1	1	1	1	1	1	1	1	1	1	1	1	1	1
1	1	1	1	1	1	1	1	1	1	1	1	1	1	1	1	1	1	1	1	1	1	1	1	1	1	1	1	1	1	1	1	1	1	1	1	1	1	1	1	1	1	1	1	1

Column 136 through 168

1	1	1	1	1	1	1	1	1	1	1	1	1	1	1	1	1	1	1	1	1	1	1	1	1	1	1	1	1	1	1	1	1
1	1	1	1	1	1	1	1	1	1	1	1	1	1	1	1	1	1	1	1	1	1	1	1	1	1	1	1	1	1	1	1	1
1	1	1	1	1	1	1	1	1	1	1	1	1	1	1	1	1	1	1	1	1	1	1	1	1	1	1	1	1	1	1	1	1
1	1	1	1	1	1	1	1	1	1	1	1	1	1	1	1	1	1	1	1	1	1	1	1	1	1	1	1	1	1	1	1	1
1	1	1	1	1	1	1	1	1	1	1	1	1	1	1	1	1	1	1	1	1	1	1	1	1	1	1	1	1	1	1	1	1
1	1	1	1	1	1	1	1	1	1	1	1	1	1	1	1	1	1	1	1	1	1	1	1	1	1	1	1	1	1	1	1	1
1	1	1	1	1	1	1	1	1	1	1	1	1	1	1	1	1	1	1	1	1	1	1	1	1	1	1	1	1	1	1	1	1
1	1	1	1	1	1	1	1	1	1	1	1	1	1	1	1	1	1	1	1	1	1	1	1	1	1	1	1	1	1	1	1	1
1	1	1	1	1	1	1	1	1	1	1	1	1	1	1	1	1	1	1	1	1	1	1	1	1	1	1	1	1	1	1	1	1
1	1	1	1	1	1	1	1	1	1	1	1	1	1	1	1	1	1	1	1	1	1	1	1	1	1	1	1	1	1	1	1	1
1	1	1	1	1	1	1	1	1	1	1	1	1	1	1	1	1	1	1	1	1	1	1	1	1	1	1	1	1	1	1	1	1
1	1	1	0	0	1	0	0	0	1	1	1	1	1	1	1	1	1	1	1	1	1	1	1	1	1	1	1	1	1	1	1	1
1	1	1	1	1	1	1	1	1	0	1	1	1	1	1	0	0	1	0	0	0	1	1	1	1	1	1	1	1	1	1	1	1
1	1	1	1	1	1	1	1	1	1	1	1	1	1	1	1	1	1	1	1	1	0	1	1	1	1	1	0	0	1	0	0	0

APPENDIX D: LINE AND LOAD DATA OF THIMI-SALLAGHARI DISTRIBUTION SYSTEM

Bus No.	Load Data	
	Active Power (kW)	Reactive Power (kVAR)
1.	0	0
2.	80	60
3.	96	128
4.	128	96
5.	120	160
6.	90	120
7.	189	252
8.	80	60
9.	80	60
10.	160	120
11.	80	60

Bus No.		Line Data	
From	To	R(Ohms)	X(Ohms)
1	2	1.695	1.575
2	3	0.968	0.8995
3	4	0.9705	0.9018
4	5	1.017	0.945
2	6	0.678	0.63
6	7	1.017	0.945
7	8	0.5755	0.5348
8	9	0.5713	0.5309
9	10	0.6056	0.5627
10	11	0.6441	0.5985

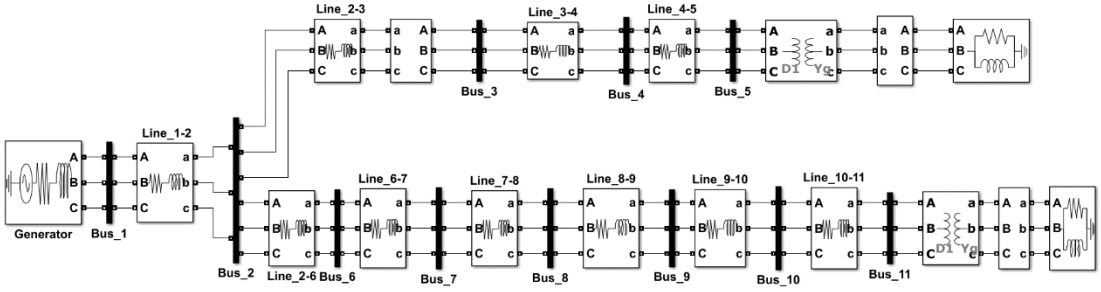

Figure D-1: Simulink Model of Thimi-Sallaghari distribution System

APPENDIX E: THIMI-SALLAGHARI DISTRIBUTION SYSTEM TRAIN DATA SAMPLES FOR ANN

Train data samples: 10×120 matrix where 10 rows represent the load buses and 120 columns represents the 10 load buses × 3 phases × 4 faults

Fault at bus 2- Column 1 to 3: L-G fault voltage, Column 4 to 6: LL fault voltage, Column 7 to 9: LLG fault voltage, Column 10 to 12: LLLG fault voltage for bus 2 and similarly other columns represents the voltage values for faults for other remaining buses 3-11 as in bus 2

Column 1 through 18

0.250	0.975	0.971	0.653	0.371	0.966	0.250	0.250	0.976	0.251	0.250	0.250	0.403	0.974	0.970	0.684	0.497	0.966
0.249	0.972	0.968	0.651	0.370	0.962	0.249	0.250	0.973	0.251	0.249	0.249	0.187	0.970	0.967	0.605	0.390	0.962
0.248	0.970	0.965	0.649	0.369	0.959	0.248	0.250	0.971	0.252	0.249	0.249	0.187	0.968	0.965	0.604	0.389	0.959
0.247	0.968	0.964	0.649	0.369	0.957	0.248	0.250	0.970	0.252	0.249	0.249	0.186	0.967	0.964	0.603	0.389	0.957
0.248	0.971	0.967	0.650	0.370	0.961	0.249	0.250	0.972	0.251	0.249	0.249	0.401	0.969	0.966	0.681	0.495	0.961
0.246	0.966	0.961	0.647	0.368	0.954	0.247	0.250	0.968	0.251	0.248	0.248	0.397	0.963	0.960	0.677	0.493	0.954
0.246	0.964	0.959	0.646	0.368	0.951	0.246	0.250	0.966	0.251	0.248	0.248	0.396	0.961	0.958	0.675	0.492	0.951
0.245	0.962	0.957	0.645	0.367	0.949	0.245	0.250	0.964	0.251	0.248	0.248	0.395	0.960	0.956	0.674	0.491	0.949
0.245	0.961	0.956	0.644	0.367	0.947	0.244	0.251	0.963	0.251	0.247	0.248	0.394	0.958	0.954	0.673	0.491	0.947
0.245	0.961	0.955	0.643	0.367	0.947	0.244	0.251	0.963	0.251	0.247	0.247	0.394	0.958	0.954	0.673	0.490	0.947

Column 19 through 36

0.404	0.405	0.975	0.406	0.404	0.404	0.512	0.973	0.970	0.722	0.586	0.966	0.513	0.514	0.974	0.515	0.513	0.514
0.188	0.187	0.972	0.188	0.187	0.187	0.322	0.969	0.967	0.631	0.473	0.962	0.323	0.323	0.971	0.324	0.323	0.323
0.187	0.188	0.970	0.189	0.187	0.187	0.149	0.967	0.965	0.577	0.403	0.959	0.150	0.149	0.969	0.150	0.149	0.149
0.187	0.188	0.969	0.189	0.187	0.187	0.149	0.966	0.964	0.576	0.403	0.957	0.150	0.150	0.968	0.151	0.149	0.149
0.402	0.403	0.971	0.404	0.402	0.403	0.509	0.968	0.965	0.719	0.584	0.961	0.510	0.511	0.969	0.513	0.511	0.511
0.399	0.401	0.965	0.403	0.400	0.400	0.505	0.962	0.959	0.714	0.580	0.954	0.506	0.508	0.963	0.510	0.508	0.508
0.398	0.400	0.963	0.402	0.399	0.400	0.503	0.960	0.957	0.713	0.579	0.951	0.505	0.507	0.961	0.509	0.507	0.507
0.397	0.399	0.962	0.402	0.399	0.399	0.502	0.958	0.955	0.711	0.578	0.949	0.504	0.506	0.960	0.508	0.506	0.506
0.396	0.399	0.960	0.401	0.398	0.398	0.501	0.956	0.953	0.710	0.577	0.947	0.503	0.505	0.958	0.508	0.505	0.505
0.396	0.399	0.960	0.401	0.398	0.398	0.500	0.956	0.953	0.710	0.577	0.947	0.503	0.505	0.958	0.507	0.505	0.505

Column 37 through 54

0.590	0.972	0.970	0.756	0.651	0.966	0.591	0.591	0.973	0.593	0.591	0.592	0.363	0.975	0.971	0.673	0.464	0.966
0.430	0.968	0.966	0.667	0.548	0.962	0.431	0.431	0.970	0.432	0.431	0.431	0.361	0.971	0.968	0.671	0.463	0.962
0.273	0.966	0.964	0.599	0.465	0.959	0.273	0.274	0.968	0.275	0.273	0.274	0.359	0.969	0.965	0.669	0.462	0.959
0.123	0.965	0.963	0.558	0.414	0.957	0.123	0.123	0.967	0.124	0.123	0.123	0.359	0.967	0.964	0.668	0.461	0.957
0.586	0.967	0.965	0.752	0.648	0.961	0.587	0.588	0.968	0.590	0.588	0.589	0.203	0.970	0.967	0.616	0.384	0.961
0.582	0.961	0.958	0.747	0.644	0.954	0.583	0.584	0.962	0.587	0.585	0.585	0.201	0.965	0.962	0.613	0.382	0.954
0.580	0.958	0.956	0.745	0.642	0.951	0.582	0.583	0.960	0.585	0.583	0.583	0.200	0.963	0.959	0.612	0.382	0.951
0.578	0.956	0.954	0.744	0.641	0.949	0.580	0.582	0.958	0.584	0.582	0.582	0.200	0.962	0.958	0.611	0.381	0.949
0.577	0.955	0.952	0.743	0.640	0.947	0.579	0.581	0.957	0.584	0.581	0.581	0.200	0.960	0.957	0.610	0.381	0.947
0.577	0.954	0.952	0.742	0.640	0.947	0.579	0.580	0.956	0.583	0.581	0.581	0.200	0.960	0.956	0.610	0.381	0.947

Column 55 through 72

0.363	0.363	0.976	0.365	0.363	0.363	0.491	0.974	0.971	0.714	0.568	0.966	0.492	0.492	0.975	0.493	0.492	0.492
0.362	0.362	0.973	0.364	0.362	0.362	0.488	0.970	0.967	0.712	0.566	0.962	0.490	0.490	0.972	0.492	0.490	0.490
0.361	0.362	0.970	0.364	0.361	0.361	0.487	0.968	0.965	0.710	0.565	0.959	0.488	0.489	0.969	0.491	0.489	0.489
0.360	0.361	0.969	0.363	0.361	0.361	0.486	0.966	0.963	0.709	0.564	0.957	0.488	0.488	0.968	0.490	0.488	0.488
0.203	0.203	0.972	0.204	0.203	0.203	0.350	0.970	0.967	0.646	0.483	0.961	0.351	0.351	0.971	0.353	0.351	0.351
0.202	0.204	0.967	0.205	0.202	0.202	0.158	0.964	0.962	0.580	0.398	0.954	0.158	0.158	0.967	0.159	0.158	0.158
0.201	0.204	0.966	0.205	0.202	0.202	0.157	0.963	0.960	0.579	0.397	0.951	0.158	0.159	0.965	0.160	0.158	0.158
0.200	0.204	0.964	0.205	0.202	0.202	0.157	0.961	0.958	0.579	0.397	0.949	0.157	0.159	0.964	0.160	0.158	0.158
0.200	0.204	0.963	0.205	0.202	0.202	0.157	0.960	0.957	0.578	0.397	0.947	0.157	0.159	0.962	0.160	0.158	0.158
0.200	0.204	0.963	0.205	0.202	0.202	0.157	0.959	0.956	0.578	0.397	0.947	0.157	0.159	0.962	0.160	0.158	0.158

Column 73 through 90

0.543	0.973	0.971	0.735	0.611	0.966	0.544	0.544	0.974	0.546	0.545	0.545	0.585	0.973	0.970	0.754	0.646	0.966
0.541	0.970	0.967	0.733	0.609	0.962	0.542	0.542	0.971	0.544	0.542	0.543	0.583	0.969	0.966	0.751	0.644	0.962
0.539	0.967	0.964	0.731	0.608	0.959	0.540	0.541	0.968	0.543	0.541	0.541	0.581	0.966	0.964	0.749	0.642	0.959
0.538	0.966	0.963	0.730	0.607	0.957	0.540	0.540	0.967	0.542	0.540	0.540	0.580	0.965	0.962	0.748	0.642	0.957
0.417	0.969	0.966	0.667	0.530	0.961	0.418	0.418	0.971	0.419	0.418	0.418	0.470	0.969	0.966	0.688	0.570	0.961
0.232	0.964	0.961	0.591	0.436	0.954	0.233	0.233	0.966	0.234	0.233	0.233	0.301	0.963	0.961	0.608	0.474	0.954
0.140	0.962	0.959	0.567	0.404	0.951	0.141	0.140	0.964	0.141	0.140	0.140	0.208	0.961	0.959	0.576	0.435	0.951
0.140	0.960	0.958	0.566	0.404	0.949	0.140	0.141	0.963	0.142	0.140	0.140	0.126	0.960	0.957	0.556	0.409	0.949
0.139	0.959	0.956	0.565	0.404	0.947	0.140	0.141	0.962	0.142	0.140	0.140	0.126	0.959	0.956	0.555	0.409	0.947
0.139	0.959	0.956	0.565	0.403	0.947	0.140	0.141	0.961	0.142	0.140	0.140	0.126	0.958	0.956	0.555	0.409	0.947

Column 91 through 108

0.586	0.587	0.974	0.588	0.587	0.587	0.622	0.972	0.970	0.771	0.677	0.966	0.623	0.623	0.973	0.625	0.623	0.624
0.584	0.584	0.970	0.586	0.585	0.585	0.619	0.969	0.966	0.768	0.674	0.962	0.620	0.621	0.970	0.623	0.621	0.621
0.582	0.583	0.968	0.585	0.583	0.583	0.617	0.966	0.963	0.766	0.673	0.959	0.619	0.619	0.967	0.621	0.619	0.619
0.581	0.582	0.966	0.584	0.582	0.582	0.616	0.964	0.962	0.765	0.672	0.957	0.618	0.618	0.966	0.620	0.618	0.618
0.471	0.472	0.970	0.473	0.472	0.472	0.517	0.968	0.966	0.708	0.606	0.961	0.518	0.519	0.969	0.520	0.519	0.519
0.302	0.302	0.965	0.303	0.302	0.302	0.362	0.963	0.960	0.628	0.512	0.954	0.363	0.363	0.965	0.365	0.363	0.363
0.209	0.209	0.964	0.210	0.209	0.209	0.276	0.961	0.958	0.592	0.469	0.951	0.277	0.277	0.963	0.278	0.277	0.277
0.126	0.126	0.962	0.127	0.126	0.126	0.193	0.959	0.957	0.565	0.436	0.949	0.194	0.194	0.961	0.195	0.193	0.193
0.126	0.127	0.961	0.127	0.126	0.126	0.114	0.958	0.956	0.547	0.414	0.947	0.114	0.114	0.960	0.115	0.114	0.114
0.126	0.127	0.961	0.128	0.126	0.126	0.114	0.958	0.955	0.547	0.414	0.947	0.114	0.114	0.960	0.115	0.114	0.114

Column 109 through 120

0.654	0.972	0.970	0.787	0.704	0.966	0.655	0.655	0.973	0.657	0.656	0.656
0.651	0.968	0.966	0.784	0.701	0.962	0.652	0.653	0.969	0.654	0.653	0.653
0.649	0.965	0.963	0.781	0.699	0.959	0.650	0.651	0.966	0.653	0.651	0.651
0.647	0.964	0.962	0.780	0.698	0.957	0.649	0.650	0.965	0.652	0.650	0.650
0.558	0.967	0.965	0.727	0.638	0.961	0.560	0.560	0.969	0.561	0.560	0.560
0.416	0.962	0.960	0.648	0.548	0.954	0.418	0.418	0.964	0.420	0.418	0.418
0.337	0.960	0.958	0.611	0.505	0.951	0.338	0.338	0.962	0.340	0.338	0.338
0.259	0.958	0.956	0.580	0.468	0.949	0.260	0.260	0.960	0.262	0.260	0.261
0.179	0.957	0.955	0.555	0.438	0.947	0.180	0.180	0.959	0.181	0.180	0.180
0.103	0.957	0.954	0.539	0.419	0.947	0.103	0.103	0.959	0.104	0.103	0.103

APPENDIX F: THIMI-SALLAGHARI DISTRIBUTION SYSTEM TEST DATA SAMPLES FOR ANN

Column 1 through 45

0	1	1	1	1	1	0	0	1	0	0	0	1	1	1	1	1	1	1	1	1	1	1	1	1	1	1	1	1	1	1	1	1	1	1	1	1	1	1	1	1	1	1	1	1
1	1	1	1	1	1	1	1	1	1	1	1	0	1	1	1	1	1	0	0	1	0	0	0	1	1	1	1	1	1	1	1	1	1	1	1	1	1	1	1	1	1	1	1	1
1	1	1	1	1	1	1	1	1	1	1	1	1	1	1	1	1	1	1	1	1	1	1	1	0	1	1	1	1	1	0	0	1	0	0	0	1	1	1	1	1	1	1	1	1
1	1	1	1	1	1	1	1	1	1	1	1	1	1	1	1	1	1	1	1	1	1	1	1	1	1	1	1	1	1	1	1	1	1	1	1	0	1	1	1	1	1	0	0	1
1	1	1	1	1	1	1	1	1	1	1	1	1	1	1	1	1	1	1	1	1	1	1	1	1	1	1	1	1	1	1	1	1	1	1	1	1	1	1	1	1	1	1	1	1
1	1	1	1	1	1	1	1	1	1	1	1	1	1	1	1	1	1	1	1	1	1	1	1	1	1	1	1	1	1	1	1	1	1	1	1	1	1	1	1	1	1	1	1	1
1	1	1	1	1	1	1	1	1	1	1	1	1	1	1	1	1	1	1	1	1	1	1	1	1	1	1	1	1	1	1	1	1	1	1	1	1	1	1	1	1	1	1	1	1
1	1	1	1	1	1	1	1	1	1	1	1	1	1	1	1	1	1	1	1	1	1	1	1	1	1	1	1	1	1	1	1	1	1	1	1	1	1	1	1	1	1	1	1	1
1	1	1	1	1	1	1	1	1	1	1	1	1	1	1	1	1	1	1	1	1	1	1	1	1	1	1	1	1	1	1	1	1	1	1	1	1	1	1	1	1	1	1	1	1
1	1	1	1	1	1	1	1	1	1	1	1	1	1	1	1	1	1	1	1	1	1	1	1	1	1	1	1	1	1	1	1	1	1	1	1	1	1	1	1	1	1	1	1	1

Column 46 through 90

1	1	1	1	1	1	1	1	1	1	1	1	1	1	1	1	1	1	1	1	1	1	1	1	1	1	1	1	1	1	1	1	1	1	1	1	1	1	1	1	1	1	1	1	1
1	1	1	1	1	1	1	1	1	1	1	1	1	1	1	1	1	1	1	1	1	1	1	1	1	1	1	1	1	1	1	1	1	1	1	1	1	1	1	1	1	1	1	1	1
1	1	1	1	1	1	1	1	1	1	1	1	1	1	1	1	1	1	1	1	1	1	1	1	1	1	1	1	1	1	1	1	1	1	1	1	1	1	1	1	1	1	1	1	1
0	0	0	1	1	1	1	1	1	1	1	1	1	1	1	1	1	1	1	1	1	1	1	1	1	1	1	1	1	1	1	1	1	1	1	1	1	1	1	1	1	1	1	1	1
1	1	1	0	1	1	1	1	1	0	0	1	0	0	0	1	1	1	1	1	1	1	1	1	1	1	1	1	1	1	1	1	1	1	1	1	1	1	1	1	1	1	1	1	1
1	1	1	1	1	1	1	1	1	1	1	1	1	1	1	0	1	1	1	1	1	0	0	1	0	0	0	1	1	1	1	1	1	1	1	1	1	1	1	1	1	1	1	1	1
1	1	1	1	1	1	1	1	1	1	1	1	1	1	1	1	1	1	1	1	1	1	1	1	1	1	1	0	1	1	1	1	1	0	0	1	0	0	0	1	1	1	1	1	1
1	1	1	1	1	1	1	1	1	1	1	1	1	1	1	1	1	1	1	1	1	1	1	1	1	1	1	1	1	1	1	1	1	1	1	1	1	1	1	0	1	1	1	1	1
1	1	1	1	1	1	1	1	1	1	1	1	1	1	1	1	1	1	1	1	1	1	1	1	1	1	1	1	1	1	1	1	1	1	1	1	1	1	1	1	1	1	1	1	1
1	1	1	1	1	1	1	1	1	1	1	1	1	1	1	1	1	1	1	1	1	1	1	1	1	1	1	1	1	1	1	1	1	1	1	1	1	1	1	1	1	1	1	1	1

Column 91 through 120

1	1	1	1	1	1	1	1	1	1	1	1	1	1	1	1	1	1	1	1	1	1	1	1	1	1	1	1	1	1
1	1	1	1	1	1	1	1	1	1	1	1	1	1	1	1	1	1	1	1	1	1	1	1	1	1	1	1	1	1
1	1	1	1	1	1	1	1	1	1	1	1	1	1	1	1	1	1	1	1	1	1	1	1	1	1	1	1	1	1
1	1	1	1	1	1	1	1	1	1	1	1	1	1	1	1	1	1	1	1	1	1	1	1	1	1	1	1	1	1
1	1	1	1	1	1	1	1	1	1	1	1	1	1	1	1	1	1	1	1	1	1	1	1	1	1	1	1	1	1
1	1	1	1	1	1	1	1	1	1	1	1	1	1	1	1	1	1	1	1	1	1	1	1	1	1	1	1	1	1
1	1	1	1	1	1	1	1	1	1	1	1	1	1	1	1	1	1	1	1	1	1	1	1	1	1	1	1	1	1
0	0	1	0	0	0	1	1	1	1	1	1	1	1	1	1	1	1	1	1	1	1	1	1	1	1	1	1	1	1
1	1	1	1	1	1	0	1	1	1	1	1	0	0	1	0	0	0	1	1	1	1	1	1	1	1	1	1	1	1
1	1	1	1	1	1	1	1	1	1	1	1	1	1	1	1	1	1	0	1	1	1	1	1	0	0	1	0	0	0

APPENDIX G: SARFI VALUE

For IEEE 15 bus system

S.N.	DVR Location	SARFI Index
1.	1-2	14.21428571
2.	2-3	**10.64285714**
3.	3-4	12.07142857
4.	4-5	14.14285714
5.	2-6	12.64285714
6.	6-7	14.21428571
7.	6-8	14.21428571
8.	2-9	13.35714286
9.	9-10	14.21428571
10.	3-11	12.64285714
11.	11-12	13.35714286
12.	12-13	14.21428571
13.	4-14	14.21428571
14.	4-15	14.21428571

For Thimi-Sallaghari distribution system

S.N.	DVR Location	SARFI Index
1.	1-2	9.909090909
2.	2-3	8.727272727
3.	2-6	**7.545454545**
4.	3-4	9.272727273
5.	4-5	9.818181818
6.	6-7	8.090909091
7.	7-8	8.272727273
8.	8-9	8.636363636
9.	9-10	9.181818182
10.	10-11	9.909090909

APPENDIX H: ORIGINALITY REPORT

ORIGINALITY REPORT

12%	6%	7%	10%
SIMILARITY INDEX	INTERNET SOURCES	PUBLICATIONS	STUDENT PAPERS

PRIMARY SOURCES

1	Submitted to Institute of Engineering, Pulchock Campus, Tribhuvan University Student Paper	1%
2	Submitted to Higher Education Commission Pakistan Student Paper	<1%
3	Bach Quoc Khanh. "On Optimally Positioning a Multiple of Dynamic Voltage Restorers in Distribution System for Global Voltage Sag Mitigation", 2019 IEEE Asia Power and Energy Engineering Conference (APEEC), 2019 Publication	<1%
4	www.iaescore.com Internet Source	<1%
5	Submitted to Victoria University Student Paper	<1%
6	Submitted to Jawaharlal Nehru Technological University Student Paper	<1%

7	Basanta Pancha, Rajendra Shrestha, Ajay Kumar Jha. "Optimal Integration of Distributed Generation in Distribution System: A Case Study of Sallaghari Feeder from Thimi Switching Station, Bhaktapur, Nepal", Journal of the Institute of Engineering, 2020 Publication	<1%
8	Jian Ye, Hoay Beng Gooi, Benfei Wang, Yuanzheng Li, Yun Liu. "Elliptical restoration based single-phase dynamic voltage restorer for source power factor correction", Electric Power Systems Research, 2019 Publication	<1%
9	Submitted to Rajarambapu Institute of Technology Student Paper	<1%
10	Emiyamrew Minaye Molla, Chien-Hsun Liu, Cheng-Chien Kuo. "Power quality improvement using microsystem technology for wind power plant", Microsystem Technologies, 2019 Publication	<1%
11	Submitted to University of Queensland Student Paper	<1%
12	Submitted to NCC Education Student Paper	<1%
13	repository.ntu.edu.sg	